

4-2018

DEVELOPMENT OF WASTE-BASED-THERMOPLASTIC COMPOSITE HEAT INSULATORS

Waseem Yousef Hittini

Follow this and additional works at: https://scholarworks.uaeu.ac.ae/mechan_theses



Part of the [Mechanical Engineering Commons](#)

Recommended Citation

Yousef Hittini, Waseem, "DEVELOPMENT OF WASTE-BASED-THERMOPLASTIC COMPOSITE HEAT INSULATORS" (2018). *Mechanical Engineering Theses*. 12.
https://scholarworks.uaeu.ac.ae/mechan_theses/12

This Thesis is brought to you for free and open access by the Mechanical Engineering at Scholarworks@UAEU. It has been accepted for inclusion in Mechanical Engineering Theses by an authorized administrator of Scholarworks@UAEU. For more information, please contact mariam_aljaberi@uaeu.ac.ae.

United Arab Emirates University

College of Engineering

Department of Mechanical Engineering

DEVELOPMENT OF WASTE-BASED-THERMOPLASTIC
COMPOSITE HEAT INSULATORS

Waseem Yousef Hittini

This thesis is submitted in partial fulfilment of the requirements for the degree of
Master of Science in Mechanical Engineering

Under the Supervision of Professor Abdel-Hamid Ismail Mourad

April 2018

UAEU Library



1000502043



Declaration of Original Work

I, Waseem Yousef Hittini, the undersigned, a graduate student at the United Arab Emirates University (UAEU), and the author of this thesis entitled "*Development of Waste-Based-Thermoplastic Composites Insulators*", hereby, solemnly declare that this thesis is my own original research work that has been done and prepared by me under the supervision of Professor Abdel-Hamid Ismail Mourad, in the College of Engineering at UAEU. This work has not previously been presented or published, or formed the basis for the award of any academic degree, diploma or a similar title at this or any other university. Any materials borrowed from other sources (whether published or unpublished) and relied upon or included in my thesis have been properly cited and acknowledged in accordance with appropriate academic conventions. I further declare that there is no potential conflict of interest with respect to the research, data collection, authorship, presentation and/or publication of this thesis.

Student's Signature: 

Date: 7/5/2018

Approval of the Master Thesis

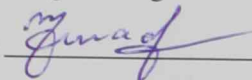
This Master Thesis is approved by the following Examining Committee Members:

- 1) Advisor (Committee Chair): Dr. Abdel-Hamid Ismail Mourad

Title: Professor

Department of Mechanical Engineering

College of Engineering

Signature 

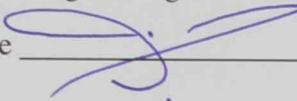
Date 12/4/2018

- 2) Co-Advisor: Dr. Basim Abu-Jdayil

Title: Professor

Department of Chemical and Petroleum Engineering

College of Engineering

Signature 

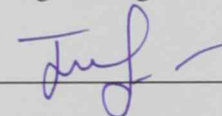
Date 12/4/2018

- 3) Member: Dr. Jaber Abu Qudeiri

Title: Associate Professor

Department of Mechanical Engineering

College of Engineering

Signature 


Date 12/4/2018

- 4) Member (External Examiner): Dr. Autar Kaw / Dr. Tarig Darabsch

Title: Professor

Department of Mechanical Engineering

Institution: University of South Florida, USA

Signature 

Date 12/4/2018

This Master Thesis is accepted by:

Dean of the College of Engineering: Professor Sabah Alkass

Signature  Date 7/5/2018

Dean of the College of Graduate Studies: Professor Nagi T. Wakim

Signature  Date 8/5/2018

Copy 7 of 8

Copyright © 2018 Waseem Yousef Hittini
All Rights Reserved

Advisory Committee

1) Advisor: Prof. Abdel-Hamid Ismail Mourad

Title: Professor

Department of Mechanical Engineering

College of Engineering

2) Co-advisor: Prof. Basim Abu-Jdayil

Title: Professor

Department of Chemical and Petroleum Engineering

College of Engineering

3) Member: Dr. Jaber Abu Qudeiri

Title: Associate Professor

Department of Mechanical Engineering

College of Engineering

4) Member: Prof. Autar Kaw

Title: Professor

Department of Mechanical Engineering

University of South Florida, USA

Abstract

The main scope of this research is to develop polymer-filler thermal insulators utilizing natural and industrial local waste such as date pit powder (DPP), devulcanized tire rubber (DVR) and buffing dust (BD). Recycling and reuse of these local wastes as fillers in insulation materials has significant benefit for the UAE environment. An objective of this work was to study the effect of combination of these local wastes with polystyrene (PS) on the physical, mechanical and thermal properties of the developed thermal insulators. PS was used as a matrix, mixed in different proportions with the waste fillers. Each mixture was then exposed to heat and pressure in a hot press to form a solid sample. The formed composites were tested to evaluate their physical (water absorption and bulk density), mechanical (compression strength, compression modulus, tensile strength, tensile modulus, flexural strength and flexural modulus) and thermal properties (thermal conductivity and thermogravimetric analysis (TGA)). The results established that DPP, DVR and BD were suitable as fillers in thermal insulation materials. Use of DPP and DVR waste in ratios ranging from 0 wt. % to 30 wt. % affected thermal conductivity minimally and resulted in an acceptable reduction in mechanical properties. Replacing 50 wt. % of PS by DPP increased the thermal conductivity by only 9.1%. Adding 10 wt. % of BD to the PS reduced thermal conductivity by 13.29 %, with negligible effect on the mechanical properties. Similarly, low DVR rubber content led to a slight reduction in thermal conductivity (4 %). However, higher proportions of DVR and BD content had a negative effect on the thermal and mechanical properties. Prior treatment of the waste fillers with NaOH, enhanced mechanical performance in composites prepared from the treated fillers. Scanning electron microscopy (SEM) was used to investigate the microstructure of the prepared composites. In addition, the waste fillers were analyzed by infrared

spectroscopy (FTIR) to identify the main functional groups in the fillers. To study the effect of the chemical treatment on the main functional groups, these fillers were analyzed by FTIR after the treatment. Although addition of the three types of waste reduced mechanical strength, all prepared composites with a waste filler concentration below 30 wt. % displayed good mechanical properties, compared with available commercial thermal insulators. Moreover, replacing one-third of the thickness of a building wall with DPP-polystyrene, DVR-PS and BD-PS composites reduced the heat transfer coefficient by 85 %, 87.8 % and 83 %, respectively. Therefore, recycling of the local wastes DPP, BD and DVR as filler materials in thermal insulators presents an opportunity for significant benefit to the UAE economy.

Keywords: Thermal insulators, composites, polystyrene, waste, buffing dust, date pits, tire devulcanized rubber.

Title and Abstract (in Arabic)

تطوير عوازل حرارية معتمدة على اللدائن الحرارية والمخلفات

المخلص

الهدف الرئيسي من هذا البحث هو تطوير عوازل حرارية معتمدة على الخليط الناتج من اللدائن الحرارية و المخلفات المحلية الطبيعية منها و الصناعية مثل بذور التمر، مخلفات الدباغة و مطاط إطارات السيارات المعالج بالحرارة. تدوير هذه المواد و استخدامها كمواد مألثة له تأثير كبير على طبيعة دولة الإمارات العربية المتحدة. أحد أهداف هذه الأطروحة دراسة تأثير إضافة أنواع مختلفة من هذه المخلفات المحلية على الخواص الفيزيائية، الميكانيكية و الحرارية للعوازل الحرارية المطورة. البوليسترين أستخدم كقالب و خلط مع نسب مختلفة من المخلفات باستخدام خلاط تجاري. و من ثم تم تعريض الخليط الناتج إلى الضغط و الحرارة باستخدام آلة الضغط و الحرارة لانتاج العينات الصلبة. لقد تم فحص هذه العينات من ناحية الخواص الفيزيائية (امتصاص الماء و الكثافة)، الخواص الميكانيكية (قوة الضغط، معامل الضغط، قوة الشد، معامل الشد، قوة الانتشاء و معامل الانتشاء) و الخواص الحرارية (قابلية توصيل الحرارة و التحلل الحراري). و لقد أظهرت النتائج أن بذور التمر، مخلفات الدباغة و مطاط الإطارات المعالج بالحرارة يمكن استخدامها كمواد مألثة في العوازل الحرارية. إضافة بذور التمر و مطاط الإطارات المعالج بالحرارة بنسبة تتراوح بين 0-30 % من الوزن له تأثير ضئيل على قابلية التوصيل الحراري و أدى إلى انخفاض الخواص الميكانيكية بشكل مقبول. على سبيل المثال، تبديل 50 % من وزن البوليسترين ببذور التمر، أدى إلى زيادة 9.1 % فقط بالموصلية الحرارية. بالنسبة لمخلفات الجلود، إضافة 10 % من هذا النوع من المخلفات للبوليسترين أدت إلى انخفاض الموصلية الحرارية بنسبة 13.29 % و كان لها تأثير طفيف على الخواص الميكانيكية. و بشكل مشابه، إضافة

نسب قليل من مطاط السيارات المعالج بالحرارة أدى إلى انخفاض بسيط في الموصلية الحرارية. غير أن إضافة نسب أعلى من مخلفات الدباغة و مطاط الإطارات المعالج بالحرارة له تأثير سلبي على الخواص الحرارية و الميكانيكية. عندما تمت معالجة أسطح الخلفات كيميائياً، للخليط المحضر من المخلفات المعالجة و البوليسترين أظهر خواص ميكانيكية أفضل. المجهر الإلكتروني قد استخدم للتحقق من التشكل المجهرى للعينات المحضرة. بالإضافة إلى ذلك، المخلفات المستخدمة قد فحصت باستخدام الأشعة تحت الحمراء للتعرق على المجموعات الوظيفية الأساسية المتواجدة في المخلفات المستخدمة. لدراسة التأثير الناتج من استخدام المعالجة الكيميائية على المجموعات الوظيفية للمخلفات المستخدمة، هذه المخلفات قد فحصت بالأشعة تحت الحمراء بعد المعالجة أيضاً. على الرغم من أن إضافة الأنواع الثلاث من المخلفات أدت إلى انخفاض في الخواص الميكانيكية، كل العينات المصنوعة من نسب مخلفات أقل من 30% لها خواص ميكانيكية جيدة عندما تقارن مع العوازل الحرارية التجارية المتاحة. علاوة على ذلك، استبدال ثلث سماكة جدران الأبنية بخليط بذور التمر و البوليستيرين ، مخلفات الدباغة و الوليستيرين و مخلفات مطاط الإطارات المعالج بالحرارة و البوليستيرين خفض معامل انتقال الحرارة بنسبة 85%، 87.8% و 83%، على التوالي. و من الجدير بالذكر هنا، تدوير هذه المخلفات و استخدام بذور التمر، مخلفات الدباغة و مطاط الإطارات المعالج حرارياً كمادة مألثة بالمواد العازلة حرارياً، له تأثير كبير على اقتصاد دولة الإمارات العربية المتحدة و هذا التأثير يعد تأثير رئيسي على هذه الدولة.

كلمات البحث الرئيسية: العوازل الحرارية، البوليستيرين، المخلفات، مخلفات الدباغة، بذور التمر، مطاط إطارات السيارات المعالج.

Acknowledgements

I would like to thank God for giving me the strength to complete this work. My first thanks go to my main supervisor Prof. Abdel-Hamid Ismail Mourad, Department of Mechanical Engineering, UAE University, and my co-supervisor Prof. Basim Abu-Jdayil, Department of Chemical and Petroleum Engineering, UAE University, who guided me through the two years of research. I would like to thank them for providing me with the precious academic time to pursue my research goals. In addition, I would like to thank Eng. AbdulSattar Nour-Eldin at the Department of Mechanical Engineering, UAE University, for his assistance in the mechanical properties testing. Moreover, I would like to thank them for sharing their knowledge and thoughts throughout my research. In addition, I would like to thank Eng. Suhaib Hameedi, Zayed University, for sharing his valuable knowledge of laboratory equipment, and for teaching me to operate and maintain the equipment safely.

I would to thank all my colleagues and family for supporting and encouraging me to complete this work. Finally, I would like to thank the chair and all members of the Department of Mechanical Engineering at the United Arab Emirates University for assisting me all during my studies and research. I would like to thank the examination committee for their assistance throughout my preparation of this thesis.

This work was supported financially by the Emirates Center of Energy and Environment Research at the United Arab Emirates University (grant number 31R041).

Dedication

To my beloved parents, family and friends

Table of Contents

Title	i
Declaration of Original Work	ii
Copyright	iii
Advisory Committee	iv
Approval of the Master Thesis	v
Abstract	vii
Title and Abstract (in Arabic)	ix
Acknowledgements	xi
Dedication	xii
Table of Contents	xiii
List of Tables.....	xv
List of Figures	xvi
List of Abbreviations.....	xix
Chapter 1: Introduction	1
1.1 Overview	1
1.2 Statement of the Problem	2
1.3 Relevant Literature.....	3
1.3.1 Natural fillers and date pits	4
1.3.2 Plastics and rubber waste	10
1.3.3 Buffing dust waste	18
1.3.4 Chemical treatments	21
Chapter 2: Materials and Research Methods	27
2.1 Materials.....	27
2.1.1 Polystyrene.....	27
2.1.2 Date pit powder.....	28
2.1.3 Devulcanized rubber	28
2.1.4 Buffing dust	29
2.2 Moulds and Composite Fraction	31
2.2.1 Moulds	31
2.2.2 Composites.....	32
2.3 Measurements Methods	32
2.3.1 Mechanical tests.....	32
2.3.2 Structure.....	34
2.3.3 Bulk density	34
2.3.4 Thermal conductivity.....	35

2.3.5	Themogravimetric analysis.....	36
2.3.6	IR spectroscopy.....	36
2.3.7	Water retention	36
2.4	Chemical treatment	37
Chapter 3: Results and Discussion.....		38
3.1	Mechanical Properties.....	38
3.1.1	Compression properties	38
3.1.2	Tensile properties.....	49
3.1.3	Flexural properties	62
3.2	Microstructure	71
3.2.1	Fillers	71
3.2.2	Composites.....	73
3.3	Density	78
3.3.1	Date pits	78
3.3.2	Devulcanized rubber	80
3.3.3	Buffing Dust	81
3.4	Thermal conductivity	83
3.4.1	Date pits	83
3.4.2	Devulcanized rubber	88
3.4.3	Buffing dust	91
3.4.4	Treated fillers	94
3.5	Thermogravimetric analyses	96
3.5.1	Date pits	96
3.5.2	Devulcanized rubber	98
3.5.3	Buffing dust	100
3.5.4	Treated fillers	103
3.6	IR spectroscopy	107
3.7	Water retention.....	110
3.7.1	Date pits	110
3.7.2	Devulcanized rubber	111
3.7.3	Buffing dust	112
Chapter 4: Conclusion.....		114
References		120

List of Tables

Table 1: Compression properties of the DPP-PS composites	41
Table 2: Compression properties of DVR-PS composites.....	44
Table 3: Compression properties of BD-PS composites.....	47
Table 4: Tensile properties of the developed composites	52
Table 5: Tensile properties of DVR-PS composites	56
Table 6: Tensile properties of BD-PS composites	59
Table 7: Flexural properties of the DPP-PS composites.....	64
Table 8: Flexural properties of DVR-PS composites.....	67
Table 9: Flexural properties of BD-PS composites	70
Table 10: DPP-PS fitting parameters	88
Table 11: DVR-PS fitting parameters	91
Table 12: BD-PS fitting parameters	94
Table 13: Decomposition temperature of the DPP-PS composites.....	98
Table 14: Decomposition temperature of DVR-PS composites	100
Table 15: Decomposition temperature of BD-PS composites	103

List of Figures

Fig. 1: Building energy consumption (2010)	1
Fig. 2: PS beads	27
Fig. 3: DPP particle size distribution	28
Fig. 4: DVR	29
Fig. 5: BD cylinders	30
Fig. 6: BD particle size distribution	30
Fig. 7: Moulds for (a) thermal conductivity measurements; (b) compression strength and water retention measurements; (c) tensile strength measurements; (d) flexural strength measurements	31
Fig. 8: Prepared samples for (a) compression test; (b) tensile test; (c) flexural test	34
Fig. 9: Prepared sample for thermal conductivity test	35
Fig. 10: Stress-strain curve for DPP-PS composites	40
Fig. 11: Compression strength of the DPP-PS composites	40
Fig. 12: Compression modulus of the DPP-PS composites	41
Fig. 13: Stress-strain curve for DVR-PS composites	43
Fig. 14: Compression strength of DVR-PS composites	43
Fig. 15: Compression modules of DVR-PS composites	44
Fig. 16: Stress-strain curve for BD-PS composites	46
Fig. 17: Compression strength of BD-PS composites	46
Fig. 18: Compression modulus of BD-PS composites	47
Fig. 19: Compression strength after NaOH treatment	48
Fig. 20: Compression modulus after NaOH treatment	49
Fig. 21: Tensile sample with metallic parts	49
Fig. 22: Tensile strength of the developed composites	51
Fig. 23: Tensile strength of the developed composites	51
Fig. 24: Modulus of elasticity for the developed composites	52
Fig. 25: Stress-strain curve for DVR-PS composites	55
Fig. 26: Tensile strength for the DVR-PS composites	55
Fig. 27: Modulus of elasticity for the DVR-PS composites	56
Fig. 28: Stress-strain curve for BD-PS composites	58
Fig. 29: Tensile strength for the BD-PS composites	58
Fig. 30: Modulus of elasticity for the BD-PS composites	59
Fig. 31: Tensile strength after NaOH treatment	60
Fig. 32: Modulus of elasticity after NaOH treatment	61
Fig. 33: Treated DVR	61
Fig. 34: Load extension curve for DPP-PS composites	63
Fig. 35: Flexural yield strength of the DPP-PS composites	63
Fig. 36: Flexural modulus of the DPP-PS composites	64

Fig. 37: Load extension curve for DVR-PS composites	66
Fig. 38: Flexural yielding strength of the DVR –PS composites.....	66
Fig. 39: Flexural modulus of the DVR-PS composites.....	67
Fig. 40: Load extension curve for BD-PS composites.....	68
Fig. 41: Flexural yielding strength of the BD-PS composites	69
Fig. 42: Flexural modulus of the BD-PS composites.....	69
Fig. 43: Flexural strength after NaOH treatment	71
Fig. 44: Flexural modulus after NaOH treatment	71
Fig. 45: SEM micrograph for (a) raw DPP; (b) DPP after chemical treatment.....	72
Fig. 46: SEM micrograph for (a) raw DVR; (b) DVR after chemical treatment.....	73
Fig. 47: SEM micrograph for (a) raw BD; (b) BD after chemical treatment.....	73
Fig. 48: Filler agglomeration in 50-DPP composite	75
Fig. 49: Crack propagation in the composite	76
Fig. 50: The used filler as reinforcement agent.....	76
Fig. 51: SEM images: (a) 30-DPP composite; (b) treated 30-DPP composite	77
Fig. 52: SEM images of: (a) 30-DVR composite; (b) treated 30-DVR composite	77
Fig. 53: SEM images of: (a) 30-BD composite; (b) treated 30-BD composite	78
Fig. 54: DPP-PS composite density for different filler contents.....	79
Fig. 55: Voids in the pure PS sample and DPP-PS composite.....	79
Fig. 56: DVR-PS composite density with varying filler content	81
Fig. 57: Voids in the pure PS sample and DVR-PS composite	81
Fig. 58: BD-PS composites density for varying filler content.....	82
Fig. 59: Voids in the pure PS sample and BD-PS composite	83
Fig. 60: Thermal conductivity variation of DPP-PS composites at 25 °C.....	86
Fig. 61: Relationship between DPP-PS density and thermal conductivity at 25 °C.	87
Fig. 62: Thermal conductivity of the DPP-PS composites	87
Fig. 63: Thermal conductivity variation of DVR-PS composites at 25 °C.....	90
Fig. 64: Relationship between DVR-PS density and thermal conductivity at 25 °C.	90
Fig. 65: Thermal conductivity of DVR-PS composites	91
Fig. 66: Variation in thermal conductivity of BD-PS composites at 25 °C.....	93
Fig. 67: Thermal conductivity in BD-PS composites	94
Fig. 68: Thermal conductivity of treated fibers composites	95
Fig. 69: Thermograms of DPP–PS composites with different filler content	97
Fig. 70: DTGA curve of DPP.....	97
Fig. 71: Thermograms of DVR-PS composites for different filler content	99
Fig. 72: DTGA curve of DVR.....	100
Fig. 73: Thermograms of BD-PS composites for different filler content	102

Fig. 74: DTGA curve of BD	102
Fig. 75: Thermograms of untreated DPP and treated DPP	105
Fig. 76: Thermograms of untreated DVR and treated DVR	106
Fig. 77: Thermograms of untreated BD and treated BD	106
Fig. 78: FTIR spectra of DPP and treated DPP	108
Fig. 79: FTIR spectra of DVR and treated DVR	109
Fig. 80: FTIR spectra of BD and treated BD	109
Fig. 81: Water retention of DPP-PS composites.....	111
Fig. 82: Water retention of DVR-PS composites.....	112
Fig. 83: Water retention of BD-PS composites.....	113
Fig. 84: Effect of different fillers on the compression strength	114
Fig. 85: Effect of different fillers on tensile strength.....	115
Fig. 86: Effect of different fillers on flexural strength.....	116
Fig. 87: Effect of different fillers on thermal conductivity	117
Fig. 88: Effect of different fillers on water retention	117
Fig. 89: Thermal conductivity comparison	118
Fig. 90: Mechanical strength comparison	119

List of Abbreviations

BD	Buffing dust
CW	Coring wool
DPP	Date pit powder
DTGA	Differential thermogravimetric analysis
DVR	Devulcanized rubber
DW	Doper wool
FTIR	Fourier transform infrared spectroscopy
HDPE	High density polyethylene
NFPC	Natural-fiber polymer composite
PS	Polystyrene
RPET	Recycled polyethylene terephthalate
SBR	Styrene butadiene rubber
SEM	Scanning electron microscopy.
TGA	Thermogravimetric analysis
XRD	X-ray diffraction

Chapter 1: Introduction

1.1 Overview

Air and soil pollution are a major global problem today. Carbon emissions formed by electricity generation are a major source of air pollution, and the pollution from these emissions is increasing as energy consumption continues to rise. Space heating and cooling is a major contributor to energy consumption in buildings (Fig. 1). Soil pollution may result from the disposal to landfill of solid industrial wastes such as date pit powder (DPP), buffing dust (BD) and tire rubber. In addition, non-biodegradable wastes such as used tires may result in serious environmental hazards.

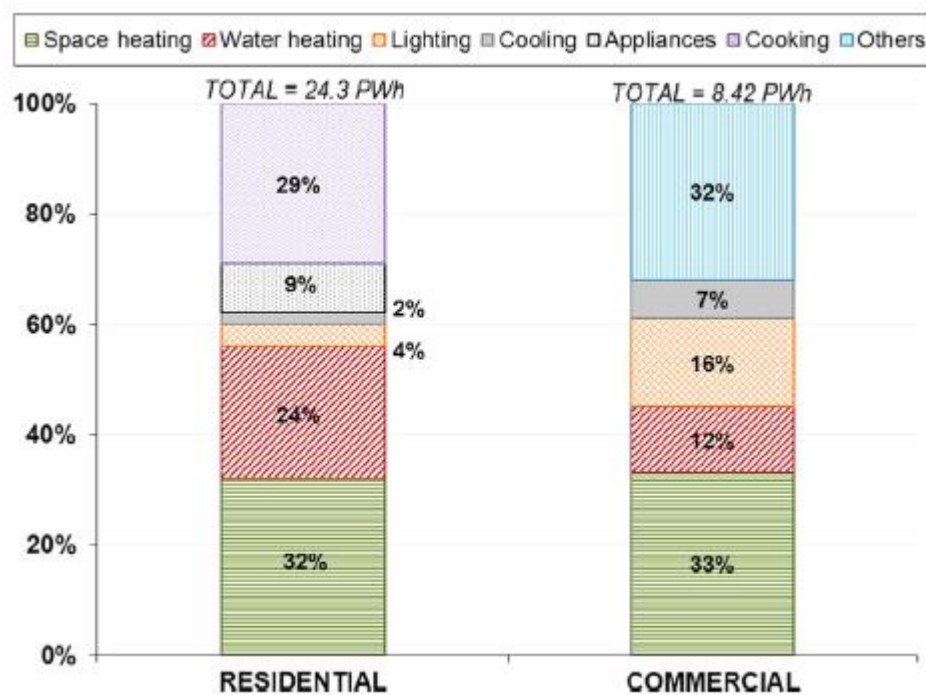


Fig. 1: Building energy consumption (2010) [1]

1.2 Statement of the Problem

In 2016, 39.5 % of the world's energy was consumed in residential and commercial buildings [2]. Residential and commercial buildings were responsible for 16, 843 and 15, 082 trillion Btu in 2016, respectively [2]. According to U.S. Energy Information Administration agency report [3], 52 % of total energy consumed in US homes in 2016 was for space heating. It is likely this energy portion is higher in hot climate countries such as the United Arab Emirates (UAE). By 2012, electricity consumption in the UAE had reached a value of 10.17 MWh per capita [2]. In fact, energy consumption per capita in UAE is considered to be among the highest worldwide [4]. Moreover, it was reported that the electric power demand in the UAE was increasing by 10 % yearly [5]. Because of these factors, research is underway to develop new ways to lower energy consumption.

The date palm tree (*Phoenix dactylifera*) is planted in many areas of the world, and dates are harvested from the trees. In 2006, worldwide date production was seven million tons [6]. Almana and Mahmoud [7] reported that date pits make up around 10 % of the date weight. The date pits from homes and date packaging factories are considered a source of waste. Some researchers have suggested methods to utilize this waste in animal feed and the production of activated carbon.

Used tires are a common source of pollution worldwide. More than 500 million used tires are disposed of annually without any treatment [8], which is a major environmental concern globally. In response, the UAE government and other governments have launched tire waste recycling programs.

Leather production is also a significant source of waste in the UAE and an environmental concern. Processing one metric tonne of raw hide produces 200 kg of

leather as a final product, along with 250 kg of non-tanned waste, 200 kg of tanned waste and 50,000 kg of wastewater. Thus, only 20 % of the raw material by weight is converted to final leather [9].

This research is aimed at the possibility of using available local wastes such as DPP, BD and DVR in developing thermal insulators. The proposed thermal insulators are intended for use in the residential and commercial sectors of the building industry. It is expected these insulation products would improve the efficiency of building cooling systems and minimize the required energy. This, in turn, would reduce electricity consumption and, consequently, carbon emissions. In addition, commonly available thermal insulators are relatively expensive and non-biodegradable; adding local waste to the insulators may reduce cost and environmental impacts.

1.3 Relevant Literature

Natural and industrial wastes cause environmental problems worldwide. Due to the high amount of waste produced, finding new recycling methods is an important challenge. One suggested recycling method is to use waste materials in developing thermal insulation composites. The benefits in using waste in thermal insulation composites is not limited to recycling, but also to develop better thermal insulation materials in residential and commercial buildings and thereby reduce energy consumption. As a result, electricity usage would decrease, resulting in lower costs and carbon emissions. Although the recycling of many kinds of waste as fillers offers advantages such as low density and low cost, they often also have disadvantages such as agglomeration and poor compatibility with polymers. Because of this, researchers are studying chemical treatments and coupling agents to enhance the desirable properties

of waste-polymer composites. This chapter discusses three types of wastes generally and then focuses on the use of these wastes in building materials composites. They are:

- Natural fillers and date pits
- Plastics and rubber waste
- Buffing dust (BD).

Chemical treatments to enhance the properties of composites will also be discussed.

1.3.1 Natural fillers and date pits

Some researchers are focused on using natural fibers and fillers in insulation materials because their internal structure exhibits high porosity. Cellulose is one such fiber, recently used as the main raw material in different insulation products. Cellulose is widely used in paper and cardboard manufacturing [10].

Asdrubali et al. [11] investigated the acoustic and thermal insulation properties of corrugated cardboard panels made from waste paper. The corrugated cardboard panels, which are typically used in packaging, are self-supporting and fully recyclable. The internal geometry of panels allows air to be stored in the flutes, thus enhancing the thermal performance of the panel.

The panels are made from overlapping a number of boards with flutes sandwiched between them. The flutes have two shapes (C-flute and E-flute) with different standardized height (4.1 mm and 1.9 mm, respectively). Both concordant and orthogonal arrangements were used in making samples. The researchers observed that the C-flute sample with a concordant arrangement gave peak transmission loss of 80 dB in the 800 to 1600 Hz frequency range, the transmission loss increasing with

sample thickness. The thermal conductivity of the C-flute concordant samples was measured at 0.053 W/m-K, whereas the thermal conductivity of the E-flute was 0.060 W/m-K [11].

Balčiūnas, Žvironaitė, Vėjelis, Jagniatinskis, and Gaidučis [12] produced an insulating composite from hemp shives with sapropel as a binder and paper production waste as a reinforcement filler. They investigated the thermal conductivity, sound absorption, compressive stress, short-term water absorption and water vapor diffusion resistance of the composite. Thermal conductivity values varied from 0.055 to 0.076 W/m-K, with the variation essentially due to density changes. A correlation formula was derived which correlated thermal conductivity with particle size and density.

Dieye et al. [13] investigated the possibility of using *Typha Australis* fibers as a building material, with clay as a binder. Measured values of compression strength, tensile strength and thermal conductivity ranged from 0.279 to 0.796 MPa, from 0.340 to 0.969 MPa, and from 0.117 to 0.153 W/m-K, respectively, for a clay content of 77 % to 85 %. It was reported that the thermal conductivity of the composite rose with increasing moisture content.

Belkharchouche and Chaker [14] evaluated the effect of mixing building materials lightened with vegetable fibers on the thermal and mechanical properties of heat insulators. Their research focused on the influence of the water content on these properties. Increasing vegetable fibers in concrete resulted in a significant decrease in the density and thermal parameters of the composite. It was reported that thermal conductivity rose considerably with increasing water content. Moreover, it was found that vegetable fibers enhanced mechanical performance slightly.

Balo et al. [15] investigated the thermal, environmental and economical properties of insulation materials developed from clay, fly ash, rice husk ash and epoxidized tall oil. Clay, fly ash and rice husk ash formed the base material with epoxidized tall oil used as binder. The clay, fly ash and epoxidized tall oil had thermal conductivities of 0.93, 0.511 and 0.133 W/m-K, respectively. While the rice husk content was fixed at 10 %, the weight contents of clay and fly ash varied from 30 to 60 wt. %. Epoxidized tall oil was added to the final mixture in proportions of 40 %, 45 % or 50 %. Thermal conductivity of samples varied from 0.537 W/m-K (for 60 % clay, 30 % fly ash, 10 % rice husk ash and epoxidized tall oil 40 %, cured at 165 °C) to 0.256 W/mK (for 30 % clay, 60 % fly ash, 10 % rice husk ash and epoxidized tall oil 50 %, cured at 205 °C). Results showed that thermal conductivity decreased with the increasing of epoxidized tall oil and fly ash content, while it increased with increasing clay content.

An economical analysis was performed assuming a hypothetical house with external composite structure and a 10-year life cycle. The study considered different types of fuels suitable for heating purposes. The study calculated project payback periods of 3.62, 2.28, 2.02 and 1.88 years for natural gas, fuel oil, coal and LPG, respectively. The optimal insulator thickness was calculated to be 0.14, 0.25, 0.30 and 0.34 m for natural gas, fuel oil, coal and LPG, respectively [15].

Cotton waste and textile ash were used to develop a new lightweight insulation material by Binici, Gemci, Aksogan, and Kaplan [16]. Bricks and walls made with these wastes displayed good insulation properties.

Binici, Gemci, Kucukonder, and Solak [17] examined the possibility of using cotton waste, fly ash and epoxy resin in producing chipboard. The thermal

conductivities, acoustic insulation and bending strengths of these boards were determined. Adding cotton waste, fly ash and epoxy resin enhanced the thermal and acoustic insulation properties of the building materials. In another study, Binici, Eken, Dolaz, Aksogan, and Kara demonstrated the possibility of producing thermal insulation materials using sunflower stalks, cotton waste and stubble fibers [18].

Binici, Aksogan, and Demirhan [19] developed bio-based composite using corn-stalk particles as the reinforcement components, and investigated the thermal, mechanical and acoustical insulation properties of the developed composites. Corn-stalk particles vary in size between 0.5 and 4 mm. Epoxy resins, gypsum and cement (CEM I 42,5 R) were used as binders. For corn-stalk and epoxy, water absorption values were measured to between 18.75 and 28.12 %. The highest compaction pressure was found to produce the lowest water absorption. However, the lowest thermal conductivity (0.075 W/m-K) corresponded with the lowest compaction pressure. Compaction pressure affects void size—larger voids lower thermal conductivity but increase water absorption. For corn-stalk and gypsum, the results showed water absorption values lower than that for corn-stalks and epoxy composites.

Advantages of natural fibers such as recyclability, low cost and low density make them feasible as substitutes for glass fibers in composite materials [20]. Anand [21] developed an insulation material composite from banana wastes and binders such as epoxy and waste plastics, and he studied its insulation properties. Preparation of this material consisted of four stages: soaking, drying, grinding and sieving. The resultant fine powder was mixed in different weight ratios with epoxy resin and waste plastic as binders at different concentrations (5 to 20%). Tests showed the banana-epoxy composite was denser than the banana-plastic waste composite. Water absorption

values were in the range 2.430 to 2.961 %; with higher values for the banana-epoxy composite. Thermal conductivity ranged from 0.366 to 0.456 W/m-K for banana-epoxy composite, and from 0.334 to 0.408 W/m-K for banana-waste plastic composite.

Da Rosa, Santor, Lovato, da Rosa, and Güths [22] developed a thermal insulation board for use in solar collector insulation. The researchers made six boards using different percentages of rice husks and sunflower stalks, with gypsum as binder and jute fabric as a design element. The thermal conductivities of the boards ranged from 0.104 to 0.049 W/m-K. One of the boards, which was replaced with a solar collector insulator made from glass wool, gave a similar performance.

Damfeu, Meukam, and Jannot [23] studied the thermal conductivity of several natural plant fibers: kapok fibers, groundnut shell fibers, rattan fibers and coconut fibers. Thermal effusivity was estimated using the asymmetrical hot plate method, and specific heat capacity measured using a differential scanning calorimeter. Thermal conductivity was derived from these measurements and compared with a direct measurement of thermal conductivity using a radial flux flow method. Good agreement between the obtained results and literature values validated the developed radial flow method. The thermal conductivity of the kapok fibers, groundnut shell fibers, rattan fibers and coconut fibers were found to be 0.045 W/m-K, 0.055 W/m-K, 0.093 W/m-K and 0.072 W/m-K, respectively.

Binici and Aksogan [24] mixed different concentrations of pumice, fly ash, perlite, barite, cement and gypsum with onion skin and peanut, and studied the properties of the prepared composites, including thermal conductivity ultrasonic sound penetration coefficient, radioactive relative permeability, specific gravity, water absorption, and flexural and compressive strength. Composites containing pumice and

perlite were observed to have lower thermal conductivity. It was noted that composites with onion skin and peanut had thermal conductivity coefficients 3.5 to 5 times smaller than that of control samples.

Limam, Zerizer, Quenard, Sallee, and Chenak [25] performed an experimental study on corkwood and its composites, measuring thermal conductivity, thermal resistance, specific heat and thermal diffusivity. The samples were prepared by sandwiching cork between two wooden plates. The thermal conductivity of symmetrical and asymmetrical sandwich structures were 0.068 and 0.0656 W/m-K, respectively, and cork thermal conductivity was 0.041 W/m-K. In addition, the researchers studied the impact of moisture on the thermal properties of wood and cork.

Makul and Sua-iam [26] examined the feasibility of replacing Portland cement with incinerated sugarcane filter (ISF) cake, in proportions from 0 to 20% in lightweight foamed concrete. It was found that, as ISF increased, thermal conductivity of the mixture decreased from 0.878 W/m-K to 0.718 W/m-K.

Hamada, Hashim, and Sharif [27] studied the chemical composition of three different date pits planted in the UAE. Date pits were found to contain six ingredients: neutral detergent fiber, acid detergent fiber, ash, crude protein, crude fat and moisture.

Oushabi, Sair, Abboud, Tanane, and Bouari [28] investigated the opportunity of using date palm waste as an insulation material in refrigeration and air conditioning. Seven date palm varieties were collected: Khalt, Boufeggous, Bu-Slikhen, Mejhoul, Admou, Khalt Zhar and Tazaout. The Boufeggous varieties showed a moisture content of 3 to 5 %, a tensile strength of 253.48 MPa, a modulus of elasticity of 4.41 GPa and a thermal conductivity of 0.041 W/mK. Scanning electron microscopy (SEM) showed that the fibers had a cylindrical shape and contained microfibers in parallel assembly.

Energy dispersive spectroscopy showed that the external part of the fibers consisted mainly of oxygen and carbon, with impurities such as iron oxide, chromium oxide, nickel oxide and silicon oxide.

Alami [29] added DPP and olive husk to masonry bricks. It was noted that clay with DPP had higher toughness than clay mixed with olive husk. Alsewailem and Binkhder [30] added DPP to high-density polyethylene (HDPE) and polystyrene (PS) matrices, and studied their mechanical and thermal properties. While HDPE tensile strength was not affected by the addition of DPP, PS tensile strength reduced with increasing filler content. However, the authors did not obtain thermal conductivity, compression strength or water retention measurements.

Abu-Jdayil and Mourad [31] examined the thermal properties of composites prepared from DPP and polyester resin for use as a thermal insulator in the construction industry. The thermal conductivity of DPP-polyester composites containing 60 vol. % DPP was measured between 0.166 and 0.170 W/mK in the temperature range 0 to 60 °C.

1.3.2 Plastics and rubber waste

Plastic materials are low cost, low density and lightweight, as well exhibiting as good durability and processability. Because of these properties they are used widely in many industrial sectors, including thermal and acoustic insulation [32]. Ruiz-Herrero et al. [33] prepared samples from concrete and electrical wire plastic waste and studied its thermal and mechanical properties. It was reported that the mechanical strength, density and thermal conductivity of the samples decreased with increasing plastic waste content.

Pantnaik, Mvubu, Muniyasamy, Botha, and Anandjiwala [34] studied the thermal and acoustic properties of waste wool and recycled polyester fibers. As supplies of waste wool were limited, it was mixed with recycled polyethylene terephthalate (RPET) fibers. Two waste wool fibers were used: coring wool (CW) and dooper wool (DW). Two non-woven mats were made from these fibers and a third mat from RPET fibers. All manufactured samples displayed good acoustic absorption and thermal insulation properties, with the RPET sample showing the lowest acoustic coefficient ($\alpha = 0.61$) in a frequency range of 50 to 5700 Hz. The CW sample showed the lowest thermal conductivity coefficient (0.032 W/mK). In addition, water absorption was measured in the range 4 to 6 %. [35].

Automobile old tires are a major source of global pollution. Disposal of these tires is a serious environmental concern as the waste is not biodegradable and may result in an environmental hazard. One solution is to recycle the waste tire rubber in the construction industry. This would not only solve the disposal problem, but would also help to address shortages of natural mineral resources. Much research has focused on utilizing automobile old tires in construction, concrete and cementitious composites.

Van de Lindt, Carraro, Heyliger, and Choi [36] found that the addition of fly ash and scrap tire fiber to the fiberglass insulation used in residential construction increased the thermal efficiency of light-framed residential structures.

Catalytic polymerization of ethylene was used by Sulcis, Lotti, Coiai, Ciardelli, and Passaglia [37] to prepare composites made from HDPE matrix and powdered rubber. Piszczyk, Hejna, Formela, Danowska, and Strankowski [38] investigated the structural, mechanical and thermal properties of flexible polyurethane and ground tire

rubber foams and reported that the addition of tire rubber increased the thermal stability of the composite.

Abu-Jdayil, Mourad, and Hussain [39] used different proportions of waste rubber (0 to 40 vol. %) to develop rubber-polyester thermal insulator composites. The results showed that adding higher concentration of waste rubber had a positive effect on the thermal conductivity and density of the composite. The composites displayed low thermal conductivity which varied between 0.144 and 0.113 W/m-K, and a very low water retention (< 2.0 %).

In the second part of their study, Abu-Jdayil, Mourad, and Hussain [40] investigated the mechanical performance of rubber-polyester composites. They reported that compressive and tensile strengths were reduced due to poor compatibility between the hydrophobic filler and the hydrophilic polymer. In addition, they found that increasing the size of rubber particles induced the formation of voids in the matrix, which reduced its mechanical properties. The lowest yielding stress value using small rubber particles (less than 0.8 mm) was found to be 18.7 MPa, while the lowest yielding stress value using larger rubber particles (0.8 mm to 2.0 mm) was 8.2 MPa.

Two model rooms were built by Yesilata, Bulut, and Turgut [41] to investigate the effect of adding scrap tire rubber to concrete. The first model was built using conventional concrete; the other with concrete containing scrap rubber. Addition of scrap-tire rubber resulted in an 11 % improvement in thermal protection and a 12 % enhancement in thermal comfort.

Herrero, Mayor, and Hernández-Olivares [42] added three different sizes of crumbed tire rubber (0 to 0.6 mm, 0.5 to 2.5 mm and 2.5 to 4 mm) into plaster test

pieces in proportions varying from 30 to 60 %. They reported that addition of rubber improved density, thermal insulation and acoustic insulation, but decreased the bending and compressive strength. In addition, they noted that a smaller rubber size improved these properties in the composite.

In a study by Eiras et al. [43], natural sand replaced by crumbed rubber in a cement composite and an air-entraining agent was applied to ensure a cellular structure in the composite. As the proportion of rubber increased, the thermal conductivity decreased—the authors related this to the difference in thermal conductivity between the crumbed rubber and the aggregate. The compression strength of the composite ranged from 1 to 10 MPa, which is within the minimum requirements of mechanical strength for masonry units.

Rincon et al.[44] investigated the effect of replacing the conventional drainage layer in green roofs, usually made from pozzolana, with a drainage layer made from recycled tire rubber. The environmental impact of the four constructive systems was compared using Life Cycle Assessment. Replacing the drainage layer resulted in a 13 % reduction in energy consumption for the insulated roof.

Benazzouk, Douzane, Mezreb, Laidoudi, and Quéneudec [45] used a dry state transient plane source technique to investigate the thermal conductivity of a lightweight construction material developed by replacing part of the cement content (10 to 50%) with tire rubber particles. The researchers used an auto-homogenization model to relate the thermal conductivity of the produced composite to the dry unit weight. The thermal conductivity, compressive strength and flexural strength of the composite with 50 vol. % rubber were found to be 0.47 W/m-K, 10.5 MPa and 3.25 MPa, respectively.

Oktay, Yumrutaş, and Akpolat [46] observed that addition of rubber aggregate in proportions varying from 10 to 50 % to a cement composite reduced the thermal conductivity and diffusivity of the composite by 82 % and 74 %, respectively. However, the rubber aggregate had a negative effect on the mechanical properties. A rise in porosity was thought to be the cause of the improvement in thermal conductivity.

Normbuena-Contreras, Silva-Robles, Gonzalez-Torre, and Saravia-Montero [47] developed a membrane from recycled tire rubber powder for use in the building industry. Environmental factors such as climatic conditions tend to reduce the mechanical strength and durability over time. To combat this, the researchers added recycled HDPE in proportions of 0 to 70 %. The HDPE increased the thermal conductivity of the developed material but with a low heat transfer ability. Overall, the developed material was found suitable for thermal facing purposes.

Schiavoni, D'Aessandro, Bianchi, and Asdrubali [48] reviewed insulation materials for the construction sector. The researchers reported that recycled tire rubber used to develop innovative materials performed well—the best performance characterized by a dynamic stiffness of 61 MN/m^3 and an impact sound insulation of 26 dB. In addition, they reported that the thermal conductivity of commercial materials developed from recycled rubber ranged from 0.100 W/m-K to 0.14 W/m-K .

In a study by Mujal-Rosas, Marin-Genesca, Orrit-Prat, Rahhali, and Colom-Fajula [49], tire dust was mixed with HDPE in a range of proportions (0 %, 5 %, 10 %, 20 %, 40 %, 50 % and 70 %). The authors reported that the addition of tire dust in proportions between 10 and 15% did not affect the initial polymer microstructure;

consequently, dielectric, mechanical and thermal properties were maintained within an acceptable range.

Some researchers have worked on developing methods to devulcanize tire rubber before use. Rubber devulcanization is defined as the process of modifying the rubber structure by breaking the sulfur bonds between the rubber chains. There are three commonly-used technologies to devulcanize the rubber: supercritical fluid, ultrasonic waves and biological methods [50].

Kojima et al. [51] introduced the supercritical devulcanization technology by which supercritical carbon dioxide is used as a reaction medium for some devulcanization agents. Carbon dioxide is used because its critical point (at 31.1 °C and 7.38 MPa) can be achieved easily.

Ultrasonic devulcanization, invented by Isayev, Chen, and Tukachinsky [52], needs a continuous source of energy, but it has its advantages—the process is performed without chemicals, takes only several seconds to work, and is suitable for bulk treatments.

Biological devulcanization, reported by Romine and Romine [53], employs microorganisms with the ability to metabolize the sulfur in the rubber matrix. This method of devulcanization requires relatively low energy; however, it is limited to the surface and has low reaction yield.

Mangili et al. [50] investigated the best operational parameters for these three methods of devulcanization. The devulcanization methods were applied to ground tire rubber, then the devulcanized rubber mixed at a ratio of 10 parts per hundred with

natural rubber and tested. The researchers reported that ultrasonic devulcanization was the most effective method in terms of controlling and studying the rubber's properties.

In a study by Mangili, Collina, Anzano, Pitea, and Lasagni [54], the researchers used diphenyl disulfide as a devulcanization agent in the supercritical carbon dioxide process. The use of diphenyl disulfide increased the elongation at the break in the sulfur crosslink network and decreased the modulus.

Liu et al.[55] devulcanized tire rubber using supercritical carbon dioxide and constructed a second-level full factorial set of experiments to determine the relative effects of reaction temperature, reaction pressure, time and diphenyl disulfide agent. The researchers concluded that diphenyl disulfide treatment had the greatest effect on the devulcanization process.

In Shi et al. [56], the researchers applied four devulcanization methods to ground tire rubber: low-temperature shear reclamation, high temperature shear reclamation, twine-screw extruder reclamation and supercritical carbon dioxide reclamation. This study recommended that tire rubber devulcanization should be performed in an oxygen-free medium, with low shear force and at low temperature.

De Sousa, Scuracchio, Hu, and Hoppe [57] worked on relating chemical modification, flow and thermo-oxidative degradation behavior to the exposure time of round tire rubber irradiated with microwaves. It was noted that the final temperature was the most important factor in devulcanization. They also reported that a longer exposure was needed to achieve a high degree of devulcanization.

Aoudia et al. [58] compared two kinds of composites developed from ground tire rubber, devulcanized ground tire rubber and thermoset resin. The researchers used

ultrasonic devulcanization to devulcanize the tire rubber. They concluded that devulcanization of the rubber had a positive effect on the mechanical properties. This finding was confirmed by SEM images which showed improved coherence between the devulcanized ground tire rubber and the resin.

Piszczyk, Hejna, Formela, Danowska, and Strankowski [59] modified foamed polyurethane with the addition of two types of tire rubber, ground tire rubber and reclaimed ground tire rubber. A significant improvement in the thermal stability and compressive strength resulted from the addition of tire ground rubber.

In a study by Punnarak, Tantayanon, and Tangpasuthadol [60], reclaimed ground tire rubber was blended with HDPE to investigate the effect of blend ratios, method of vulcanization and the addition of compatibilizer on the properties of the composite. It was noted that increasing the rubber component in the blend increased impact strength, but weakened the tensile strength.

Impact strength in a rubber-polypropylene composite was studied by Tantayanon and Juikham [61]. The researchers found that the addition of reclaimed rubber significantly increased impact strength. The improvement was explained by the action of the reclaimed rubber in penetrating the polymer matrix.

Hassan, Aly, Aal, El-Masry, and Fathy [62] mixed DVR with HDPE during exposure to gamma radiation (dosages of 25, 50, 100 and 125 kGy) and at different feed rates to investigate the effect of these two parameters on the tensile strength, elongation at break and hardness of the composite.

Ground tire rubber and devulcanized ground tire rubber were added to foamed polyurethane by Zhang, Lu, Tian, Li, and Lu [63] to study the effect of

mechanochemical devulcanization on the acoustic absorption of the composites. Damping properties, acoustic absorption and cell morphology were improved by devulcanization of flexible chains in the rubber.

1.3.3 Buffing dust waste

Leather production processes create large amounts of waste worldwide, adding to environmental pollution. In leather production, just 20 % of the raw material weight is converted to final product [9]. In fact, 35 to 40% of the tannery solid waste is BD and chrome shavings, with landfill and incineration the two most common disposal methods. Other statistics reveal that 2 to 6 kg of buffing waste is produced for every ton of leather processing. For example, Indian tanneries produce around 600 000 tons of leather annually, which results in 36 million kg of BD waste a year [64]. Landfill causes soil pollution, while incineration generates serious air pollution through the emission of sulfur oxide and nitrogen oxide gases [65]. Researchers are trying to develop new methods to dispose of these wastes safely. Their efforts are focused on various areas, including activated carbon production and recycling the waste as a filler in different kinds of rubber and building materials.

Sekaran, Shanmugasundaram, and Mariappan [64] suggested a method to produce activated carbon from BD, using 6.24 mg/g BD at 3.5 pH, dye concentration of 6.25 mg/L and an activation temperature of 800 °C. The adsorption capacity of the activated carbon produced was comparable with available commercial products used in wastewater treatment.

Yılmaz, Kantarli, Yuksel, Saglam, and Yanik [66] pyrolyzed chromium-tanned shaving, vegetable-tanned shavings and BD and found that carbon residue yields were

suitable for generation of activated carbon. The carbonaceous residue (char) was activated by carbon dioxide in order to produce the activated carbon. The research indicated that BD gave the highest yield of oil (23%) and that the chromium-tanned activated carbon may be used as an adsorbent in aqueous solution.

In a study by Chrońska-Olszewska and Przepiórkowska [67], chrome shavings and BD were mixed with nitrile rubber to produce a collagen-elastomer material. The addition of these two fillers reduced the vulcanization time due to changes in viscosity.

Garcia et al. [68] manufactured a new foam composite by mixing natural rubber with leather waste in proportions varying from 0 to 60 %. This study found that increasing the leather dust content affected the structural and mechanical properties of the cell, hence improving the tensile strength and stiffness of the composite.

El-Sabbagh and Mohamed [69] treated chrome-tanned leather waste with ammonia and sodium solutions, then blended it with acrylonitrile butadiene rubber. They reported that the addition of the treated filler enhanced the mechanical properties of the composite, including tensile strength, tensile modulus, elongation, hardness and stiffness. Moreover, its addition enhanced thermal stability and aging coefficient.

In a similar study [70], BD was mixed with carboxylated butadiene rubber and acrylonitrile butadiene rubber, but without any treatment. Similar results to El-Sabbagh and Mohamed [69] were obtained; in addition, the researchers noted an improvement in the electrical insulation properties of the composite.

Ferreira, Freitas, and Almeida [71] investigated the effect of adding footwear leather fiber waste to styrene butadiene rubber and acrylonitrile rubber. Compression moulding was used to vulcanized the mixture and form the composite. The study

showed that an addition of 10 to 20 parts per hundred enhanced the tear strength and caused an acceptable reduction in tensile strength and elongation.

In a study by Andreopoulos and Tarantili [72], waste leather was used as a filler in poly(vinyl chloride). The authors reported that addition of the filler had a positive effect on density, wear resistance and hardness, but also adversely affected tensile strength.

Murugan, Swarnalatha, and Sekaran [73] aimed to produce microfiber carbon from tannery solid waste by pyrolysis of chromium-tanned BD. The study characterized the treated BD by XRD, SEM, FTIR and TGA. The treated BD was found suitable for use in pavement building materials.

Bitlisli and Karacaki [74] added fleshings and vegetable shaving waste to clay in proportions of 1 %, 3 %, 5 % and 10 % to study the possibility of producing a porous brick. Increasing the filler proportion reduced density, thermal conductivity and compressive strength. The authors recommended adding 5 % of the filler only, to maintain suitable properties within the developed material.

Lakraflı, Tahiri, A. Albizane, and El Otmani [75] studied the effect of adding two industrial leather solid wastes (chrome shavings and BD) to cement and plaster materials. The composite produced from the addition of 5 % waste had superior thermal conductivity, with the thermal conductivity of the BD and chrome shaving composites reduced by 84.6 % and 54.5 %, respectively. However, introduction of these wastes caused a huge drop in the mechanical properties, prompting the researchers to use the two wastes as a separation material in cement/sand panels and

plasterboards. In this use, the addition of chrome shavings and BD reduced the thermal conductivity of the boards by 55 % and 66 %, respectively.

In another part of their study [76], these researchers examined the use of wet-blue chrome shavings, BD, wood shavings and sawdust as fillers in insulation materials. In addition, they examined the effect of moisture content on the thermal conductivity of the materials. The research showed that thermal conductivity increased with the moisture content, and that the materials had low thermal conductivities, which would enable these materials to compete with commercially-available thermal insulators.

1.3.4 Chemical treatments

A principal component in natural fibers is cellulose. Natural fibers are hydrophilic because of the presence of the hydroxyl group ($-\text{OH}$) in cellulose, whereas many polymers are hydrophobic. This difference explains the poor compatibility and interference that occurs when polar natural fibers are mixed with non-polar polymers [77]. Moreover, fibers tend to agglomerate into bundles as hydrogen bonds form between the fibers [78, 79]. However, natural fibers have many advantages such as low density, low cost and high recyclability. Many researchers are focused on treatments of natural fibers to render them effective as reinforcement fibers in a composite material.

Chemical coupling agents may be used to enhance natural-fiber polymer composites (NFPCs). The coupling agent reacts with the hydroxyl group and the functional group of the matrix.

Alkaline solutions may disrupt hydrogen bonding to increase the roughness of the composite and surface interlocking. Alkaline treatment also increases the tensile strength and modulus of flax-epoxy composites by 40 % [80]. Vallo, Kenny, Vazquez, and Cyrus [81] exposed sisal fibers to alkaline solution and studied the effect of immersion time on the mechanical properties of the developed sisal-starch composite. The researchers reported 24 hours as the optimal immersion time, as this period resulted in an improvement in mechanical properties without damage to the fiber. Joseph, Thomas, and Pavithran [82] stated that a 4 % concentration of NaOH produced the highest mechanical strength when this treatment was applied to sisal fiber.

Acetylation treatments reduce the hydrophilic behavior of the fiber and modify the properties of the polymer so it becomes more hydrophobic. This results in much higher roughness and higher mechanical properties. Nair, Thomas, and Groeninckx [83] investigated the thermomechanical and thermogravimetric properties of sisal-PS composites. The researchers performed benzoylation, PS maleic anhydride (PSMA) and acetylation treatments on the prepared composite. They reported that acetylation treatment resulted in a very rough composite surface and enhanced the thermal stability of the composite. Benzoyl chloride is the most commonly used benzoylation treatment. This type of treatment reduces the hydrophilic behavior, and improves the matrix and thermal stability. The process requires alkaline pretreatment to activate the hydroxyl group [83].

Maleated coupling agents such as maleic anhydride modify fibers or filler surfaces. Mohanty, Nayak, Verma, and Tripathy [84] studied variations in fiber length, maleic anhydride grafted polypropylene (MAPP) concentration, time of MAPP

treatment and filler percentage on a jute–PP composite. The researchers reported that the treatment increases the flexural strength of the composite by 72.3 %.

Silane has bi-functional groups which may react with polymer and fiber to make a bridge between them. Direct mixing of silane and thermoplastic results in enhancement of adherence properties due to intermolecular entanglement or acid-base interactions. There are many types of silanes. with amino-silanes the most commonly reported in the literature. Vinyl-silanes and acryl-silanes, which need peroxide initiators, can form a covalent bond between fiber and polymer matrix. Azidosilanes are able to join inorganic fibers to thermoplastic matrix effectively, but their use is rarely discussed in the literature [85].

Silane treatment reduces the number of hydroxyl groups. In the presence of moisture, hydroxylable alkoxy groups form silanols, which react with hydroxyl groups to establish covalent bonds to the wall. In a study by Valadez-Gonzalez, Cervantes-Uc, Olayo, and Herrera-Franco [86], the researchers applied alkaline and silane to HDPE-henequén composites. They found that the composites prepared from silane-treated fibers gave higher tensile properties than those prepared from fibers treated with alkaline.

Direct mixing of silanes has a limited effect in the absence of covalent bonds. Treatment of fibers with amino-silanes enhances matrix properties due to acid-base interaction, especially if the composite has basic characteristics such as a PS matrix. Silanes with phenyl, phenylamino, amino or octadecyl show stronger acid-base interactions than other silanes [87]. Matuana, Woodhams, Balatinecz, and Park [87] focused on studying the acid-base interaction between the chemical treatment and the neutral fiber. They found that interaction between acidic PVC and treated fiber with

basic aminopropyltriethoxysilane (APS) increased the tensile strength by 36 %. However, when the same treatment is applied to fibers with PS matrix, the tensile strength increased only by 6 %.

A second result of a previously mentioned study [85] is that silane treatments generally have a limited effect on the properties of thermoplastic composites due to the absence of any reactive group in thermoplastic resins. For this reason, some researchers have focused on grafting by free radical grafting or plasma discharge. They have either grafted silane to the polymer to produce a copolymer or treated the fiber in the solution and initiated the grafting while heating at the production stage [85].

The most reported application is to graft with vinyltriethoxysilane (VTS) and maleic anhydride using benzoyl peroxide and dicumyl peroxide (Di-Cup[®]) as initiators. When the initiators decompose, hydrogen is extracted from the backbone of the thermoplastic and added to the double bond of the silane. It is reported that VTS grafting to polypropylene gives better results than maleic anhydride in terms of interfacial adhesion between the polypropylene matrix and the wood flour fiber. VTS grafting also gives 47 % higher tensile strength and 35 % lower water retention [88]. In two similar studies, VTS-treated wood grafted with polyethylene using Di-Cup[®] as initiator significantly increased the flexural strength and doubled the impact strength [89, 90]. Treatments of wood fibers using VTS or maleic anhydride with Di-Cup[®] with a low-density polyethylene composite increased the tensile strength by 62 %. However, it did not have an important effect on a PS composite [91]. The grafting effect of vinylsilanes depends on the type of thermoplastic matrix; hence, a good match between the silane treatment and the polymer is important.

Hydrolyzed azidosilanes form reactive silanols, which can react or condense with fibers. When heat is applied to an azidosilane, azide decomposes to a reactive intermediate, nitrene, and nitrogen. The nitrene then reacts with any CH bond in the thermoplastic. The required temperature for this to occur is 200 °C [92]. McFarren, Sanderson, and Schappell [93] used azidosilanes to treat mineral fillers mixed with polyolefins and polystyrene. The chemical treatment significantly improved tensile, flexural and heat distortion properties.

Maldas, Kokta, and Daneault [94] added wood fiber to PS in varying proportions and characterized the mechanical properties of the composite produced. They optimized the compression moulding conditions and applied various chemical treatments such as polyphenyl isocyanate and silanes. Isocyanate improved the adhesion and reduced the hydrophilic nature of the fiber. Isocyanate was also found to be more beneficial than silane to the mechanical properties of the composite.

Nair, Thomas, and Groeninckx [83] studied the aging effect of sisal-PS matrix with different chemical treatments, including benzylation, triethoxyoctylsilane, silane, methyltriethoxysilane, toluene diisocyanate, and PSMA. All treatments reduced the water absorption of the composite. The same study showed that all treatments improved the tensile strength by about 10 %.

Alam, Arif, and Shariq [95] developed a nanocomposite by mixing pure PS with zinc oxide (ZnO) nanoparticles. They studied the effect of concentration of ZnO nanoparticles and stirring speeds on tensile and flexural strength. Taguchi's statistical analysis showed that the composite was affected by concentration. The results showed the addition of 0.3 wt. % ZnO and 1200 rpm stirring increased tensile strength by 73.99 %.

Studies show that grafting gives better results than direct mixing. Most studies using grafting were done using silica. When nanoparticles were added to a polymer matrix, crosslinking could enhance properties. Vergnat, Roland, Pourroy, and Masson [96] prepared titanium dioxide (TiO_2)-PS composites by two methods, direct mixing or grafting. With the grafting method, the researchers used 2-bromo-2-methyl-propionic acid and 11-phosphono-undecyl ester as initiators and TiO_2 to produce a Ti-O-P bridge, which forms a covalent bond between the nanoparticle and the polymer. Nano-indentation was used to study the differences in mechanical properties. Grafting TiO_2 to PS resulted in longer polymer chains, which enhances a load transfer mechanism. Grafting 10 vol. % TiO_2 reduced the depth and modulus by 50 % and 40 %, respectively. In addition, it increased hardness and strength from 65 MPa to 78 MPa.

Chapter 2: Materials and Research Methods

2.1 Materials

2.1.1 Polystyrene

The PS used in this research was provided by a national polystyrene packaging factory in Dubai, UAE. This factory supplies PS for building construction, civil engineering, floatation, thermal insulation, architectural design, packaging and horticulture. The expanded diameter size of the PS beads was 950 μm (Fig. 2).



Fig. 2: PS beads

This polymer is inexpensive, with low water retention and superior insulation properties. PS boards are used heavily in the building sector, especially in hot climate countries such as the UAE. It has a very low thermal conductivity compared to other building materials; the thermal conductivity of this polymer is 0.036 W/m-K [97].

2.1.2 Date pit powder

The DPP used in this study was obtained from the UAE University farm in Al Foha, UAE. Date pits were crushed using a commercial milling machine and then sieved. Only DPP particles less than 300 μm in size were used to produce the composites. The particle size distribution of the DPP is shown in Fig. 3.

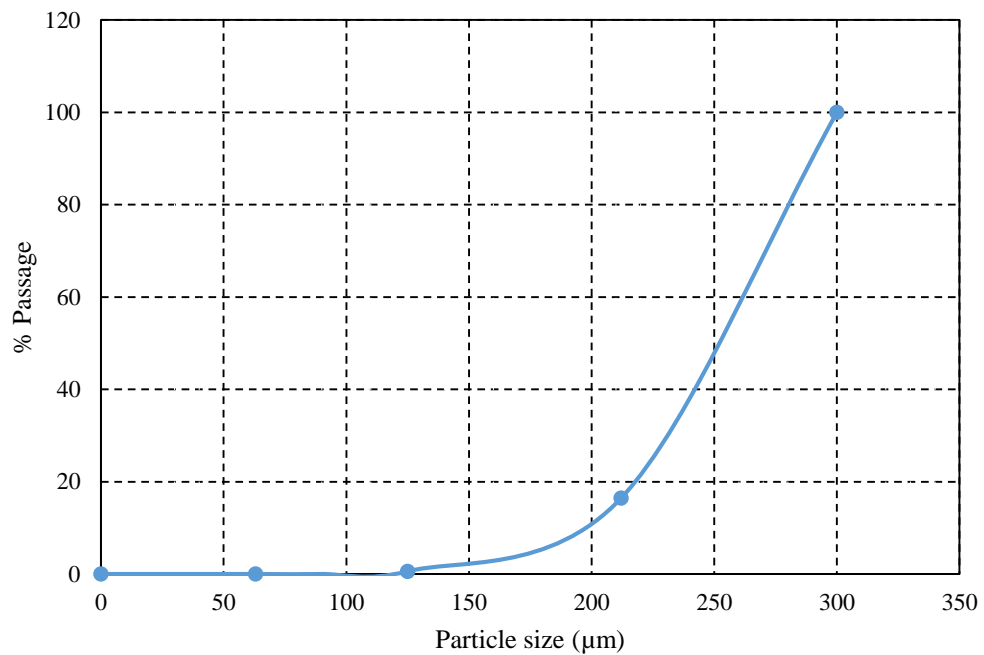


Fig. 3: DPP particle size distribution

The DPP waste used in this research is widely available in the UAE, with many facilities producing this waste, including the Al Barakah Dates factory, Emirates Dates factory and Sharjah Dates factory.

2.1.3 Devulcanized rubber

With the number of motor vehicles increasing worldwide, environmental problems related to the car are on the rise. Today, some recycling companies process used car tires. Some recyclers grind the tire rubber into small particles and sell it, others

devulcanize the rubber after grinding it. The DVR used in this research was sourced from Gulf Rubber Factory LLC in Al Ain, UAE. This kind of rubber is difficult to separate (Fig. 4), so no sieving analysis for this filler was conducted.



Fig. 4: DVR

Tire rubber was selected for this research because it is a non-degradable waste available in huge quantities in the UAE. Disposal of this waste is also a major concern globally. Furthermore, it has been reported that DVR coheres more readily with polymers than ground rubber [58].

2.1.4 Buffing dust

Leather production is a growing industry in the UAE. The BD used in this study was sourced from Al Khaznah Tannery in Abu Dhabi, UAE. The BD was provided in

the form of compressed cylinders (Fig. 5). The cylinders were cut by hands into small pieces, ground using a commercial grinder, and then sieved. The BD particles used to produce the composites were less than 300 μm in diameter; the particle size distribution is shown in Fig. 6.



Fig. 5: BD cylinders

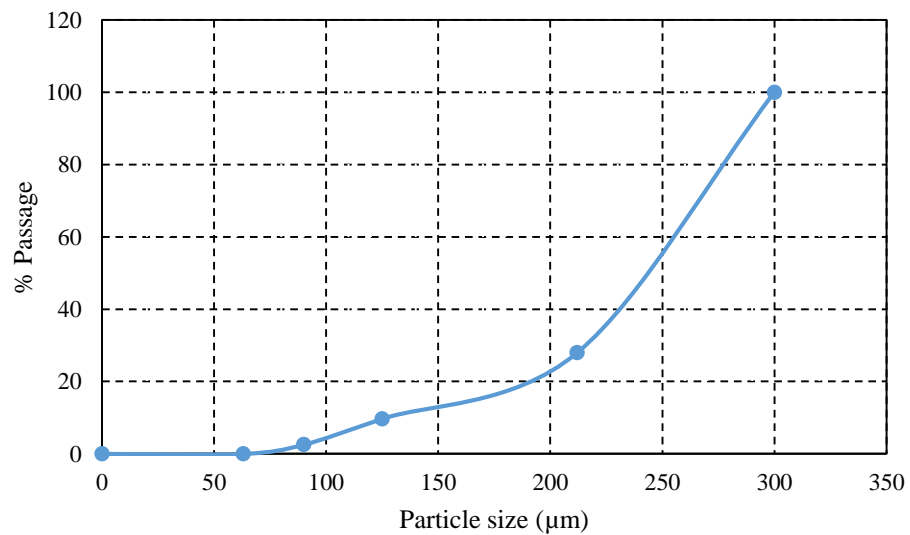


Fig. 6: BD particle size distribution

This waste was selected in order to recycle a leather tannery waste. Tannery wastes are divided into five categories: tanned splits, shaving and trimming, dyed/finished waste and BD [98]. The thermal conductivity of tannery waste is very low and some researchers have sought to develop new building materials utilizing it [73, 75, 76].

2.2 Moulds and Composite Fraction

2.2.1 Moulds

In this research, different sample shapes were needed for different physical, chemical and mechanical tests. To that aim, different moulds were fabricated from stainless steel according to the ASTM standard for each test. Al Safa Engineering Workshop in Al Ain, UAE, provided the required moulds (Fig. 7).

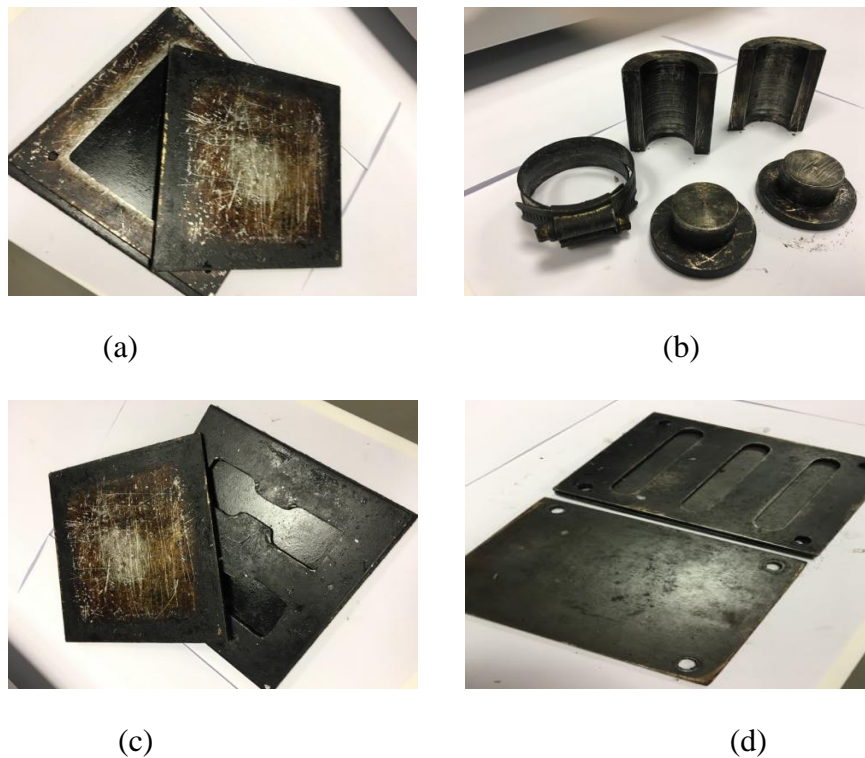


Fig. 7: Moulds for (a) thermal conductivity measurements; (b) compression strength and water retention measurements; (c) tensile strength measurements; (d) flexural strength measurements

2.2.2 Composites

To produce the DPP-polystyrene, DVR-PS and BD-PS composites, the three fillers were added to PS and the resulting materials were heated and compressed. Filler powder at various weight percentages was manually mixed with PS and poured into the appropriate steel mould. To prevent the specimens from sticking to the mould, it was sprayed with a mould release agent. For the compression samples, the heating cycle, which was chosen to minimize the size and number of voids, consists of two segments with different parameters: (1) a pressure of 500 kg at 180 °C for 20 minutes; and (2) 500 kg force at 125 °C for 20 minutes. The second segment was added to prevent the mould from opening due to the formation of hot gases inside the mould. For all other samples, only the first segment was applied (i.e., a pressure of 500 kg at 180 °C for 20 minutes). The produced samples were used for different mechanical and thermal tests. The samples were labelled using the abbreviation *<filler weight percentage>-<filler name>* For example, '10-DPP sample' is a sample in which 10 wt. % of the sample weight comprises DPP.

2.3 Measurements Methods

2.3.1 Mechanical tests

A universal testing machine (MTS model MH/20) with a load cell capacity of 100 kN was used to determine the compression strength of the produced composite. The test was stopped when the specimen fractured or the load value reduced by 10 % of the maximum load; otherwise, the test was stopped manually when a specific contraction value was reached. The dimensions of a specimen for the compression test measure 30 mm in both length and diameter (Fig. 8 (a)). All compression tests were

performed at room temperature with an overhead speed of 1 mm/min, in accordance with ASTM D 695-15 standard [99].

The same machine was used to determine the tensile strength of the produced composite. Samples were installed between the fixed and movable jaws. All tests ended when the specimen fractured. The dumbbell-shaped sample dimensions were: overall length 100 mm, gauge length 20 mm, and thickness 4 mm (Fig. 8 (b)). All tensile tests were performed at room temperature with a 2 mm/min overhead speed, in accordance with ASTM D638-14 standard [100].

The flexural strength of composites was measured using the same machine with a load cell capacity of 5 kN. The dimensions of the flexural sample were: 80 mm long, 14 mm wide and 4 mm thick (Fig. 8 (c)). Samples were measured using a three-point bending test at an overhead speed of 2 mm/min, in accordance with ASTM D 790-02 [101]. All tests were conducted at room temperature and stopped when the sample fractured.

For all tests, the results of three samples for each filler content percentage were averaged.



(a)



(b)



(c)

Fig. 8: Prepared samples for (a) compression test; (b) tensile test; (c) flexural test

2.3.2 Structure

In this research, two kinds of microscopy were used, optical microscope and SEM. The optical microscope was used to investigate void size and distribution, while the SEM was used to investigate microstructure and morphology of samples. All samples were coated in gold using gold sputtering before each test. A JEOL SEM (model JCM-5000) was used for these tests. An Olympus DP22 optical microscope was used for the void investigations.

2.3.3 Bulk density

Density is the ratio of the weight to its volume. The weight of the samples was determined up to four significant digits, and the sample volume was determined using a caliper to two significant digits. The pure PS density was measured from the prepared cylindrical samples using the above method. The filler density was determined by finding the weight of a powder sample and dividing it by the volume of the weighted sample. The linear mixing rule was used to calculate the theoretical density of the prepared composites (Equation 1).

$$\rho_{composite} = \left(\frac{w_{matrix}}{\rho_{matrix}} + \frac{w_{filler}}{\rho_{filler}} \right)^{-1} \quad \text{Eq. 1}$$

where $\rho_{composite}$, ρ_{matrix} and ρ_{filler} are the densities of composite, PS and DPP, respectively. In addition, w_{matrix} and w_{filler} are the weight fraction of PS and DPP, DVR and BD.

2.3.4 Thermal conductivity

Samples with dimensions of 110 mm × 110 mm × 3 mm were produced using a special mould, (Fig. 9). The thermal conductivity of each sample was measured using a Lasercomp FOX-200. This instrument employs the steady state method to determine thermal conductivity by measuring the temperature gradient and the input power, in accordance with ASTM C1045-07 [102].



Fig. 9: Prepared sample for thermal conductivity test

2.3.5 Thermogravimetric analysis

Thermogravimetric analysis (TGA) was used to study the change of physical and chemical properties with change of temperature. A Q50 TGA analyzer from TA Instruments was used to perform the thermal analyses. A heating rate of 10 °C/min was used to increase the temperature from 30 °C to 800 °C under a nitrogen flow of 20 mL/min.

2.3.6 IR spectroscopy

FTIR was used to investigate the main functional groups in a material. Shimadzu IR Prestige-21 FTIR spectrometers were used to study the functional groups of treated and untreated DPP, DVR and BD. Initially, 200 mg of potassium bromide (KBr) was mixed with small amount of the studied fillers and pressed into pellets. The pellets were exposed to IR spectra and analyzed over the wavelength range 400 to 4000 cm^{-1} .

2.3.7 Water retention

Cylindrical samples 25 mm in diameter and 15 mm high produced in the designed mould were used in two water retention tests, in accordance with ASTM D570-98 standard [103]. As the samples were less dense than water, each was attached to a heavy weight with plastic string to ensure complete immersion. In the two tests, samples were fully immersed in distilled water at either 25 °C or 50 °C for 24 hours. The samples were removed from the water at frequent intervals during the test period, dried with a dry cloth and weighted to nearest 0.001 g.

Equation 2 was used to find the percentage of water retention (WR %) for the developed composites:

$$WR\% = \frac{\text{weight of equilibrated sample} - \text{weight of dry sample}}{\text{weight of dry sample}} \times 100\% \quad \text{Eq.2}$$

2.4 Chemical treatment

Alkaline treatment is a well-known surface treatment to improve the mechanical properties of polymer composites. For example, alkaline treatment has been used to improve the mechanical properties of natural fiber-polymer and rubber-polymer composites [104], [[105]. In [80] and [81] researchers optimized the immersion time and sodium hydroxide concentration. Firstly, NaOH pellets were dissolved in distilled water to prepare a NaOH solution with 4 wt. % concentration. Three fillers, DPP, DVR and BD, were immersed in the prepared solution for 24 hours. The produced material was then dried in an oven at 90 °C for eight hours and ground with a commercial grinder.

Chapter 3: Results and Discussion

This chapter reports and discusses the results of measurements for compressibility, tensile and flexural strength, density, thermal conductivity, TGA and water retention. Each measured property will be discussed in its own section for the three developed composites: DPP-PS, DVR-PS and BD-PS.

3.1 Mechanical Properties

Different specimens in various shapes were produced according to ASTM standards. A MTS model MH/20 machine was used to determine the mechanical properties of compression, tensile and flexure. Three to five samples were tested at room temperature to measure these properties. The average results of these tests are reported in this section.

3.1.1 Compression properties

3.1.1.1 Date pits

The tested samples were held between two movable flat plates to compress the samples at a strain rate of 2 mm/min. The mean compression yield strength of pure PS was found to be 16 MPa.

Fig. 10 demonstrates the compression behavior of the DPP-PS composites. Initially, the curve was linear up to the first peak before the stress dropped at $< 0.1\%$ strain for all samples, which indicates brittle behavior.

Fig. 11 and Fig. 12 show the effect of the DPP contents on the compression strength and modulus of the composite, respectively. As expected, the compression strength reduced with the filler content. The compression strength reduced to

approximately 9 MPa for the 40-DPP sample. A reduction of 28 % was observed for 10-DPP. However, the compression strength remained almost constant up to 40 wt. % filler before showing a dramatic reduction of 85.7 % for the 50-DPP composite. The same trend was observed for the compression modulus, which was measured to be around 405 MPa for the pure sample. This value was reduced by 12.5% for the 10-DPP sample and remained at an almost constant value of 300 MPa up to 40 wt. % filler. Then, a remarkable reduction of 87 % was observed for the 50-DPP composite.

Fig. 10 shows that the DPP only slightly affects the yielding strain value, with strain percentage values ranging from 0.05 to 0.095 %. The mean values of modulus of compression and yield strength are presented in Table 1. Although the compression strength of the DPP–PS composites reduced with increasing filler content, these values are still higher than those of other composites used in building construction, such as composites comprising cement, sand, and waste fiber (2.4 to 3.3 MPa) [106]. Moreover, the compression strength of the DPP-PS composites was much higher than that of commonly-used commercial insulation materials such as extruded PS foam, which has a compression strength of 0.25 MPa [107].

The observed reduction in the compression properties could be attributed to two factors: poor compatibility between the natural fillers and the matrix; and agglomeration of the natural fillers. Specifically, the hydroxyl groups (–OH) present in natural fillers make them hydrophilic, whereas the polymers are hydrophobic, resulting in poor compatibility [108]. In addition, because of the presence of hydrogen bonds, natural fillers may agglomerate, due to the presence of hydrogen bonds in the filler content [85].

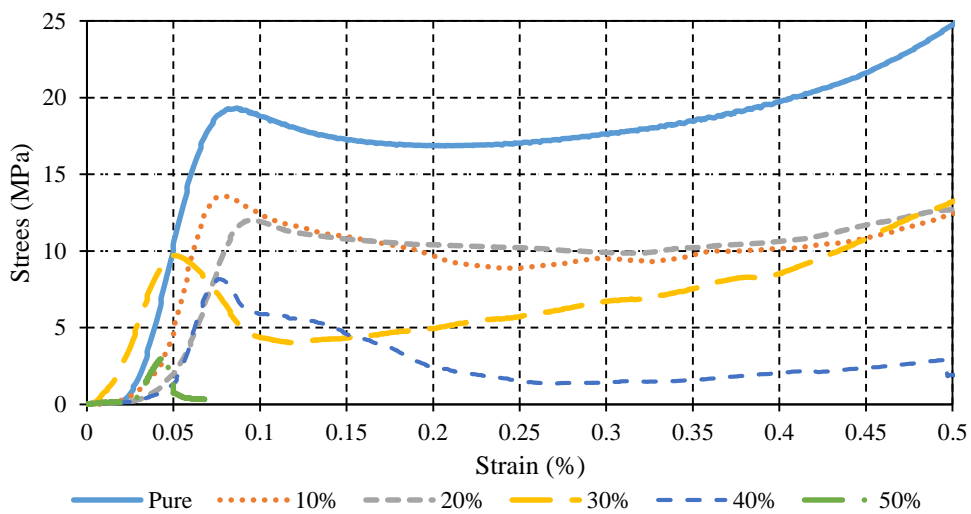


Fig. 10: Stress-strain curve for DPP-PS composites

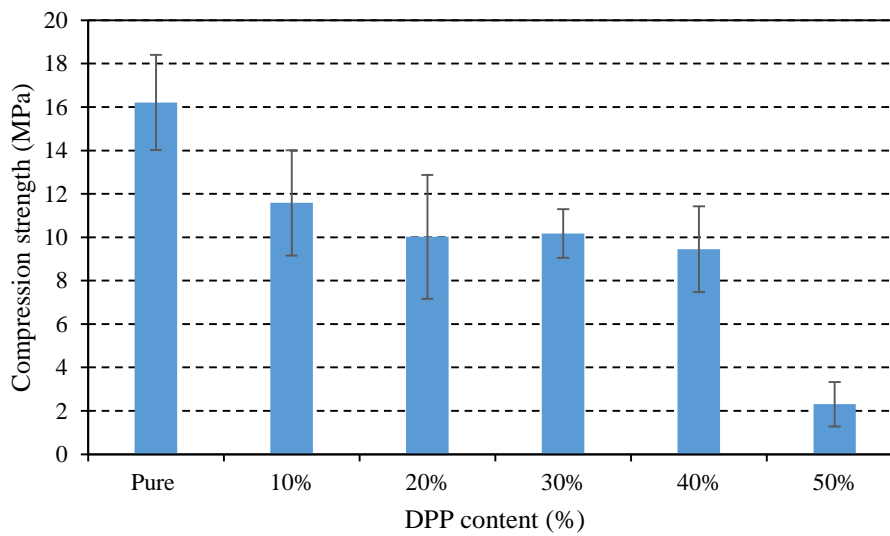


Fig. 11: Compression strength of the DPP-PS composites

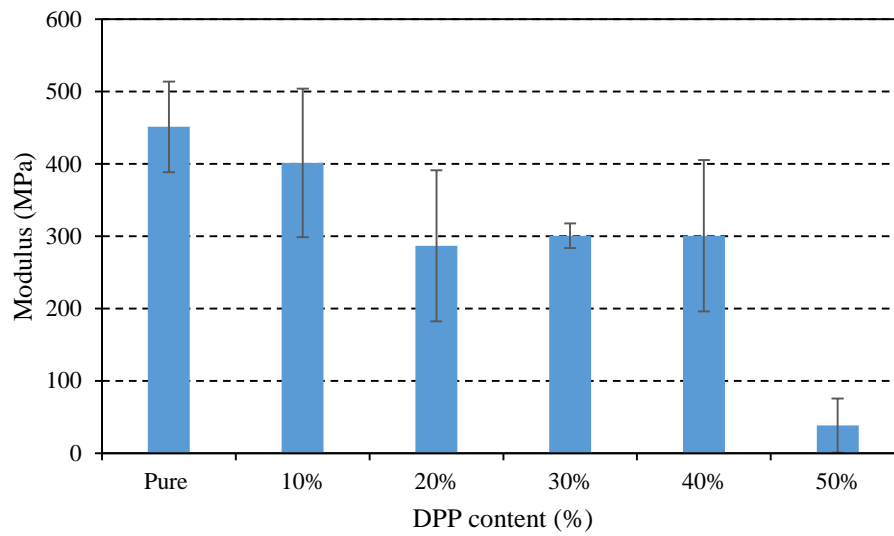


Fig. 12: Compression modulus of the DPP-PS composites

Table 1: Compression properties of the DPP-PS composites

Content	Mean Modulus (MPa)	Mean Yield Strength (MPa)
Pure	451.15 ±62.57	16.21±2.19
10-DPP	401.23±102.74	11.58±2.43
20-DPP	286.62±104.48	10.02±2.86
30-DPP	300.59±17.17	10.17±1.12
40-DPP	300.63±104.71	9.44±1.98
50-DPP	38.23±37.37	2.31±1.03

3.1.1.2 Devulcanized rubber

The compression behavior of the DVR-PS composites is shown in Fig. 13. It can be seen that yielding strain decreased with increasing DVR content. A significant reduction in yielding strain for 10-DVR and 20-DVR samples was observed; however, adding higher DVR content (30 to 50 wt. %) had a minimal effect on the yielding

strain. Furthermore, the yielding strains of the DVR composites were found to be less than 0.05 mm/mm. These low values imply that the composite had a brittle behavior and was not affected significantly by the ductility of the DVR particles. Generally, both compression strength and compression modulus reduced with increasing DVR content. The compression strength of 10-DVR, 20-DVR, 30-DVR, 40-DVR and 50-DVR was lower than the pure PS strength by 28 %, 41.64 %, 53.92 % and 63.4 %, respectively. Abu-Jdayil, Mourad, and Hussain [40] noted that the addition of scrap tire to polyester matrix significantly reduced the compression strength of the composite. They found that the addition of 40 wt. % scrap tire caused a 92 % reduction in the compression strength of the composite. On the other hand, in the current work, the addition of 40 wt. % DVR caused only a 54 % reduction in strength. Furthermore, as Fig. 15 shows, the compression moduli of DVR-PS composites with 0 to 20 wt. % DVR content were almost constant (430 MPa). For higher contents, the compression moduli dropped from 451 MPa for the pure PS to 351, 283 and 175 MPa for the 30-DVR, 40-DVR and 50-DVR composites, respectively. The maximum drop was observed for the 50-DVR composite, wherein the measured compression modulus was 61.2% less than the modulus of the pure matrix. All compression results are listed in Table 2. DVR particles may act as stress concentration points in the prepared composites. In addition, DVR may form a weak interfacial bonds with the PS matrix [109]. These two possible causes could explain the noticed drop in the mechanical properties of the composites. Although the compression strength of the composites declined with increasing DVR, the measured strength was still higher than some building insulation materials (2.4 to 3.3 MPa) [106].

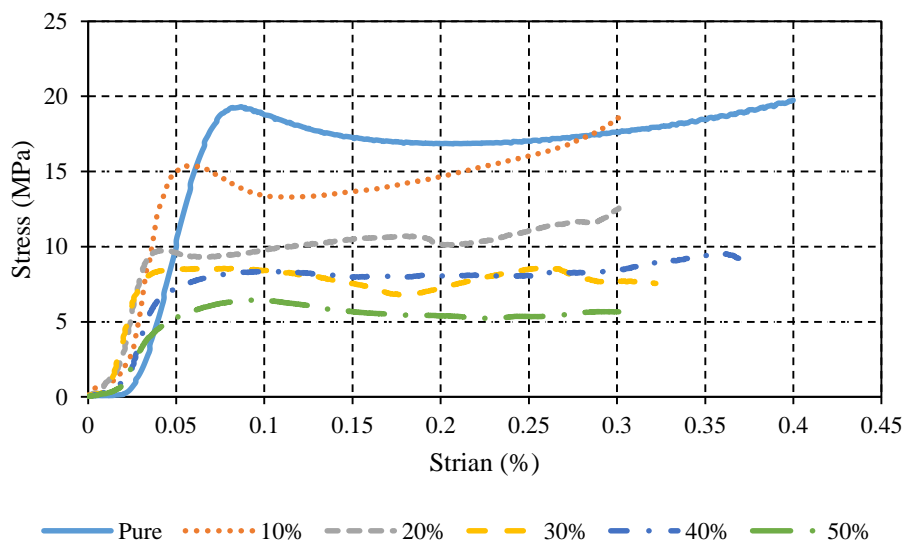


Fig. 13: Stress-strain curve for DVR-PS composites

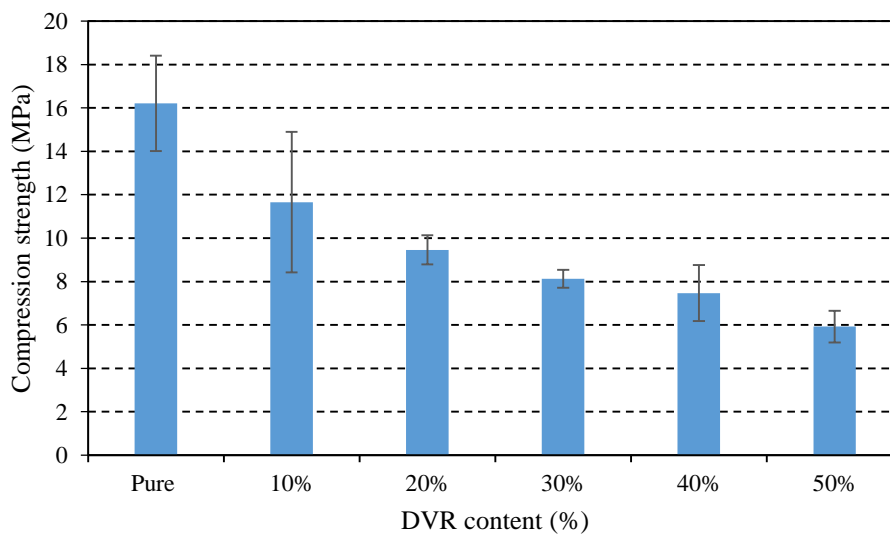


Fig. 14: Compression strength of DVR-PS composites

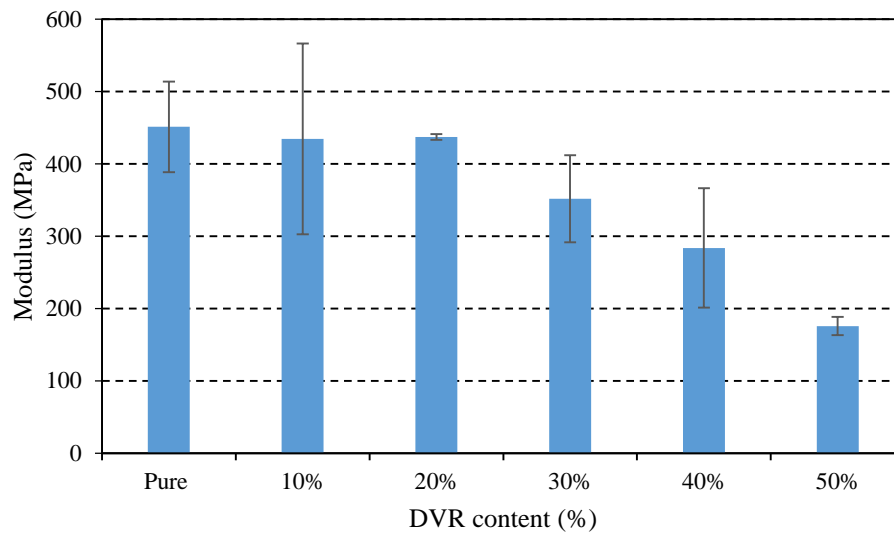


Fig. 15: Compression modules of DVR-PS composites

Table 2: Compression properties of DVR-PS composites

Content	Mean Modulus (MPa)	Mean Yielding (MPa)
Pure	451.15±62.57	16.21±2.19
10%	434.54±131.90	11.66±3.23
20%	437.17±3.95	9.46±0.67
30%	351.70±60.21	8.13±0.41
40%	283.84±82.53	7.47±1.29
50%	175.82±12.68	5.92±0.73

3.1.1.3 Buffing dust

BD-PS composites were prepared with contents of BD (0 to 50 wt.%) and compression tests performed on these composites. Table 3 summarizes the testing results. The stress-strain behavior of the developed BD-PS composites is shown in Fig. 16. The yielding strain values of all composites were less than 0.07—this illustrates

the brittle nature of the BD-PS composites. Fig. 17 shows the compression strength of the composites with different filler contents, while Fig. 18 shows the compression modulus of the composites. The pure PS compression strength was found to be 15.32 MPa; this reduced to 11.55 MPa and 10.58 MPa for 5-DB and 10-BD, respectively. Measurements of the compression strength of the other composites with higher BD contents gave a constant value of 8.6 MPa.

With compression modulus, the observed trend was similar to that for compression strength. The modulus of pure PS sample and 5-BD were 639.3 MPa and 536.5 MPa, respectively. The compression moduli of the other BD-PS composites, 10-BD, 15-BD, 20-BD and 25-BD, showed percentage reductions of 28.77 %, 25.36 %, 24.25 % and 27.98 %, respectively, compared with pure PS. As mentioned with the DVR composites, the BD particles may act as stress concentration points in the PS matrix or they may have a poor interface with the PS matrix. This may be the reason behind the observed reductions in the compression values. However, the compression properties of the developed BD-PS composites were higher than that for some insulation materials [106].

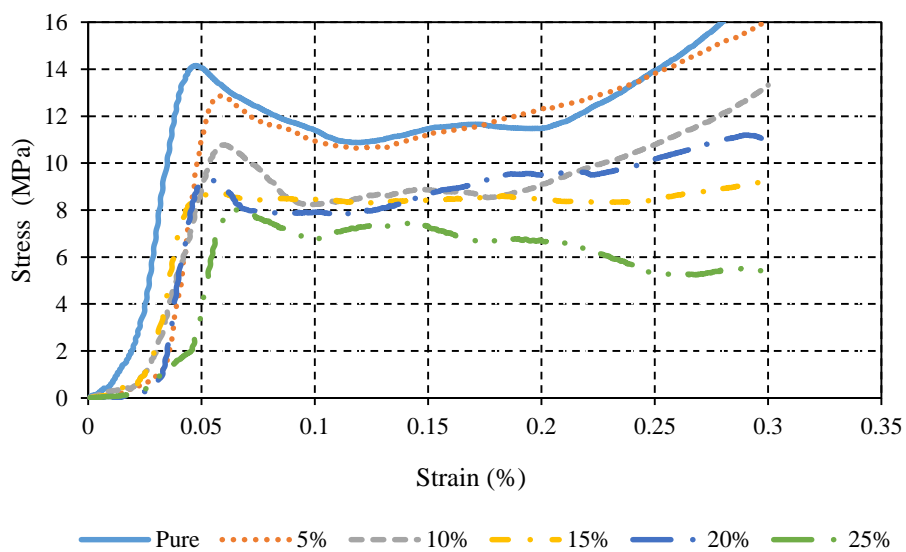


Fig. 16: Stress-strain curve for BD-PS composites

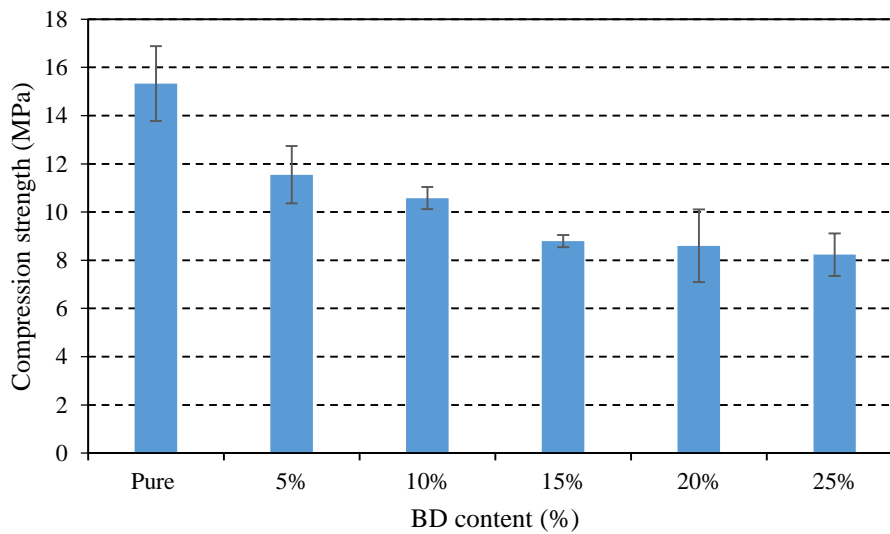


Fig. 17: Compression strength of BD-PS composites

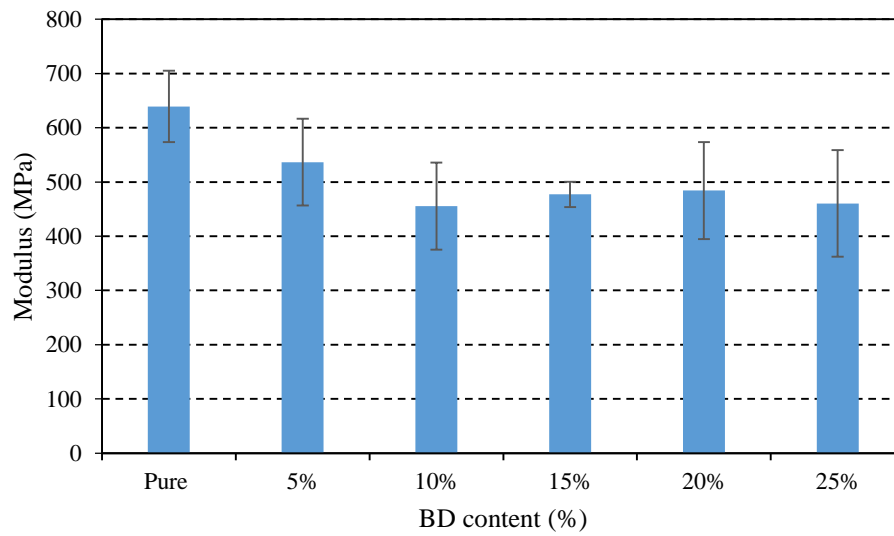


Fig. 18: Compression modulus of BD-PS composites

Table 3: Compression properties of BD-PS composites

Content	Mean Modulus (MPa)	Mean Yielding (MPa)
Pure	639.26±65.94	15.32±1.55
5%	536.56±80.12	11.55±1.19
10%	455.36±80.10	10.58±0.46
15%	477.14±23.30	8.79±0.25
20%	484.24±89.51	8.60±1.50
25%	460.41±98.04	8.23±0.88

3.1.1.4 Treated fillers

The effect of NaOH treatment on mechanical properties is discussed. Fig. 19 and Fig. 20 show the influence of the studied treatment on compression strength and modulus of the composites. Treatment of DPP with NaOH did not noticeably affect the compression strength of any composite. For example, the strength of the 30-DPP

composite before treatment was 10.17 MPa, which only rose to 10.6 MPa after treatment. The studied treatment had a negative impact on the compression moduli of three composites: DPP-PS, DVR-PS and BD-PS. The reduction in the compression moduli of DVR-PS and BD-PS was greater than the reduction for the DPP-PS composite. The modulus for the 30-DPP composite was reduced by 23.8 %, while the modulus for the DVR-PS and BD-PS composites dropped by 51.9 % and 56.7 %, respectively. Marcovich, Aranguren, and Reboredo [110] studied the effect of NaOH treatment on a wood flour-polyester composite. The researchers reported a similar trend for the compression moduli. However, they also reported a slight decrease in the compression strength. In a study by Bisanda and Ansell [111], it was found that NaOH had a positive impact on the compression properties of sisal-epoxy composites. The researchers argued that the NaOH treatment could increase wettability between the filler and the matrix, which enhanced interfacial bonding. However, Marcovich, Aranguren, and Reboredo [110], reported that the filler interfacial area was not the dominant factor.

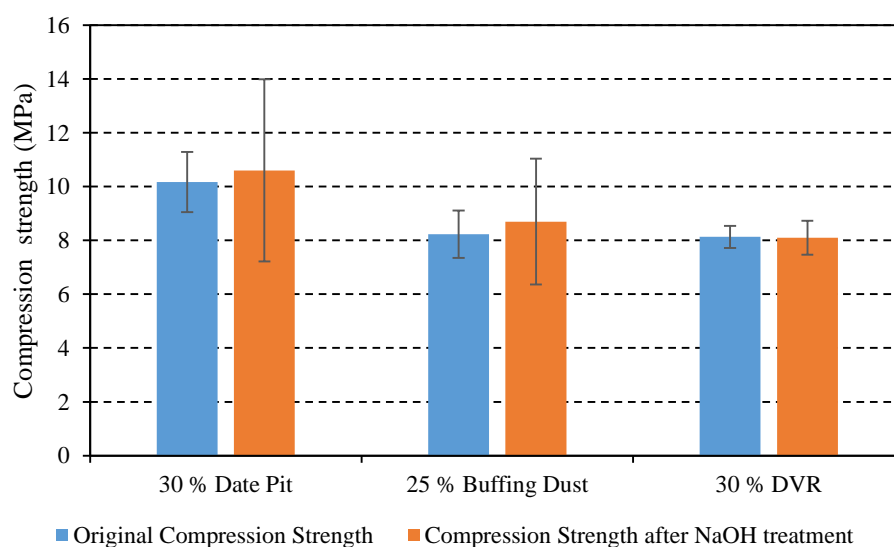


Fig. 19: Compression strength after NaOH treatment

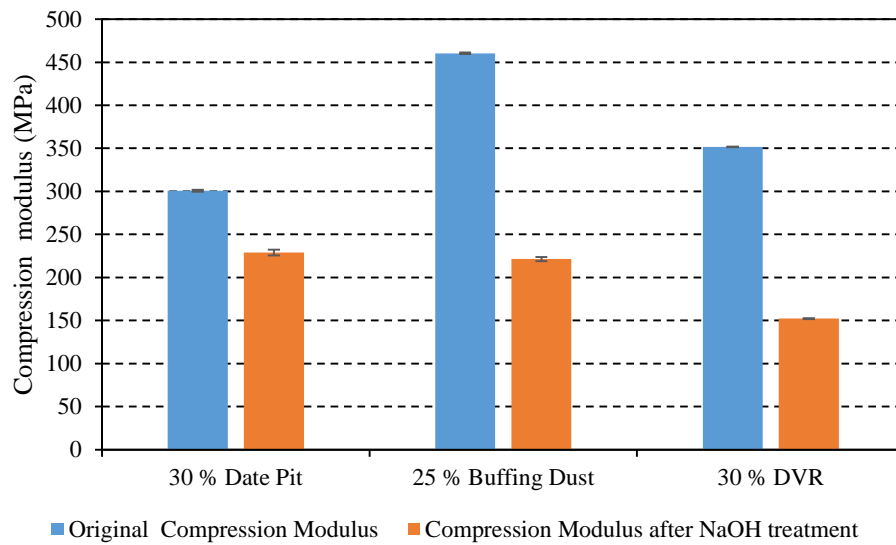


Fig. 20: Compression modulus after NaOH treatment

3.1.2 Tensile properties

A strong glue was used to attach four metallic parts to the two ends of each tensile test sample to prevent slippage, as shown in Fig. 21. Samples were inserted between the two different movable jaws of the machine to eliminate slippage between the specimen ends and the machine jaws. Samples were tested at a strain rate of 2 mm/min. The gauge length of all samples was 20 mm.



Fig. 21: Tensile sample with metallic parts

3.1.2.1 Date pits

Fig. 22 presents the tensile stress-strain behavior of the DPP composite. Generally, all samples showed brittle behavior, with a maximum fracture strain of 0.05%. The composite samples revealed a relatively higher fracture strain value than that of the pure PS samples. Meanwhile, the pure PS samples had a much higher fracture/yielding stress than that of the developed composites. The variations in the tensile strength and Young's modulus with increasing DPP content are shown in Fig. 23 and Fig. 24, respectively. The yield strength of the pure PS sample is 1.6 MPa. As the filler content increased, the yield strength decreased up to 20% filler content; then, an almost constant value of 0.375 MPa was observed for filler content of 30 to 50%. The measured values for the yield strength are 1.1, 0.8, 0.4 and 0.4 MPa for the 10-DPP, 20-DPP, 30-DPP, and 40-DPP samples, respectively, representing reductions of 29%, 50% and around 75% of the tensile yield strength for these composites, respectively.

The modulus of elasticity was almost constant at approximately 100 MPa for composites with DPP contents ranging from 0 to 20%. However, a noticeable decrease was observed for filler content higher than 20%. Above this percentage, the Young's modulus decreased, with Young's modulus values for 30-DPP, 40-DPP, and 50-DPP of 76, 24, and 25 MPa, respectively. All tensile yield strengths and moduli of elasticity values are reported in Table 4. Mıhlıyanlar, Dilmaç, and Güner [112] studied the effect of different process parameters on the mechanical properties of expanded polystyrene. For an inlet temperature of 125 °C and an outlet temperature of 80 °C, the tensile stress values were found to be between 0.86 and 2.71 MPa. The tensile strength of the produced PS (1.6 MPa) was comparable with the reported values. In addition, the

tensile strength of samples produced by a hot press was considerably lower than that of samples produced by injection molding [30, 112]. Thus, the reduction in tensile strength for samples prepared using a hot press in this study could be due to the presence of voids, as the hot press used moulds that do not allow the escape of gases which would induce voids in the sample.

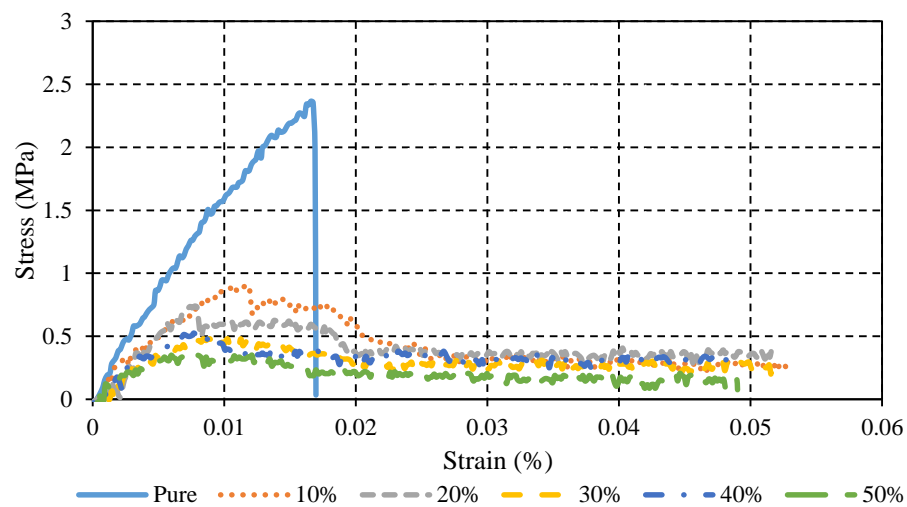


Fig. 22: Tensile strength of the developed composites

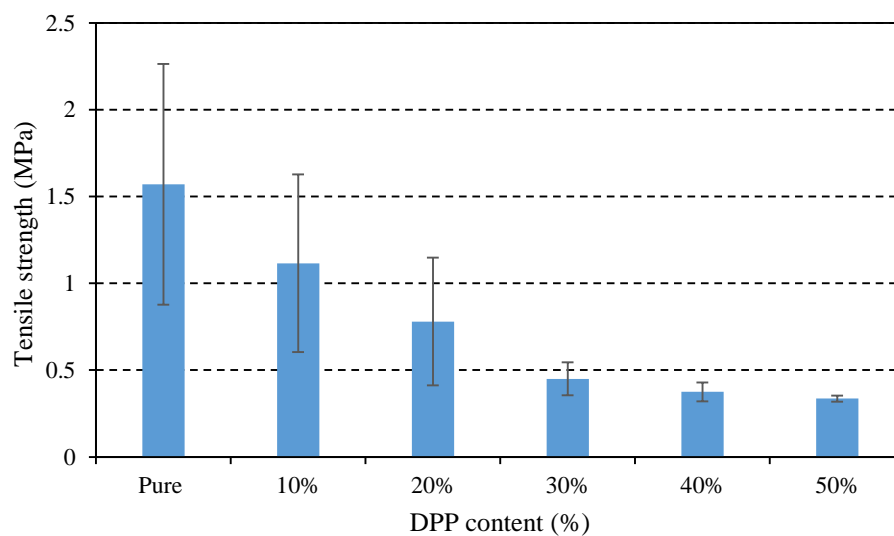


Fig. 23: Tensile strength of the developed composites

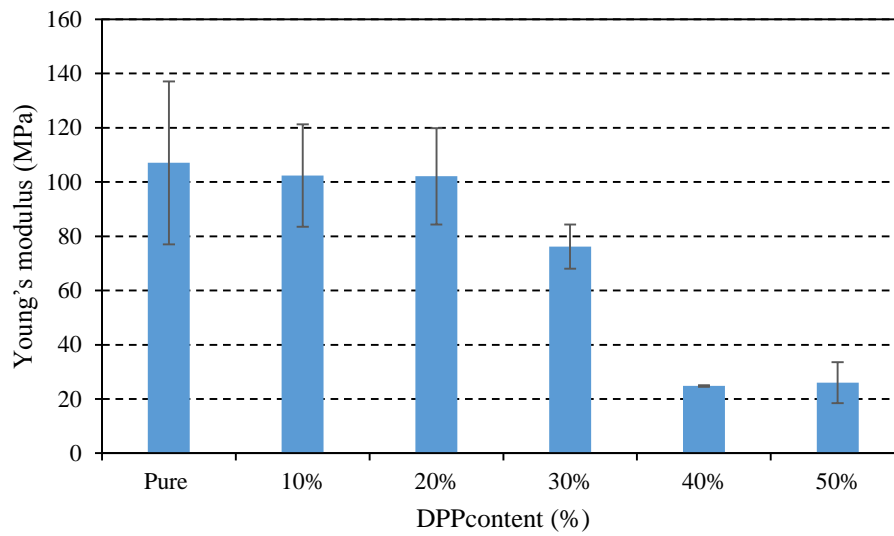


Fig. 24: Modulus of elasticity for the developed composites

Table 4: Tensile properties of the developed composites

Content	Mean Modulus (MPa)	Mean Yield strength (MPa)
Pure	107.07±1.57	1.57±0.69
10-DPP	127.98±1.12	1.12±0.51
20-DPP	68.75±0.78	0.78±0.36
30-DPP	24.80±0.38	0.45±0.09
40-DPP	76.17±0.45	0.375±0.05
50-DPP	25.99±0.34	0.34±0.02

3.1.2.2 Devulcanized rubber

The stress-strain curve of the representative samples of the DVR-PS composites is shown in Fig. 25. This curve demonstrates the brittle behavior of the developed composites—all the samples' strain to fracture value was lower than 0.025 %. It is noted that the fracture/yielding strain for the prepared composites with

a DVR content of 0 to 20 % was as much as or even higher than the fracture strain of the pure PS specimens. Averaged tensile strength and modulus values of the DVR-PS composites are summarized in Table 5. The average tensile strengths of the DVR-PS composites are presented in Fig. 26. The tensile strength of the pure sample was found to be 1.5 MPa. The tensile strength of the 10-DVR composite was 126.11 % higher than that of the pure PS. However, strength values dropped again to 2 MPa, 1.61 MPa and 1.49 MPa for the 20-DVR, 30-DVR and 40-DVR and 50-DVR composites, respectively. Despite the observed strength reduction in the 20-DVR and 30-DVR composites, the tensile strength of these composites was 27.4 % and 2.54 %, respectively, higher than that for pure PS. When the tensile strength of the 40-DVR and 50-DVR composites was compared with pure PS, it was found that these strengths were 0.67 % and 30.67 %, respectively, lower than that for pure PS. Therefore, it may be concluded that the addition of 0 to 40 wt. % of DVR does not negatively affect the tensile yielding strength. Fig. 27 demonstrates the effect of adding DVR on the elasticity modulus of the prepared composites. It is evident the elasticity moduli follow the same trend as the tensile strengths. While the Young's moduli of the 40-DVR and 50-DVR composites were 1.89 % and 50.6 % lower than pure PS modulus, respectively, values for the elasticity moduli of the 10-DVR, 20-DVR and 30-DVR composites were higher than that for pure PS by 100 %, 31 % and 11.96 %, respectively. Some researchers have studied the effect of adding different weight percentages of non-treated scrap tire rubber to polymer matrixes. For example, Abu-Jdayil, Mourad, and Hussain [40] reported different tensile behaviors for scrap tire-polyester composites. In their study, they noted that tensile strength decreased with increasing scrap tire content in a scrap tire-polyester composite. However, Mujal-Rosas, Marin-Genesca, Orrit-Prat, Rahhali, and Colom-Fajula [49] showed that the

addition of ground rubber at low percentages (0 to 15 wt. %) enhanced the tensile strength and elasticity modulus of the rubber-HDPE composite. The results of this research is consistent with the findings of the current work. Most research on the incorporation of DVR in thermoplastic polymer matrixes (e.g. [59, 61]) has focused on comparing the mechanical properties of polymer composites prepared by adding DVR and vulcanized rubber fillers, but very few studies have investigated the effect of different proportions of these fillers. In addition, some researchers have narrowed their focus to study the effect of different devulcanized methods and parameters on mechanical properties (e.g. [58, 60]). Karabork, Pehlivan, and Akdemir [113] added 10 %, 30 % or 50 % of tire rubber and DVR to styrene butadiene rubber (SBR) and studied the mechanical properties of the prepared composites. The researchers noted that DVR-SBR composites exhibited better tensile properties than tire rubber-SBR composites. They also reported that, for DVR-SBR composites, tensile strength, strain at break and elastic modulus improved for low DVR content, before it dropped at higher DVR percentages. This suggests that DVR particles may act as a reinforcement agent. DVR may interfere with the thermoplastics in the composites, which would result in strong adhesion between the DVR and the thermoplastic matrices, especially among the smaller DVR particles. It should be noted that the ductile rubber particles acted as reinforcement agents in the tensile strength test but not in the compression test; the adhesion between the DVR and the matrix was found to be more effective against pulling than against compression. However, high DVR concentrations, even among tensile samples, lowers the polymer proportion and this would worsen the interface between DVR and the polymer matrix, resulting in weak points that negatively influence the stress transformation.

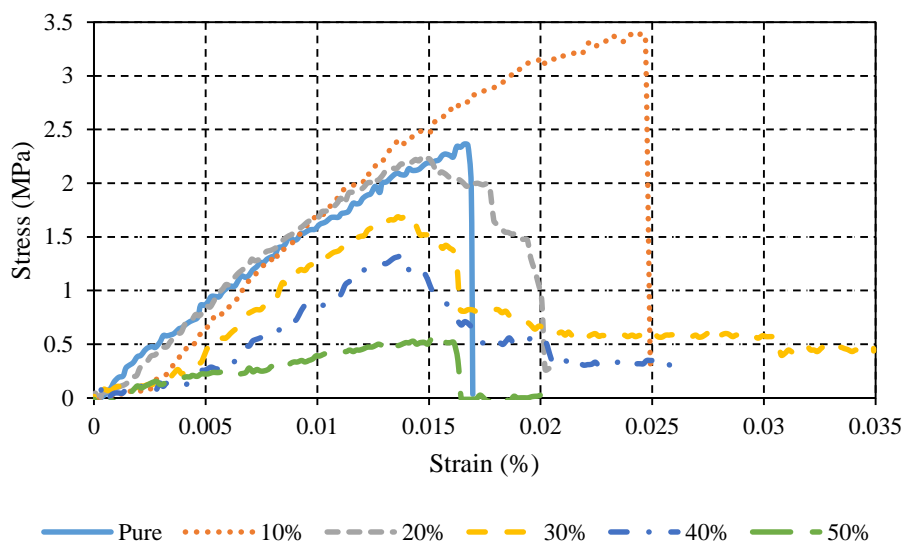


Fig. 25: Stress-strain curve for DVR-PS composites

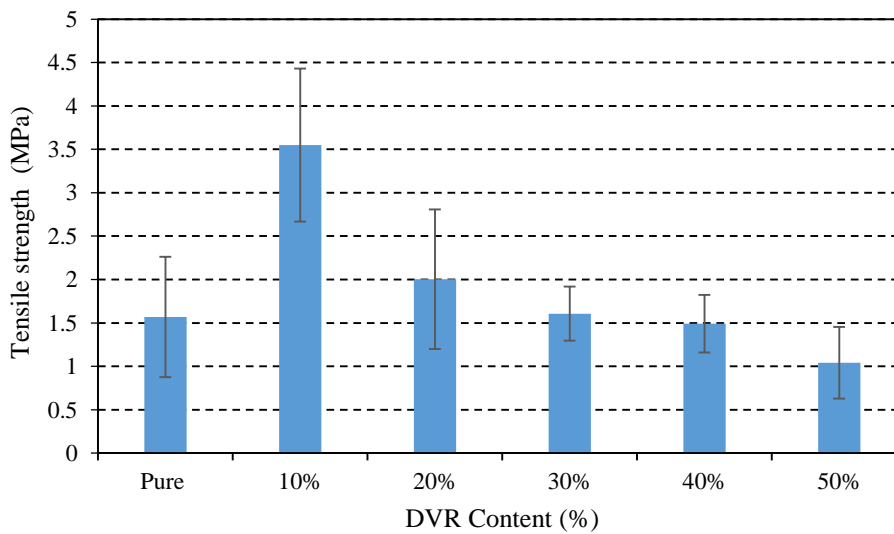


Fig. 26: Tensile strength for the DVR-PS composites

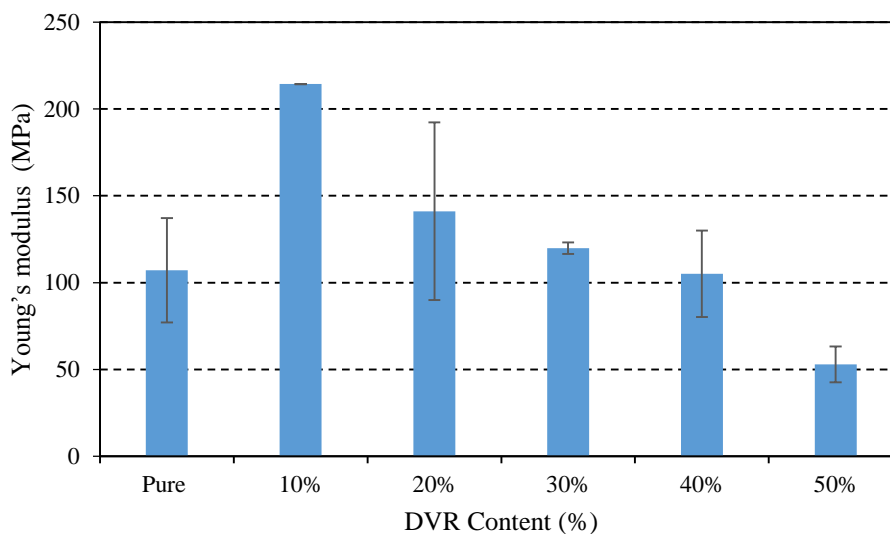


Fig. 27: Modulus of elasticity for the DVR-PS composites

Table 5: Tensile properties of DVR-PS composites

Content	Mean Modules in (MPa)	Yielding strength (MPa)
Pure	107.07±30.04	1.57±0.69
10%	214.39±0.084	3.55±0.88
20%	141.13±51.24	2.00±0.80
30%	119.88±3.33	1.61±0.31
40%	105.05±24.95	1.49±0.33
50%	52.89±10.25	1.04±0.41

3.1.2.3 Buffing dust

Fig. 28 shows the stress-strain curve of the BD-PS composites. As with the previous two composites, brittle behavior was dominant in the BD-PS composite. All measured strain rates were less than 0.02 %. Tensile yielding strengths and elasticity moduli of the composites are shown in Fig. 29 and Fig. 30, respectively. These

properties are listed in Table 6. The pure PS tensile strength was 1.57 MPa, which increased to 2.54 MPa and 2.12 MPa for BD proportions of 5 wt. % and 10 wt. %, respectively. The strength values reduced gradually to 0.95 MPa, 0.64 MPa and 0.39 MPa for the 15-BD, 20-BD and 25-BD composites, respectively. The 5-BD composite possessed the highest tensile strength, which was 61.78 % higher than that for the pure PS. An enhancement in Young's modulus was observed for composites with low BD content (0 to 10 wt. %). Modulus values rose to 160 MPa and 149 MPa for BD content of 5 wt. % and 10 wt. %, respectively. These values reduced to an almost constant value of 83 MPa for the 15-BD and 20-BD composites, respectively, prior to a drop again to 0.39 MPa. To the best of this author's knowledge, there is no similar study which used BD as a filler in polymer composite; although the improvement in tensile properties at low filler concentrations was reported in [49]. The low content of BD filler may enhance the stress transformation through matrix voids, as the BD has a needle shape which could connect the edges of the matrix voids, as illustrated in section 3.2. Similar to that for rubber, the drop in tensile properties may be due to filler aggregation and low polymer filler mass fraction in high content composites, which probably results in poor interference between the BD particles and the PS matrix.

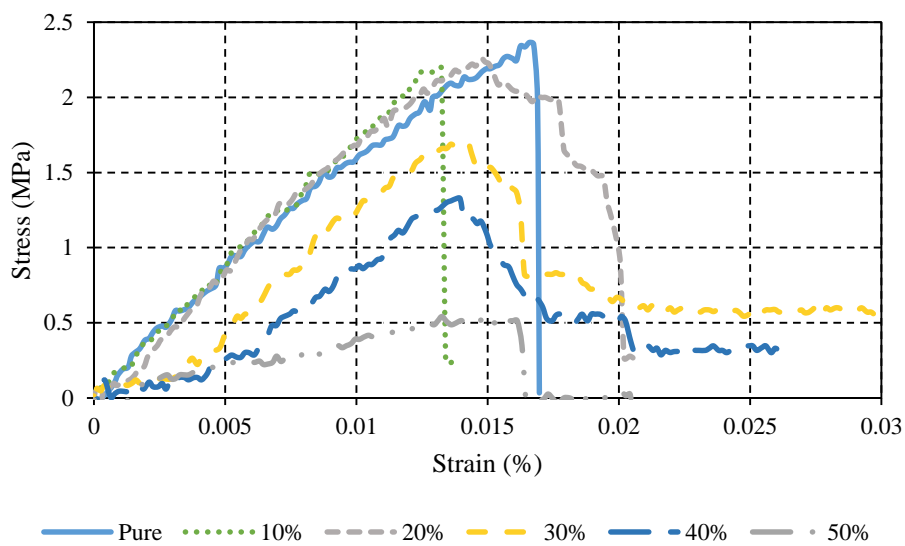


Fig. 28: Stress-strain curve for BD-PS composites

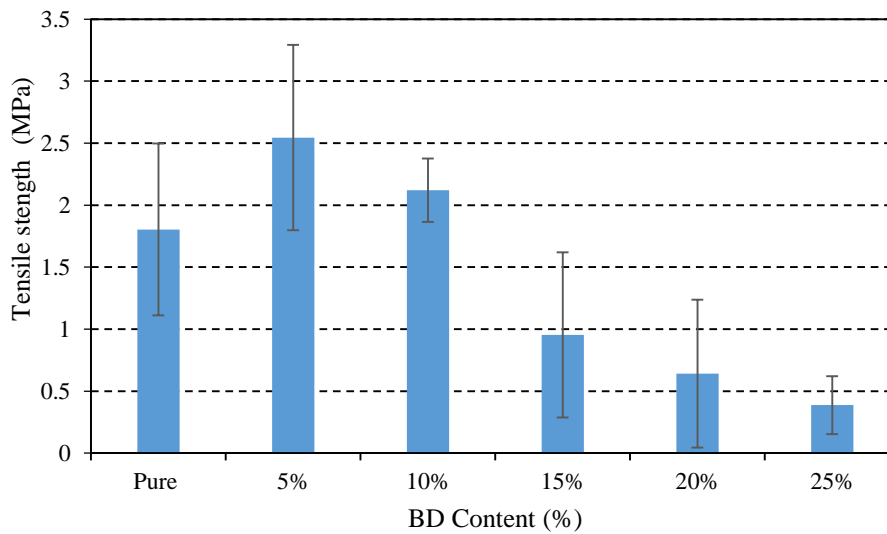


Fig. 29: Tensile strength for the BD-PS composites

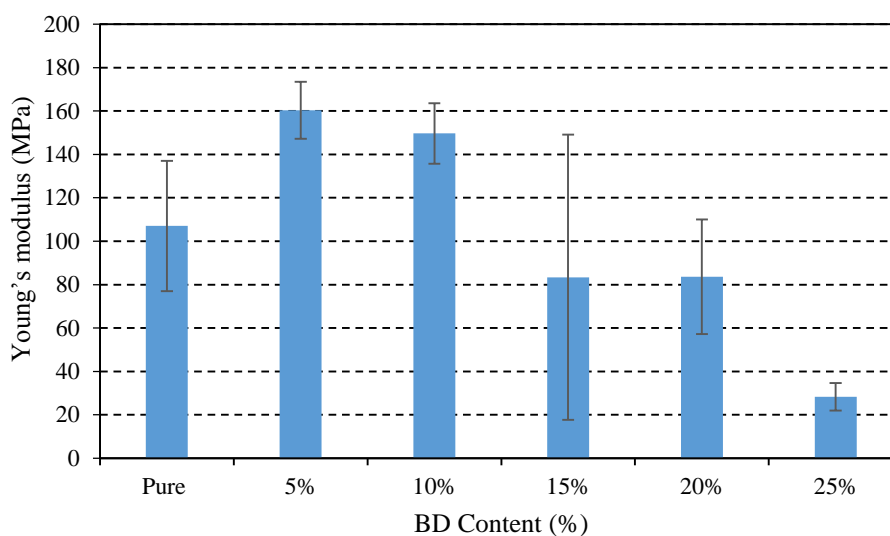


Fig. 30: Modulus of elasticity for the BD-PS composites

Table 6: Tensile properties of BD-PS composites

Content	Mean Modulus (MPa)	Yielding strength (MPa)
Pure	107.07±30.04	1.57±0.69
5%	160.305±13.15	2.54±0.74
10%	149.65±13.89	2.12±0.26
15%	83.37±65.73	0.95±0.67
20%	83.56±26.42	0.64±0.60
25%	28.31±6.34	0.39±0.23

3.1.2.4 Treated fillers

The tensile properties of composites prepared using treated fillers are discussed in this section. Significant improvement in tensile strength and elasticity modulus was observed and is reported in Fig. 31 and Fig. 32. While the tensile strength of the DPP-PS and BD-PS composites doubled, the strength of DVR-PS increased by 63.56 %. Joseph, Thomas and Pavithran [82] treated sisal fibers with NaOH and used them to

prepare sisal-polyethylene composites. The researchers noted that the tensile properties were improved by NaOH treatment. The improvement in tensile properties may be due to removal of natural and artificial impurities, which may result in better adhesion between the matrix and the used fillers. In addition, NaOH may remove lignocellulosic materials from the fillers, which would degrade the hydrophobicity of the DPP. That would increase the area of interaction between the matrix and the filler [114]. Regarding DVR, alkaline solutions may break the crosslinks within the rubber. This is apparent in comparing Fig. 4 with Fig. 33. In addition, alkali could break the S-S bond [105] and increase surface roughness. The BD-PS composite experienced a huge improvement in modulus of elasticity—the value was tripled. In addition, the NaOH treatment increased the elasticity modulus of DPP-PS composites by 63.06 %. However, NaOH treatment did not affect the elasticity modulus of the DVR-PS composite.

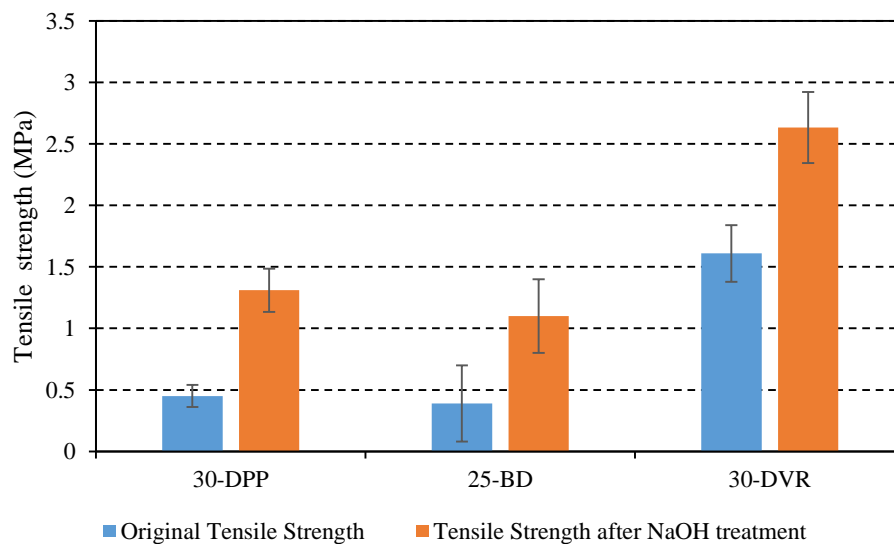


Fig. 31: Tensile strength after NaOH treatment

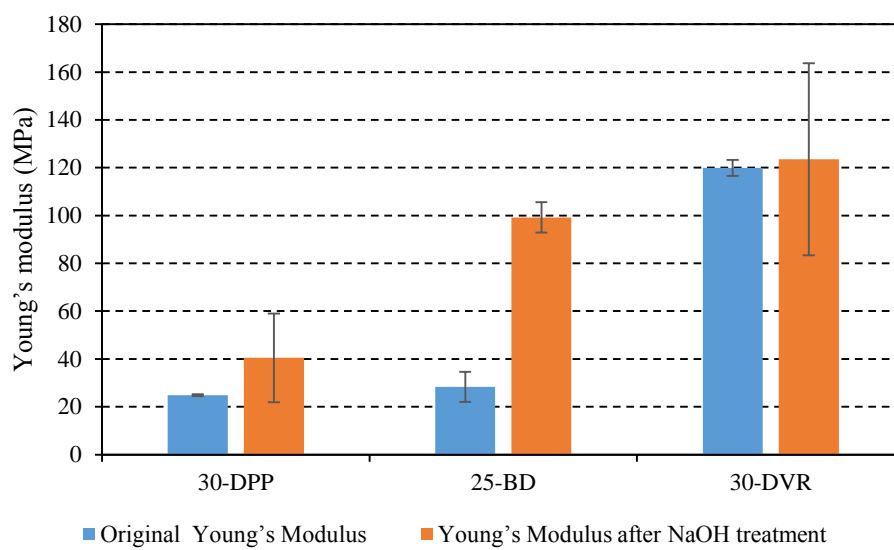


Fig. 32: Modulus of elasticity after NaOH treatment



Fig. 33: Treated DVR

3.1.3 Flexural properties

3.1.3.1 Date pits

A three-point bending test was conducted at a strain rate of 2 mm/min using a load cell with a capacity of 5 kN. The load extension curve for DPP-PS composites is shown in Fig. 34. The DPP significantly reduced the flexural yield strength of the composite, as shown in Fig. 35. In fact, 0 to 20% filler content reduced this strength by 50 %, while the 50-DPP sample strength fell by 96 %. Fig. 36 shows a similar trend for the flexural modulus, which decreased with the filler content. However, the DPP had a smaller influence on the flexural modulus than on the flexural strength, reducing the flexural modulus of the pure sample by 41 % for the 10-DPP sample. However, the modulus in the 50-DPP sample dramatically reduced by 95 % due to the poor compatibility between filler and matrix and the brittleness of both, similar to the compression testing results. All flexural moduli and yield strengths are reported in Table 7. Poletto, Dettenborn, Zeni, and Zattera [115] reported that a poly(styrene-co-maleic anhydride) coupling agent enhanced the flexural strength of the composites by improving the compatibility between wood flour and the polymer matrix. Their composites also exhibited higher flexural strength than the samples produced in this research because of differences in the mixing and processing methods. In the mentioned study [115] researchers used co-rotating twin-screw extruder for mixing and injection molding. In addition to the positive effect of the high homogenous mixture provided by the extruder, the injection moulding may have eliminated the air voids which affect the mechanical properties negatively. Nevertheless, the flexural strength for low filler content (e.g. the 10-DPP, 20-DPP and 30-DPP samples) was significantly higher than that of other thermal insulation materials, such as binderless

cotton stalk fiberboard, which had a flexural strength of 0.6 MPa [116]. Moreover, the flexural strength of the composite was much higher than that of commonly-used commercial insulation material such as extruded PS foam [107].

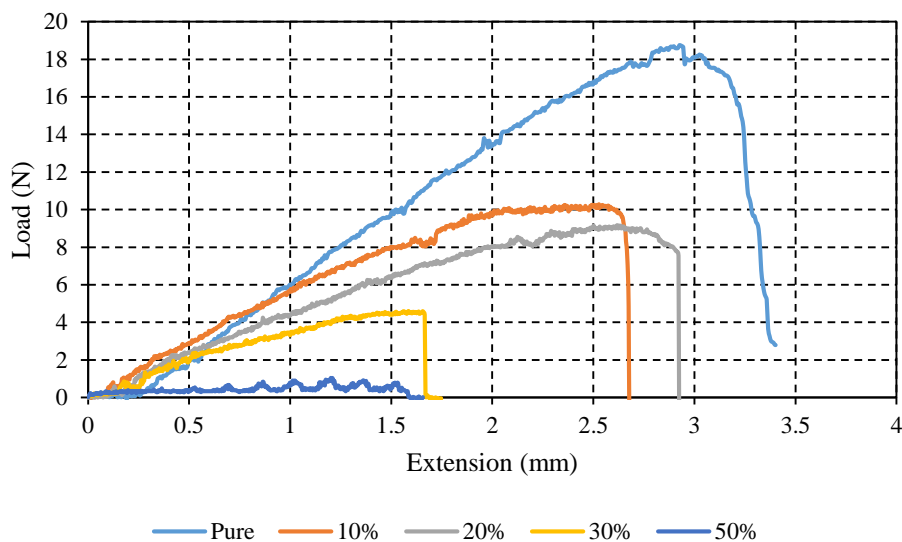


Fig. 34: Load extension curve for DPP-PS composites

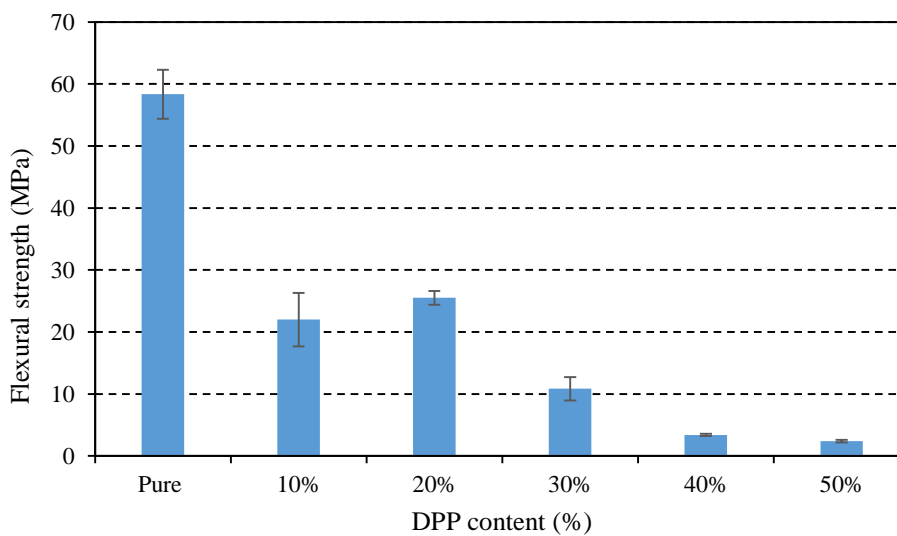


Fig. 35: Flexural yield strength of the DPP-PS composites

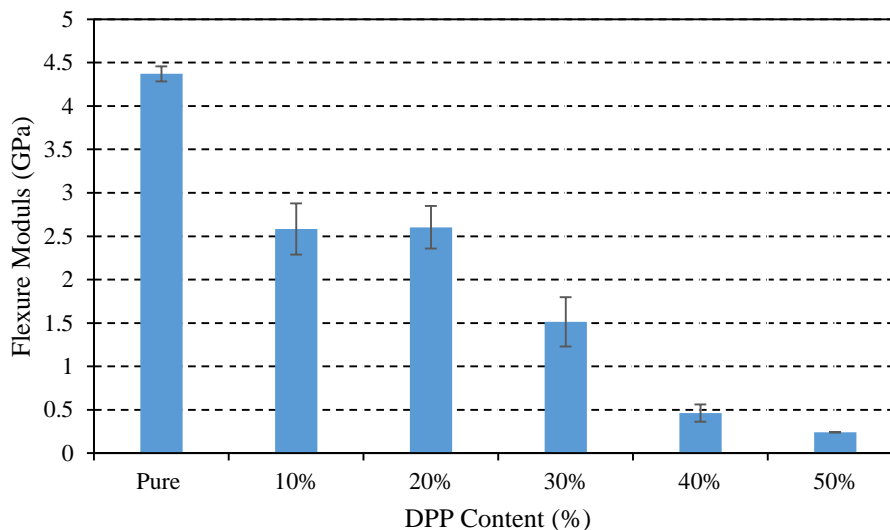


Fig. 36: Flexural modulus of the DPP-PS composites

Table 7: Flexural properties of the DPP-PS composites

Content	Mean Modulus (GPa)	Mean Yield Strength (MPa)
Pure	4.48±0.077	57.93±4.21
10-DPP	2.58±0.29	21.10±4.32
20-DPP	2.60±0.25	25.51±1.13
30-DPP	1.51±0.28	10.84±1.87
40-DPP	0.46±0.10	3.39±0.187
50-DPP	0.24±0.00	2.37±0.21

3.1.3.2 Devulcanized rubber

While Fig. 37 shows the load extension behavior of the DVR-PS composites, Fig. 38 and Fig. 39 demonstrate the change of flexural strength and flexural modulus with DVR content. In addition, averaged flexural strengths and moduli are reported in Table 8. It was noticed that the flexural strength reduced with increasing DVR content. Although the addition of DVR lowered the strength, it clearly increased the extension

values at break. As Fig. 38 shows, 10-DVR composite's strength reduces significantly; the reduction percentage is found to be 30 %. After this, the rate of reduction in the flexural strength slowed for the 20-DVR, 30-DVR and 40-DVR composites before it dropped sharply again to 6.43 MPa for the 50-DVR composite. The variation in flexure modulus of the PS-DVR composites followed a similar trend. The flexure modulus of pure PS was found to be 7.31 MPa. This value significantly reduces with addition of DVR—the flexural strength of 10-DVR composite was reduced to 2.67 MPa. Thereafter, the flexural moduli reduced slowly with higher filler content—2.67 MPa, 2.15 MPa, 1.78 MPa for the 20-DVR, 30-DVR and 40-DVR composites, respectively, and sharply to 0.65 MPa for the 50-DVR composite. The reduction in flexural strength may be due to the poor interference between the rubber and PS matrix. In fact, incorporation of rubber in the PS matrix entraps air which may cause a reduction in strength. In [43] the researchers noted a similar behavior in flexural strength when they increased the tire rubber content in a rubber-foam Portland cement composite. In [42], the flexural strength reduced with addition of tire rubber content to plaster, with the maximum reduction found to be 47 % in this composite. Medina, Medina, Hernández-Olivares, and Navacerrada [117] reported that replacing coarse aggregate with rubber aggregate also caused a reduction in flexural strength. The flexural strength of DVR-PS composite was higher than some rubber composites mentioned in the literature, such as foamed Portland cement composite [43] (10.86 to 0.27 MPa) and rubber-cement composite [45] (3.2 to 4.2 MPa).

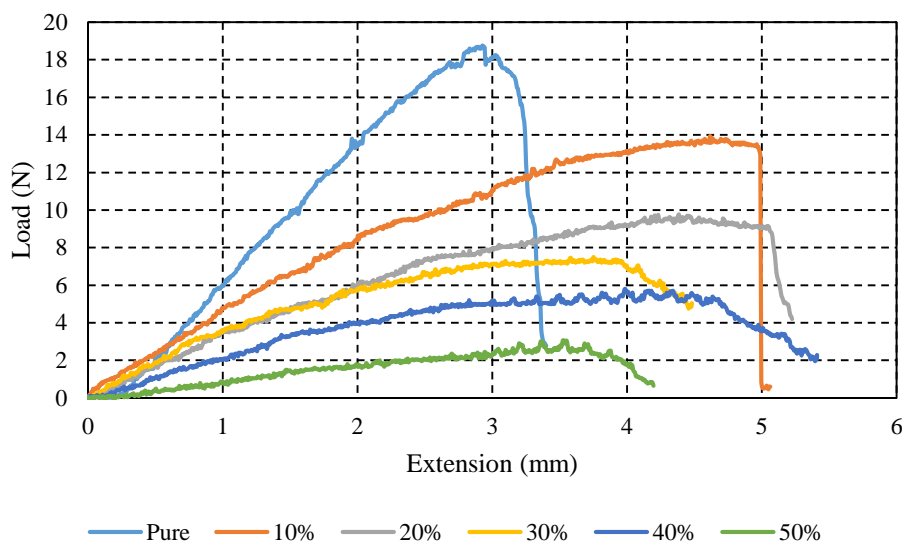


Fig. 37: Load extension curve for DVR-PS composites

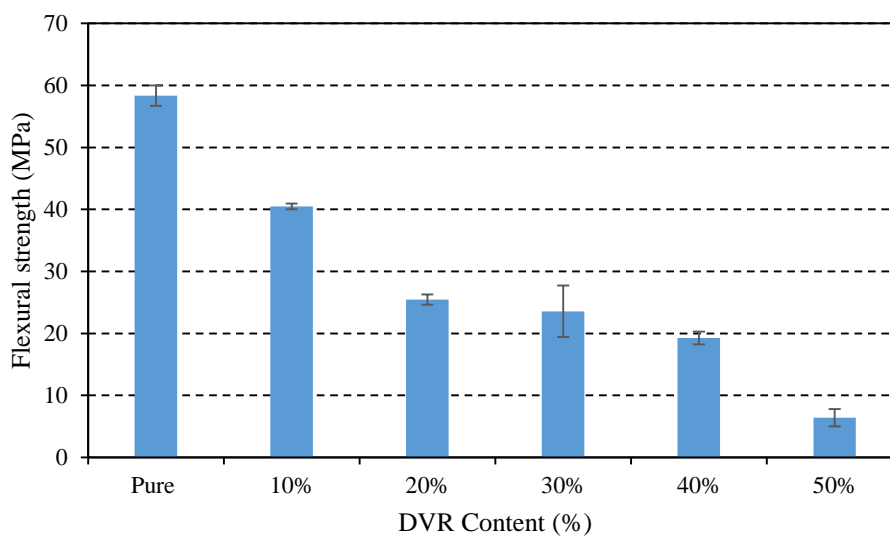


Fig. 38: Flexural yielding strength of the DVR-PS composites

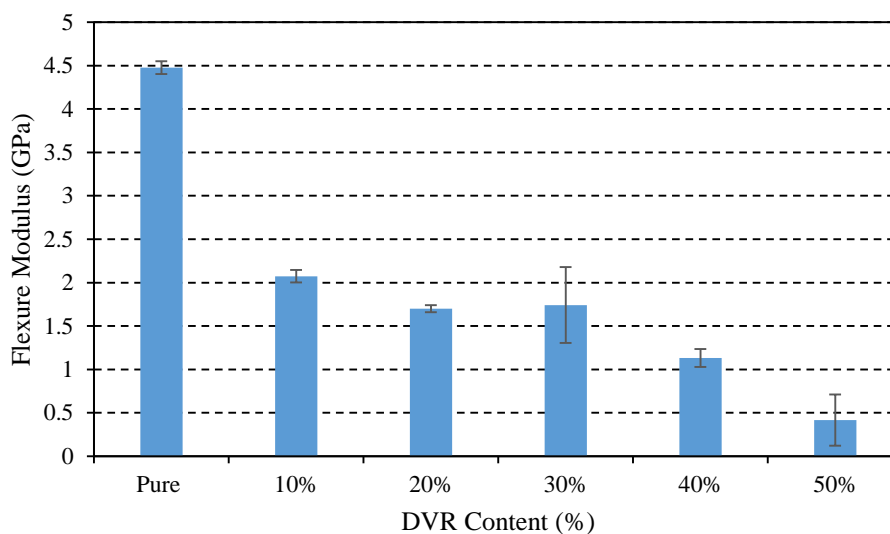


Fig. 39: Flexural modulus of the DVR-PS composites

Table 8: Flexural properties of DVR-PS composites

Content	Mean Modulus (MPa)	Mean Yielding (MPa)
Pure	4.48±0.07	58.35±1.64
10%	2.07±0.07	40.49±0.46
20%	1.70±0.04	25.46±0.82
30%	1.74±0.43	23.57±4.16
40%	1.13±0.10	19.26±1.03
50%	0.42±0.29	6.43±1.40

3.1.3.3 Buffing dust

The flexural strength and load extension curve of BD-PS composites are shown in Fig. 40 and Fig. 41, respectively. The pure sample strength was measured to be 58.35 MPa. The flexural strength reduced by 49.43 % when 5 wt. % of BD was added to a PS matrix. However, higher BD content did not further affect the strength. The flexural strength of 5-BD, 10-BD, 15-BD and 20-BD composites were almost constant,

with an average value of 28.20 MPa. For the 25-BD composite, the flexural strength, found to be 19.54 MPa, was slightly lower than the calculated average.

The flexural modulus of the prepared composites is demonstrated in Fig. 42. It was observed that the addition of BD affected the yielding strength negatively. It reduced the flexural modulus of BD-PS composites with 5 to 15 wt. % BD by 44.72 %. Both flexural strength and stiffness followed a similar trend, falling to a constant value for 5 to 15 wt. % filler content.

The BD-PS flexural properties are listed in Table 9. BD may aggregate causing poor stress transformation and this would decrease the flexural properties. However, the flexural strength of these composites were comparable with common commercial thermal insulators [107].

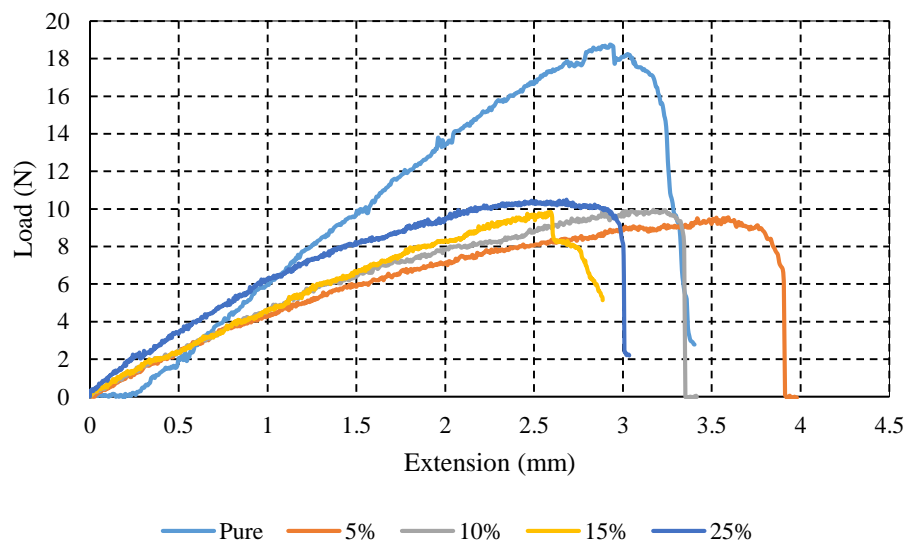


Fig. 40: Load extension curve for BD-PS composites

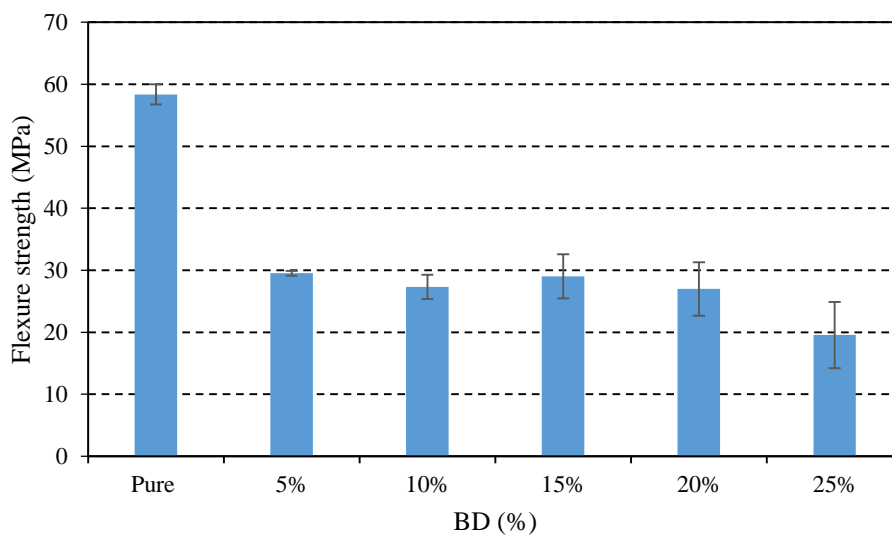


Fig. 41: Flexural yielding strength of the BD-PS composites

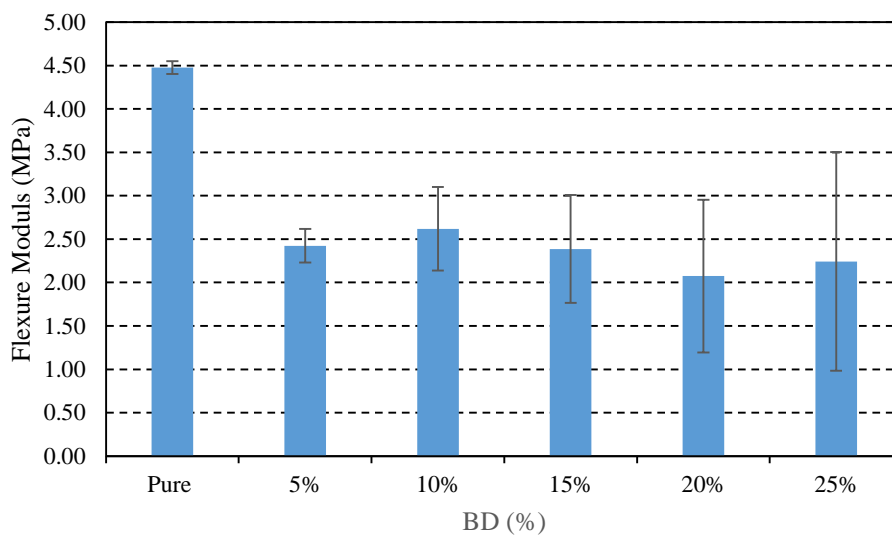


Fig. 42: Flexural modulus of the BD-PS composites

Table 9: Flexural properties of BD-PS composites

Content	Mean Modulus (Gpa)	Mean Yielding (Mpa)
Pure	4.48±0.07	58.35±1.64
5%	2.42±0.19	29.51±0.38
10%	2.62±0.48	27.29±1.96
15%	2.39±0.62	28.99±3.57
20%	2.07±0.88	26.99±4.32
25%	2.24±1.26	19.54±5.32

3.1.3.4 Treated fillers

Fig. 43 and Fig. 44 show the improvement in the flexural strength and flexural moduli of the developed composites after surface treatment. While the NaOH treatment had a significant effect on the flexural strength values, it had relatively little influence on the flexural moduli. The flexural strength of treated 30-DPP and 30-DVR composites increased from 5.42 MPa to 16.76 MPa, and from 11.785 MPa to 22.7 MPa, respectively. With treated 30-BD composite, the flexural strength increased by 23.8 %. The effect of NaOH treatment on kenaf-polyester and hemp-polyester composites has been investigated by Aziz and Ansell [104], with both composites showing a significant enhancement in flexural strength and flexural modulus. The researchers reported that alkalization of fillers improved the interlocking between the fiber and the matrix. With the rubber composites, it was reported that NaOH surface treatment improved the rubber composite adhesion and surface roughness. In addition, the treatment reduced the water absorption of the rubber particles, which would enhance the composite compatibility [118]. In the current study, the flexural modulus of the 30-DPP, 25-BD and 30-DVR treated composites improved by 79.47 %, 24.11 % and 48.26 %, respectively.

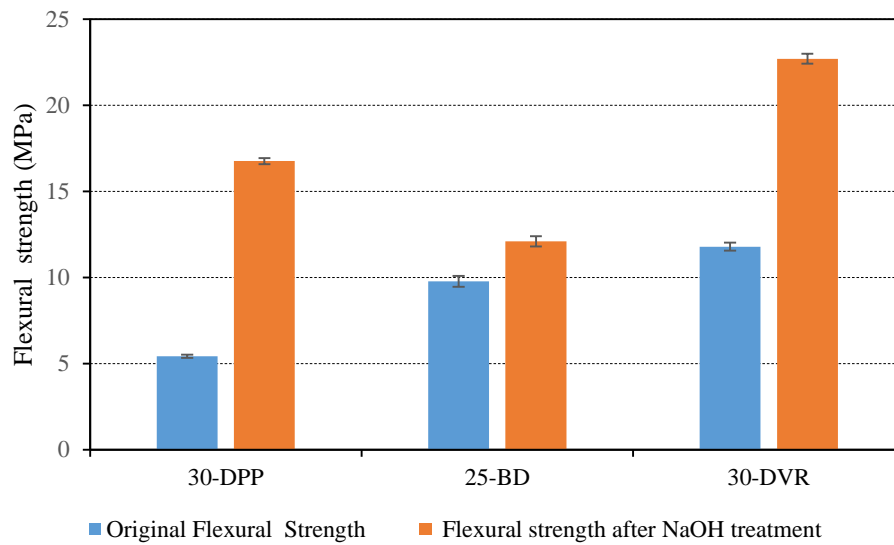


Fig. 43: Flexural strength after NaOH treatment

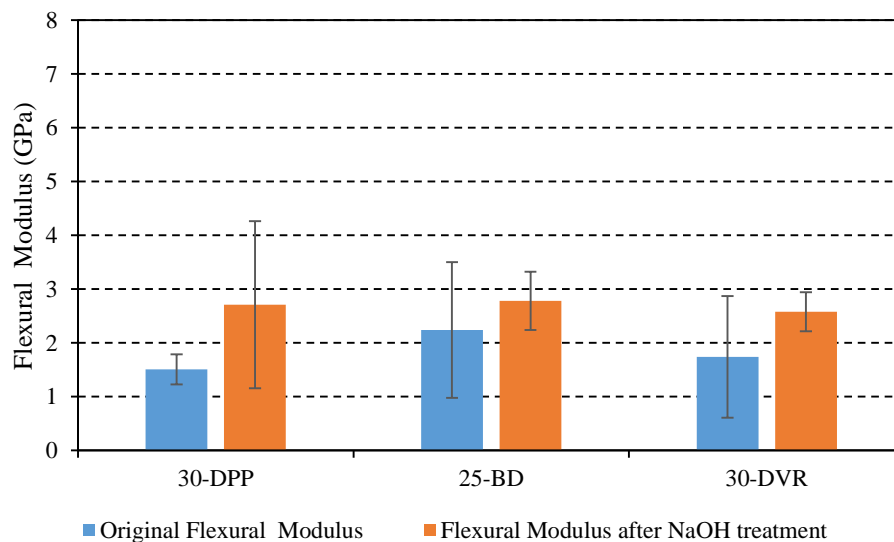


Fig. 44: Flexural modulus after NaOH treatment

3.2 Microstructure

3.2.1 Fillers

The three fillers used in the current study were imaged before and after the treatment to investigate the effect of NaOH treatment on each filler's surface and shape. As shown in Fig. 45, treatment of DPP with NaOH increased the surface

roughness of the DPP, which confirms that the treatment removed impurities on the DPP surface. A similar observation was noted in [82] when the researchers applied the treatment to sisal fiber. With DVR, roughness increased clearly, as is evident in Fig. 46, due to improved interlocking between the DVR filler and the matrix. Fig. 47 shows that the chemical treatment had a significant effect on the microstructure of the BD filler. When chemical treatment was implemented, the BD shape was changed from crossed longitudinal fibers into irregular individual particles; this change resulted in better distribution in the matrix, hence improving the mechanical properties of the composites. The SEM images of the fillers lends support to the discussion in the mechanical properties section of this study.

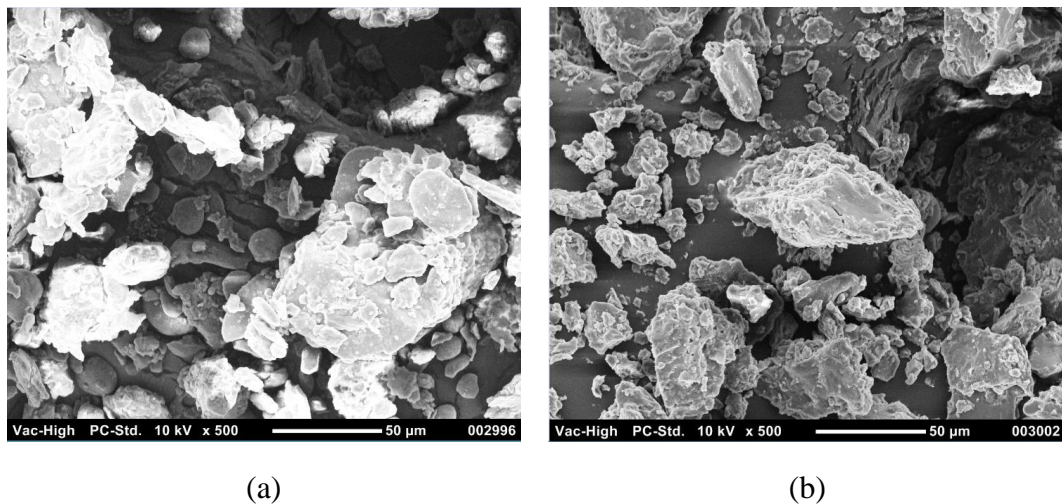


Fig. 45: SEM micrograph for (a) raw DPP; (b) DPP after chemical treatment

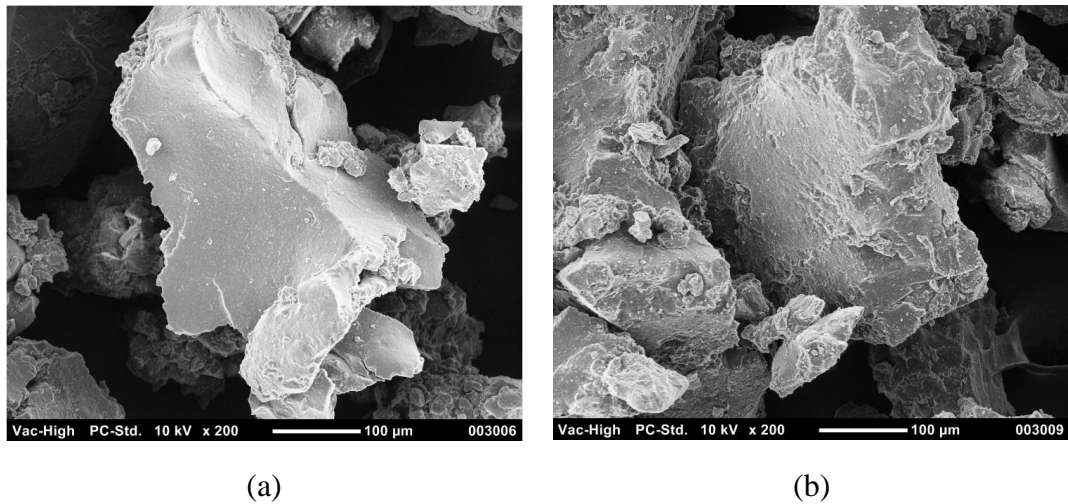


Fig. 46: SEM micrograph for (a) raw DVR; (b) DVR after chemical treatment

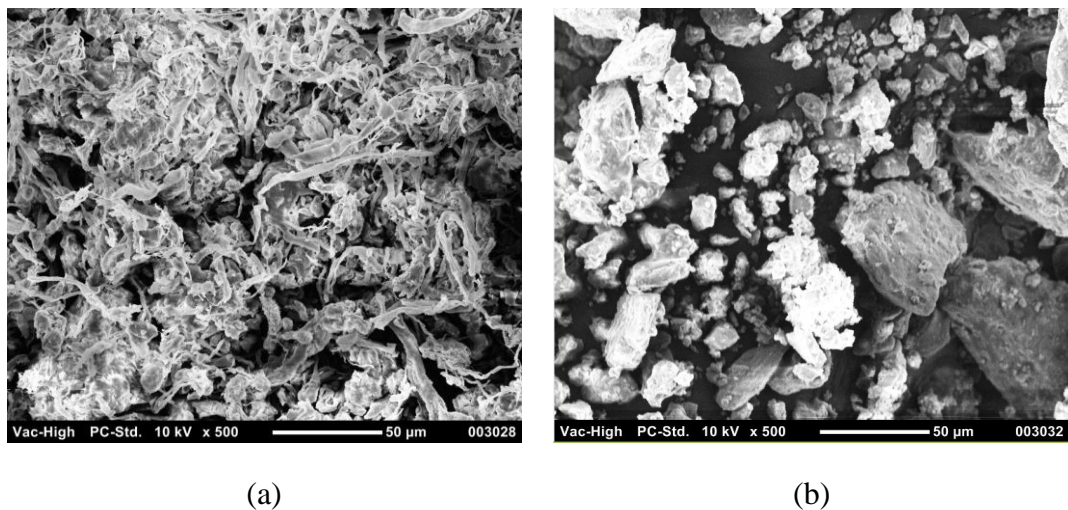


Fig. 47: SEM micrograph for (a) raw BD; (b) BD after chemical treatment

3.2.2 Composites

This section discusses the research into the morphological properties of fillers and developed composites. Tensile samples were used throughout the research for this section and the samples were imaged to investigate the adhesion between fillers and the matrix. As noted above in the mechanical properties section, two main trends were observed: a reduction of mechanical strengths with addition of different fillers; and

enhancement in mechanical properties with chemical treatment. The observed reduction was attributed to the agglomeration of fillers, creating stress concentration points, as well as poor compatibility between the fillers and the polymer matrix. As also discussed above, fillers tended to agglomerate when added to a polymer matrix. With natural fillers, this agglomeration is due to the hydrogen bonds between the particles [85]. The phenomena of filler agglomeration for DPP filler in the 50-DPP composite is clearly shown in Fig. 48. In addition, the filler particles have a weaker strength than that of the polymer matrix, thus these particles obstruct stress transfer and cause stress concentration. Fig. 49 shows that cracks were initiated from the added particles, which confirms that the particles act as stress concentration points. As a result, a reduction in mechanical strength was observed. However, the tensile properties of the DVR and BD composites increased at low filler content; here the fillers acted as reinforcement agents (Fig. 50). In addition to the discussed points, it is evident that poor compatibility between the added fillers and the PS matrix caused a reduction in mechanical properties. The reduction in mechanical properties was observed to improve with the treatment. Fig. 51 shows that the 30-DPP composite had a poor interference compared with that of the treated 30-DPP composite. This shows NaOH treatment enhanced compatibility within the composite by reducing the hydrophilicity of the DPP and removing impurities. As mentioned in section 3.1.3.2, high proportions of DVR content could affect the adhesion negatively due to the low PS matrix content. The DVR particles in the 30-DVR composite displayed poor adhesion to the PS matrix, as shown in Fig. 52. Moreover, it may be observed from the same figure that the DVR entraps air, forming large voids. Treatment of DVR with NaOH increased the DVR surface roughness (Fig. 46), due to an increase in the interaction area between the DVR and PS matrix, as discussed in section 3.1.2.4 and

indicated in Fig. 52. Fig. 53 shows that the BD had a better interference with PS matrix in the treated 30-BD composite, compared with the 30-BD composite. In addition, it shows the effect of NaOH treatment on the shape of the BD particles. The SEM images of the BD composites show that the compatibility of the BD filler improved with chemical treatment and enhanced the mechanical properties significantly, as shown in Fig. 19, Fig. 31 and Fig. 43.

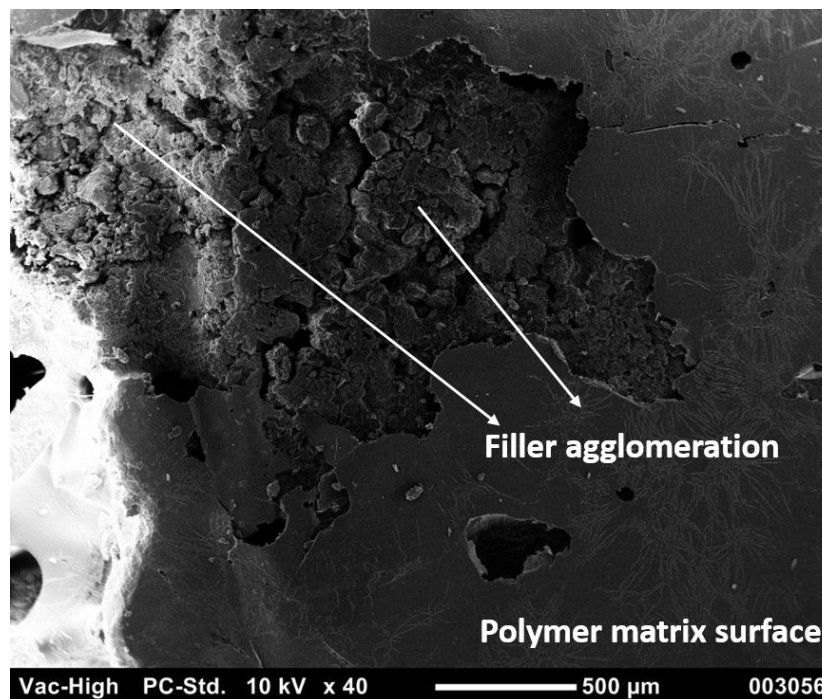


Fig. 48: Filler agglomeration in 50-DPP composite

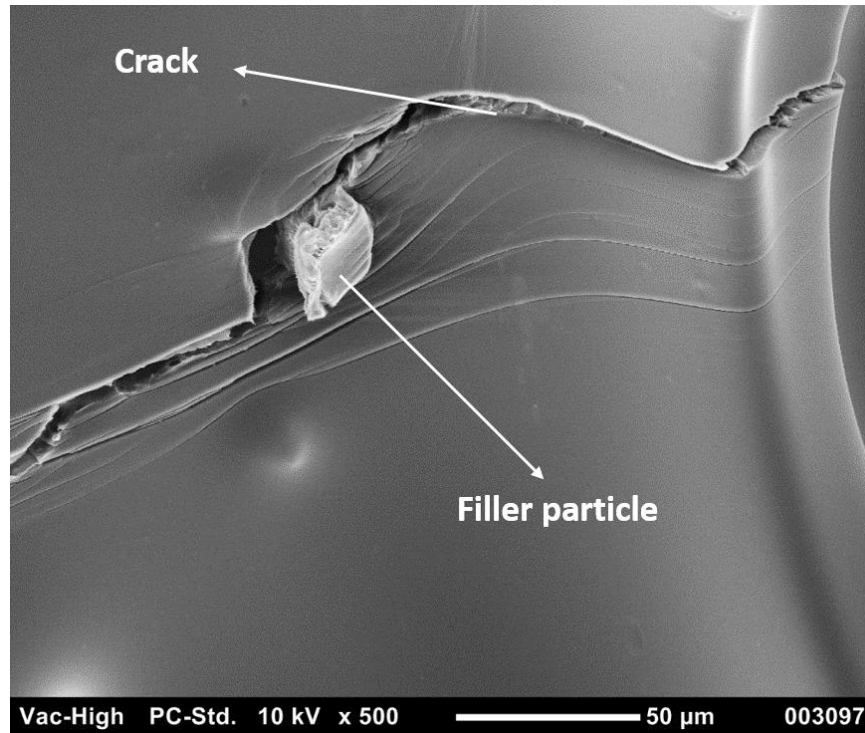


Fig. 49: Crack propagation in the composite

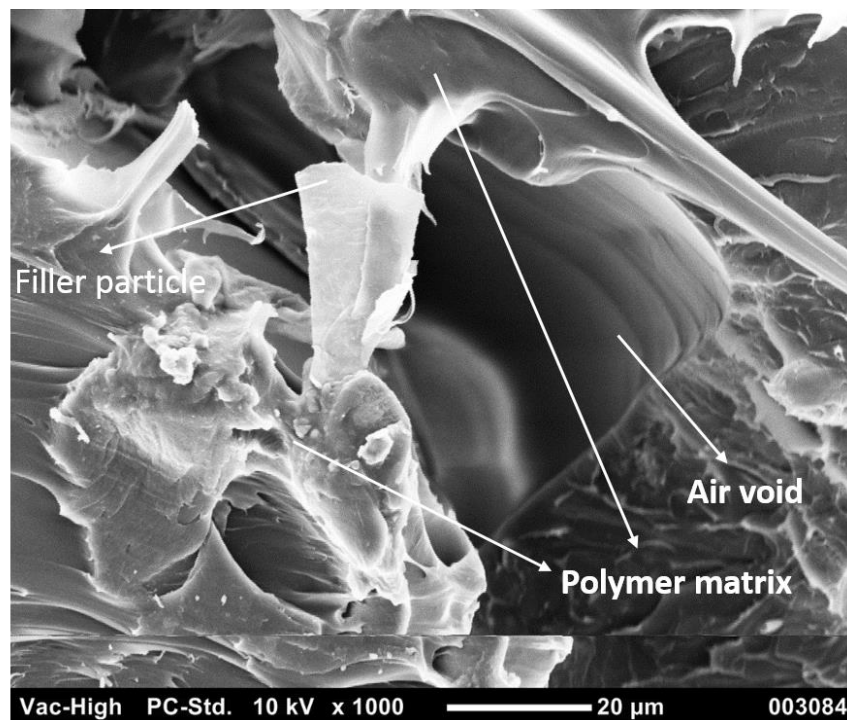


Fig. 50: The used filler as reinforcement agent

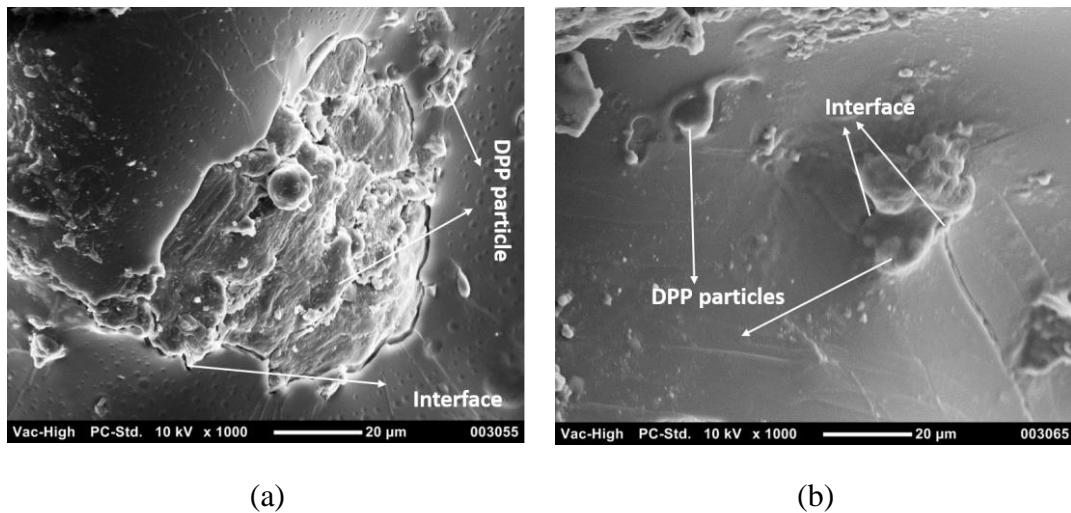


Fig. 51: SEM images: (a) 30-DPP composite; (b) treated 30-DPP composite

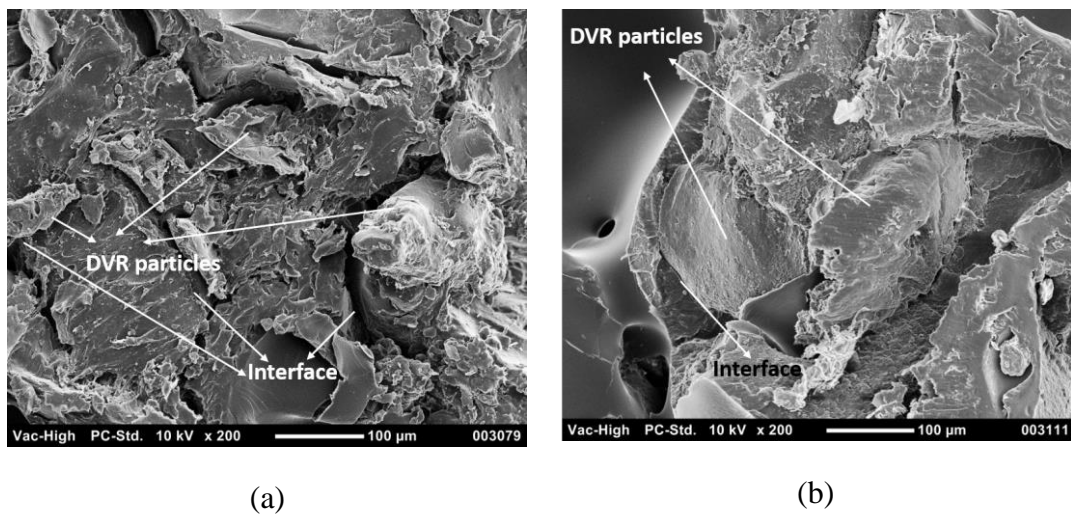


Fig. 52: SEM images of: (a) 30-DVR composite; (b) treated 30-DVR composite

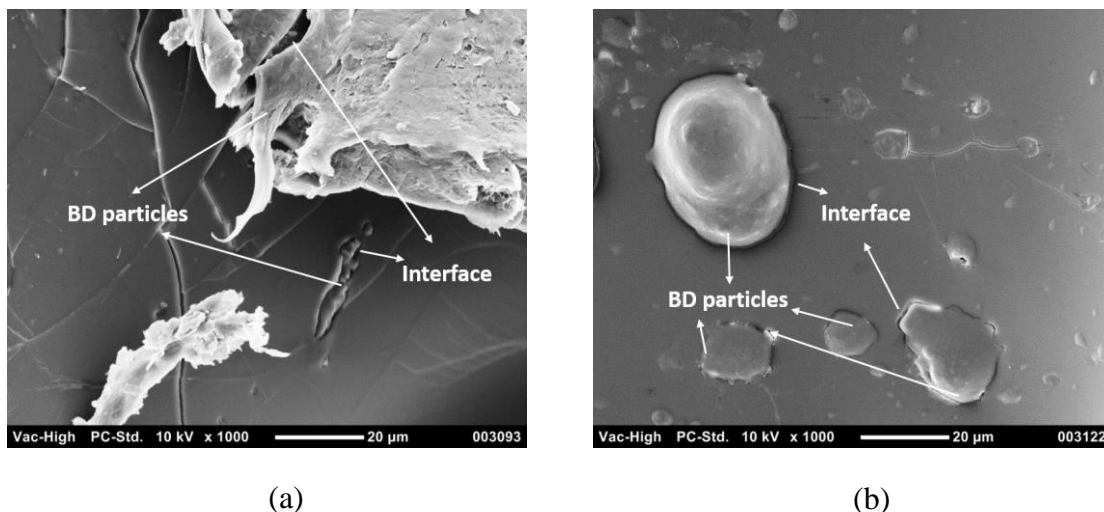


Fig. 53: SEM images of: (a) 30-BD composite; (b) treated 30-BD composite

3.3 Density

3.3.1 Date pits

Fig. 54 shows the theoretical and experimental density of the composites for different fillers. The theoretical density was calculated using Equation 1, while the experimental density was found by dividing the prepared sample weight by the measured volume. The densities of pure PS and DPP used in Equation 1 were measured experimentally to be 457 and 534 kg/m³, respectively. The theoretical density increased linearly with increasing DPP content due to the higher density of the DPP. Although the composite density increased with the filler content, the density of the 50-DPP composite remained lower than those of some reported composites, such as that of a wood-plastic composite and a date seed-concrete composite, which was found to be around 1200 kg/m³ [119]. The experimental density was higher than the theoretical density for all filler contents, and the increase was larger than the theoretically predicted increase. Natural fillers are known to induce voids when mixed with hydrophobic polymers, and the fillers agglomerate because of their hydrogen

bonds [85, 108]. Furthermore, in [39] the researchers reported that inducing voids in the matrix reduced the density. However, pure PS samples have air voids, which appear as white spots in Fig. 55. DPP may be agglomerated inside these voids, thereby filling them. The voids in 20-DPP composite were noticeably smaller than the voids in pure PS. This could explain the more dramatic increase in composite density observed experimentally.

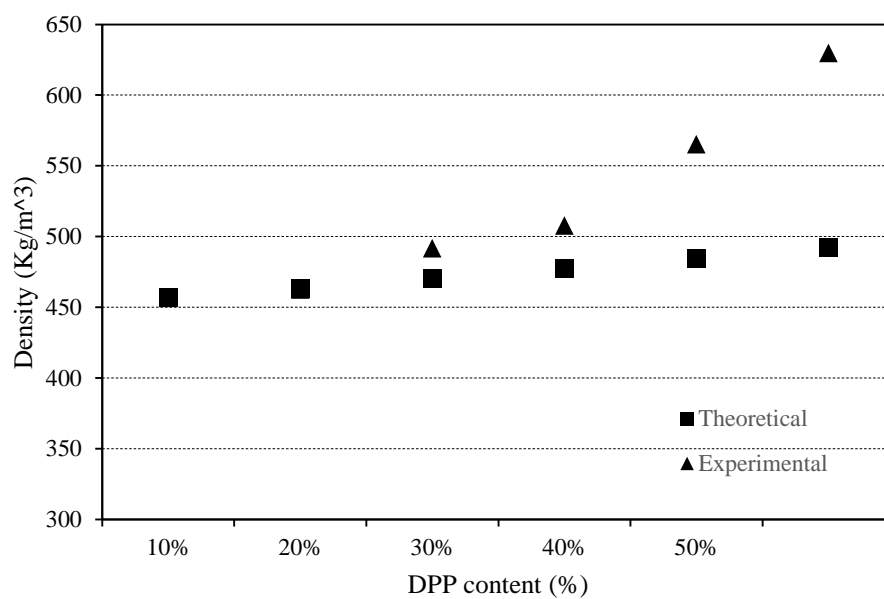


Fig. 54: DPP-PS composite density for different filler contents

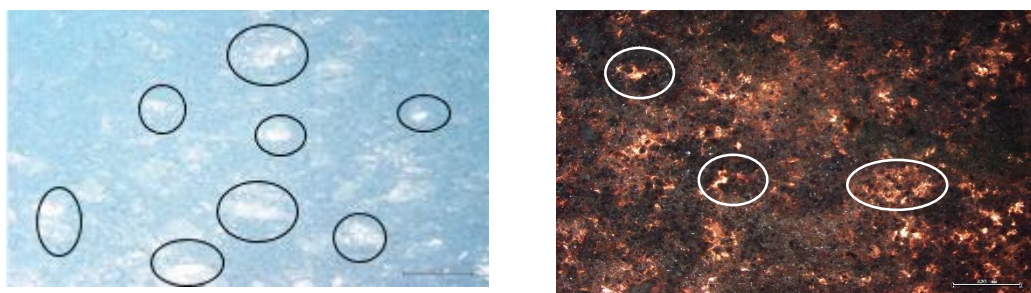


Fig. 55: Voids in the pure PS sample and DPP-PS composite

3.3.2 Devulcanized rubber

In this section, the effect of adding DVR on the density of the PS composite is discussed. Experimental and theoretical densities of the developed DVR-PS composites are shown in Fig. 56. The theoretical density of the composites was determined using Equation 1. The densities of pure PS and DVR were found to be 457 kg/m^3 and 527 kg/m^3 , respectively. The densities of PS and DVR were measured experimentally and these were used for the theoretical calculations. As shown in Fig. 56, the theoretical density of the composite increased linearly with increasing DVR content. The experimental results showed that the addition of 10 wt. % of DVR sharply increased the composite density. This was followed by slight density increase for higher DVR content. The tire rubber particles are known to entrap air inside the matrix when they are added [43, 117]. However, similar to the DPP-PS composite case, the added DVR could fill the existing air voids in the matrix, as shown in Fig. 57. The observed sharp increase in the density of 10-DVR composite was mainly due to replacing air voids in the composite with rubber particles. Furthermore, replacing the PS with rubber particles caused an additional small increase in the density. The density continued to increase slightly for DVR-PS composites with a rubber content varying between 20 and 50 wt. %, since the air voids were already filled with 10 wt. % DVR and the small density difference between PS and DVR was the dominant factor. The 50-DVR composite had the highest density (577 kg/m^3). Yet the value is much lower than that of some rubber thermal insulation composites such as foamed Portland cement composite [43] and plaster composite boards [42].

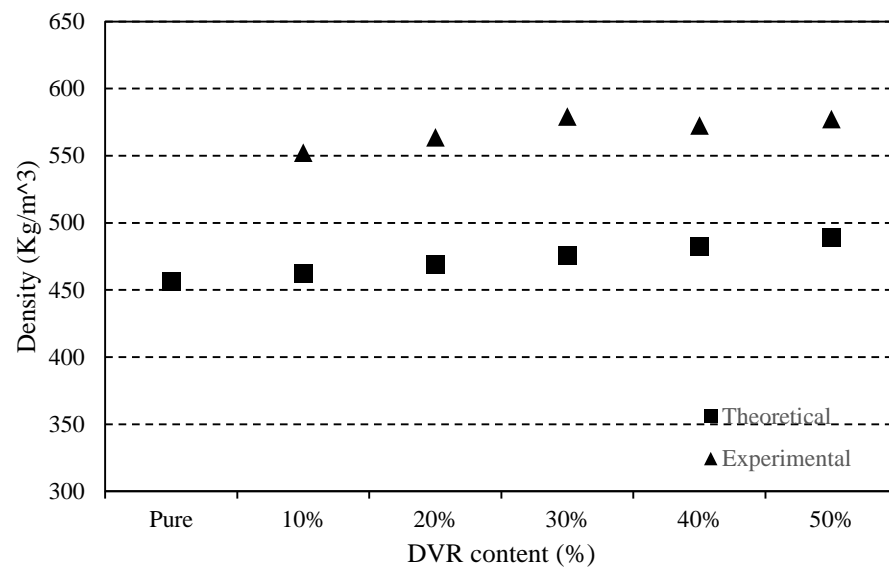


Fig. 56: DVR-PS composite density with varying filler content

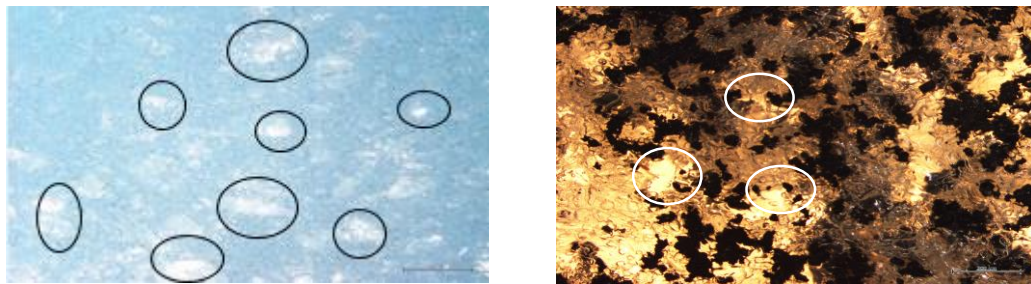


Fig. 57: Voids in the pure PS sample and DVR-PS composite

3.3.3 Buffing Dust

Fig. 58 demonstrates the effect of adding BD to the PS matrix on the theoretical and experimental density of the composite. Both the densities of BD and PS, used in Equation 1, were measured experimentally. The BD density was measured to be 326 kg/m^3 while the PS density was measured to be 577 kg/m^3 . It was observed that composite density decreased with increasing filler content due to the low density of BD. Similar results were reported in Lakraflı, Tahiri, Albizane, and El Otmani study [75]. Both experimental and theoretical results reduced linearly with filler content. There was a maximum 30 % difference between the experimental and predicted

results. Furthermore, as with DVR, a high rate of increase was observed for 5-BD composite in the experimental results. Again, this was due to the presence of air voids in the pure PS specimen that were filled by the filler. Optical microscopy was used to investigate the density of the voids and their size. The images in Fig. 59 show that the number of voids reduced with increasing filler content. In [75], the researchers studied the effect of BD incorporation into cement and plaster samples. It may be concluded that the BD-PS composites had superior density when compared with BD-cement and BD-plaster composites. To the best of the author's knowledge, no previous research in the literature has utilized BD waste in insulating polymeric composites.

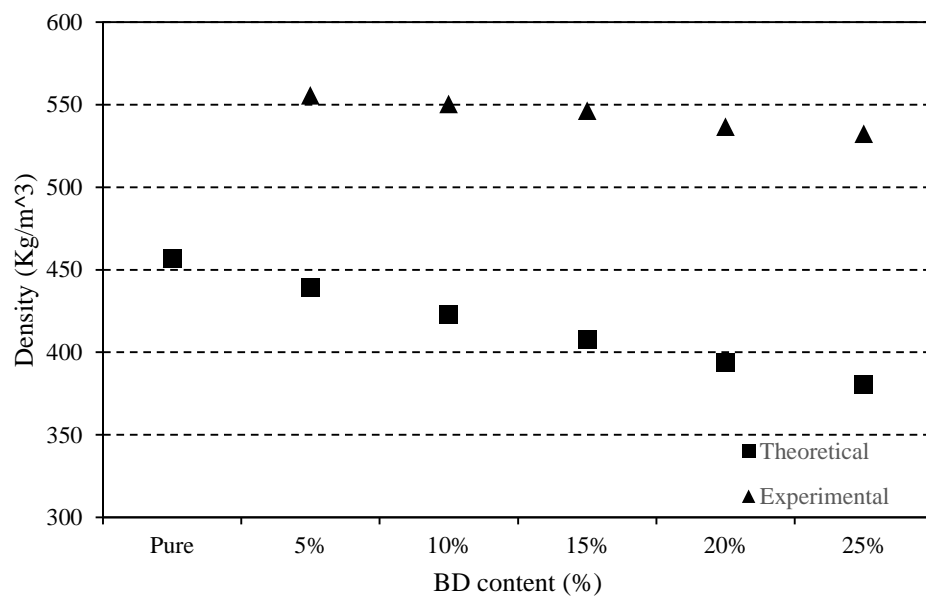


Fig. 58: BD-PS composites density for varying filler content

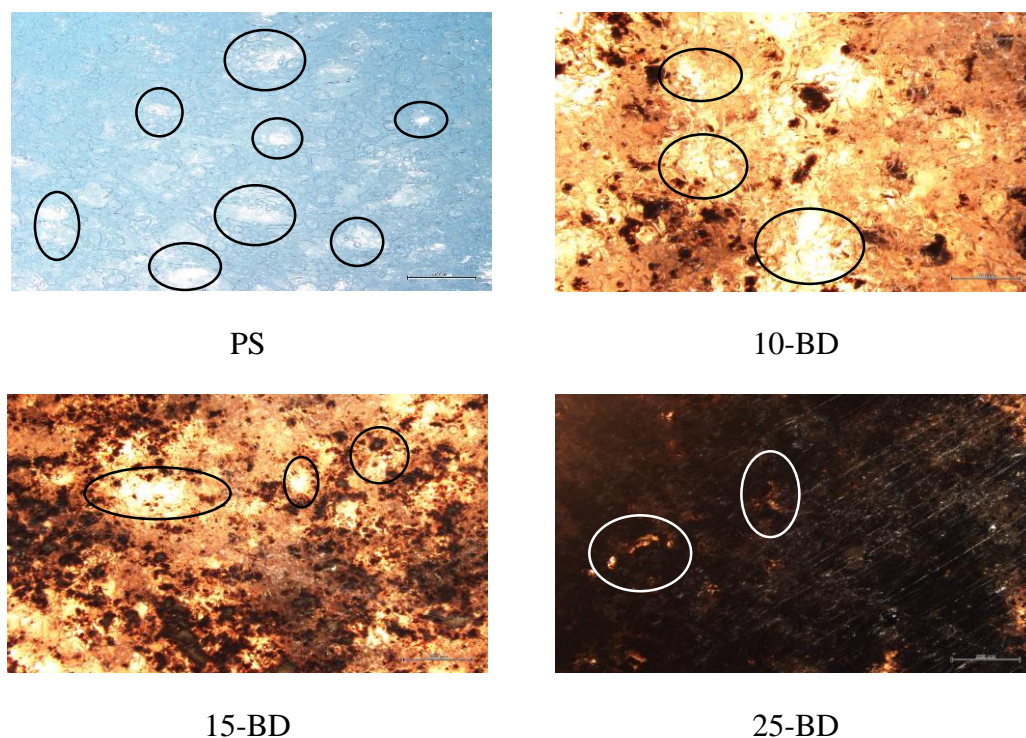


Fig. 59: Voids in the pure PS sample and BD-PS composite

3.4 Thermal conductivity

3.4.1 Date pits

The thermal conductivity of the DPP-PS composites was measured at different temperatures from 5 to 50 °C. The thermal conductivity coefficients of the composites varied between 0.0470 and 0.0600 W/m-K, with DPP contents ranging from 0 % to 50 %, respectively. Fig. 60 demonstrates the effect of the filler content on the thermal conductivity of the DPP-PS composites at room temperature. The thermal conductivity of pure PS was measured experimentally to be 0.0515 W/m-K at room temperature (25 °C). The thermal conductivity of the 50-DPP composite was 0.0562 W/m-K, which is only 9.2 % greater than that of pure polystyrene. The 10-DPP, 20-DPP, 30-DPP and 40-DPP composites exhibited small increases in the thermal conductivity coefficients relative to that of pure PS (i.e., increases of 0.37 %, 2.86 %, 8.27 % and

8.4 %, respectively, at 25 °C). In [39], the researchers related the voids in a composite structure to its thermal conductivity values. They reported that the voids increased with filler content in the polyester matrix, thereby reducing thermal conductivity. However, as discussed in section 3.3.1, the voids in the areas shown in Fig. 55 decreased in size within the DPP composite. Considering the difference in the thermal conductivity of air and DPP may explain the slight increase in thermal conductivity.

Demirboğa and Gül [120], Abu-Jdayil, Mourad, and Hassan [39, 121], and Al Rim, Ledhem, Douzane, Dheilily, and Queneudec [122] reported a linear relationship between thermal conductivity and density, which is given in Equation 3:

$$k = A + B \times \rho_{composite} \quad \text{Eq.3}$$

where A and B are constants, and ρ (in $\frac{kg}{m^3}$) is the density.

Fig. 61 shows the change in the thermal conductivity with density. The linear fitting parameters are $k = 0.0384 + 3 \times 10^{-5} \rho_{composite}$ with an R^2 value of 0.9359. Note that higher densities are associated with higher thermal conductivity values, possibly due to the higher number of voids in lower-concentration composites, which have more air inside the composite.

Fig. 62 shows the thermal conductivities of all composites over the studied temperature range (5 to 50 °C), which demonstrates that the thermal conductivity coefficient of the samples linearly depends on the temperature change. This linear dependency can be expressed by Equation 4:

$$k = C + mT \quad \text{Eq. 4}$$

where k is the thermal conductivity coefficient, C and m are constants, and T (in °K) is the temperature.

The extremely small m values in Table 10 indicate that the thermal conductivity of the DPP–PS composite is weakly dependent on temperature. This is considered an advantage of the composite as its thermal conductivity coefficient will not change significantly with temperature in building construction applications, especially in hot-climate countries.

Although increasing the proportion of date pits increased the thermal conductivity of the composite, the thermal conductivity was still lower than that of some other date-pit composites, e.g. polyester-date-pit composites [123]. In addition, this composite enables the replacement of 50 % of the polystyrene, which is often used in the thermal insulation industry, with a natural filler derived from waste, without significantly increasing thermal conductivity. PS is known to be non-biodegradable [124].

Walls made from building bricks, concrete stone and reinforced concrete, have thermal conductivities of 0.72, 0.93 and 1.73 W/m-K, respectively. The overall thermal conductivity without insulation is calculated to be 1.01 W/m-K, using Equation 5:

$$\frac{1}{K_{overall}} = \sum_{i=1}^n \frac{w_i}{k_i} \quad \text{Eq.5}$$

where $K_{overall}$ is the average thermal conductivity, K_i is the thermal conductivity of the component, and w_i is the weight fraction of the component.

If one-third of the wall by weight was made from the 50-DPP composite, the overall all thermal conductivity would be:

$$\frac{1}{K_{overall}} = \sum_{i=1}^n \frac{w_i}{k_i} = \frac{0.667}{1.01} + \frac{0.333}{0.05624} = 6.58 \text{ m} - \text{K/W}$$

$$K_{overall} = 0.1519 \text{ m} - \text{K/W}$$

Thus, using a DPP–PS composite would lead to a huge reduction in the thermal conductivity of the wall, resulting in an overall thermal conductivity of 0.1519 W/m-K, representing a reduction of 84.8 %.

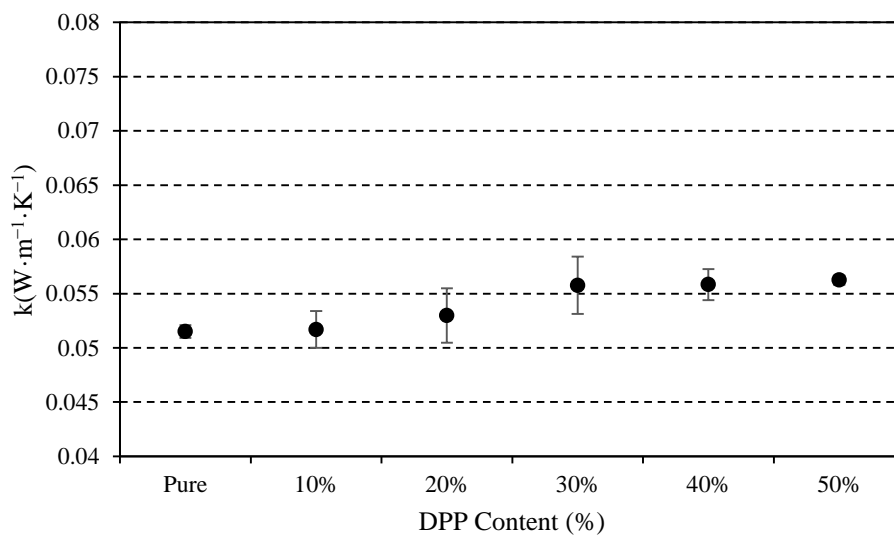


Fig. 60: Thermal conductivity variation of DPP-PS composite at 25 °C

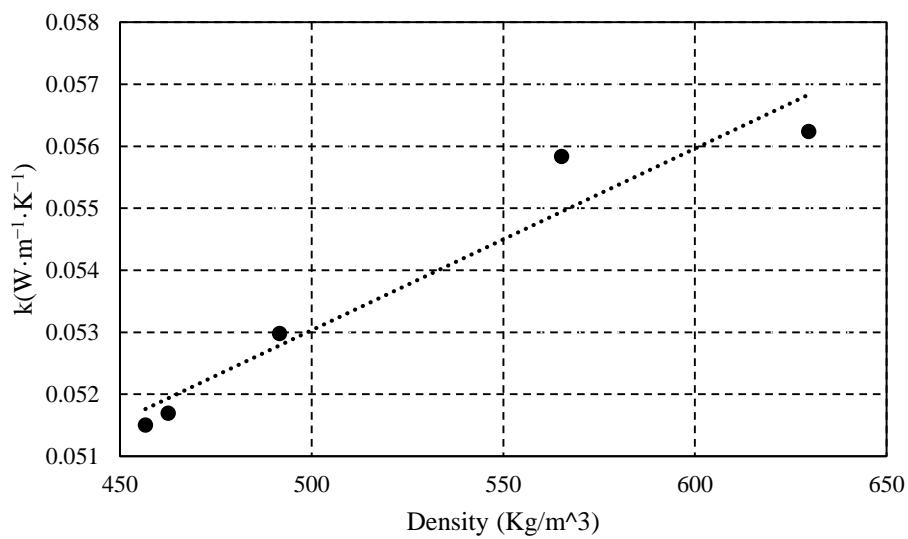


Fig. 61: Relationship between the DPP-PS composites density and thermal conductivity at 25 °C

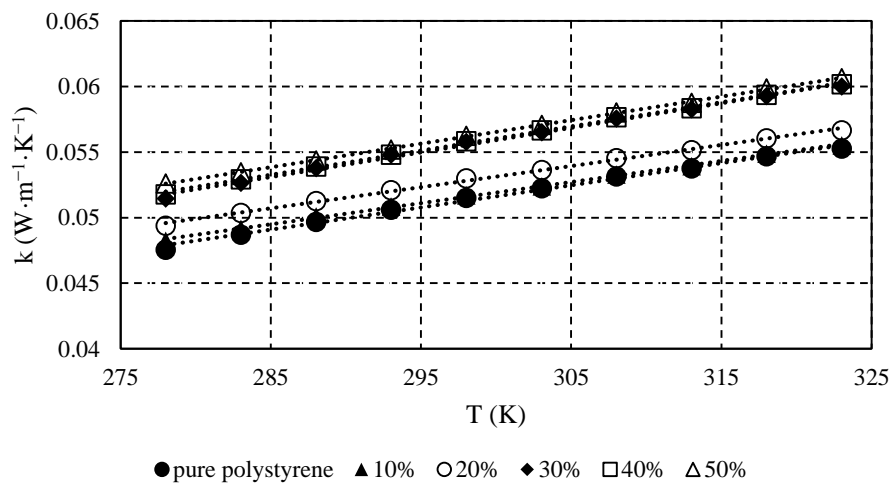


Fig. 62: Thermal conductivity of the DPP-PS composites

Table 10: DPP-PS fitting parameters

Content	C ($\text{W}\cdot\text{m}^{-1}\cdot\text{K}^{-1}$)	$m \times 10^{-3}$ ($\text{W}\cdot\text{m}^{-1}\cdot\text{K}^{-2}$)	R^2
Pure	0.0.00078	0.17	0.9974
10-DPP	0.0.00355	0.16	0.9986
20-DPP	0.00481	0.16	0.9974
30-DPP	0.00035	0.19	0.9959
40-DPP	0.00071	0.18	0.9983
50-DPP	0.00266	0.18	0.9994

3.4.2 Devulcanized rubber

In this section, the effect of adding different proportions of DVR to PS matrix on DVR-PS thermal conductivity is discussed. The thermal conductivity of composites was tested over a temperature range of 5 to 50 °C. Fig. 63 shows the thermal conductivity measurements for the 10-DVR, 20-DVR, 30-DVR, 40-DVR and 50-DVR composites at room temperature. It is noted that the thermal conductivity of 10-DVR was slightly less than that of pure PS. For low DVR content, the rubber may be well distributed in the PS matrix and hence there is a high possibility of air entrapment around the particles. However, the DVR may agglomerate in the DVR-PS composites with higher DVR contents. This may induce two negative effects: DVR particles could agglomerate inside the existing voids; and these particles may entrap less air around them. Further, the DVR thermal conductivity was 0.191 W/m-K [125], while the PS thermal conductivity was measured to be 0.0515 W/m-K. The aforementioned two effects and the difference in thermal conductivity between the DVR and the PS could explain the observed increase in thermal conductivity among the high DVR composites. It was observed that the 50-DVR composite had the highest thermal

conductivity (0.07356 W/m-K), which was 30.8 % higher than the thermal conductivity of the pure sample. It is worth mentioning that the thermal conductivity of composites with less than 30 wt. % DVR content increased only by 15 % compared with that of the pure PS. In contrast, the thermal conductivity of the 10-DVR composite was less than that of pure PS by 4 %. The entrapped air due to the incorporation of the DVR particles is negligible if compared with replacement of air voids with DVR particles. The sharp increase in density shown in Fig. 56 and the tensile mechanical properties of the 10-DVR composite demonstrate that the incorporation of DVR reduced the presence of air in the composite. Therefore, the observed reduction in thermal conductivity for 10-DVR composite appeared to be mainly due to the improvement in measurement accuracy.

The measured thermal conductivity of the 30-DVR composite was lower than that of the scrap rubber-polyester composite, crumbed rubber-concrete panel and the plaster-rubber board, by 46.5 %, 73.34 % and 54.11 %, respectively. This positions DVR-PS developed composites as viable alternatives in building insulation. Moreover, using these composites would help reduce the use of non-biodegradable PS [124].

Fig. 65 demonstrates a linear relationship between the temperature and the thermal conductivity. The linear fitting parameters of thermal conductivity results are presented in Table 11. As the slope values are small, the DVR-PS composites maintained their thermal conductivity values at high temperatures.

Furthermore, if one-third of a wall with a thermal conductivity of 1.01 W/m-K were replaced with 30-DVR composite, the thermal conductivity would be reduced by 83.1 %, according to Equation 4:

$$\frac{1}{K_{overall}} = \sum_{i=1}^n \frac{w_i}{k_i} = \frac{0.667}{1.01} + \frac{0.333}{0.064235} = 5.84 \text{ m} - \text{K/W}$$

$$K_{overall} = 0.1711 \text{ m} - \text{K/W}$$

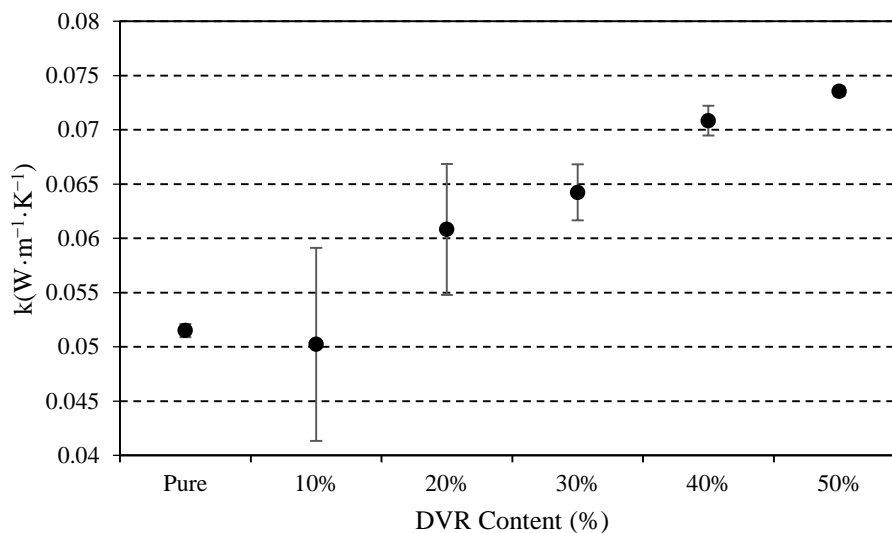


Fig. 63: Thermal conductivity variation of DVR-PS composites 25 °C

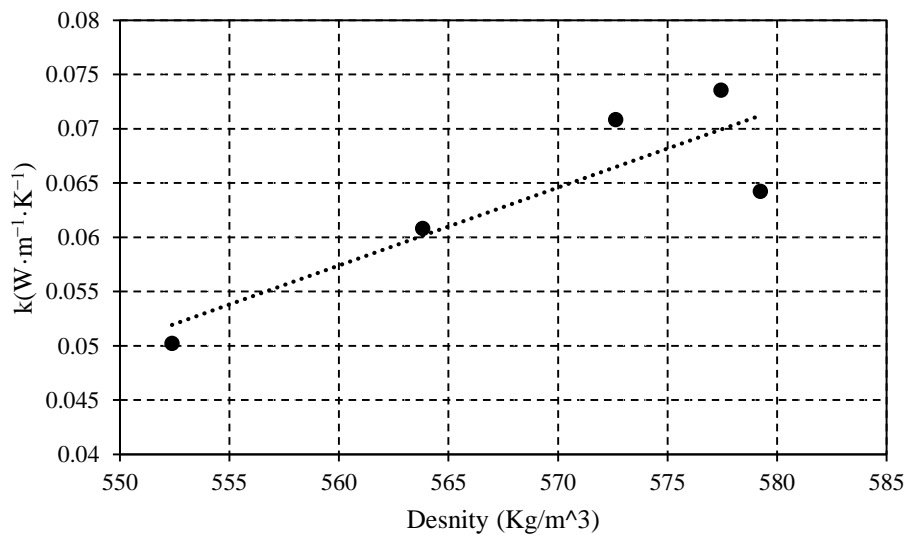


Fig. 64: Relationship between DVR-PS density and thermal conductivity at 25 °C

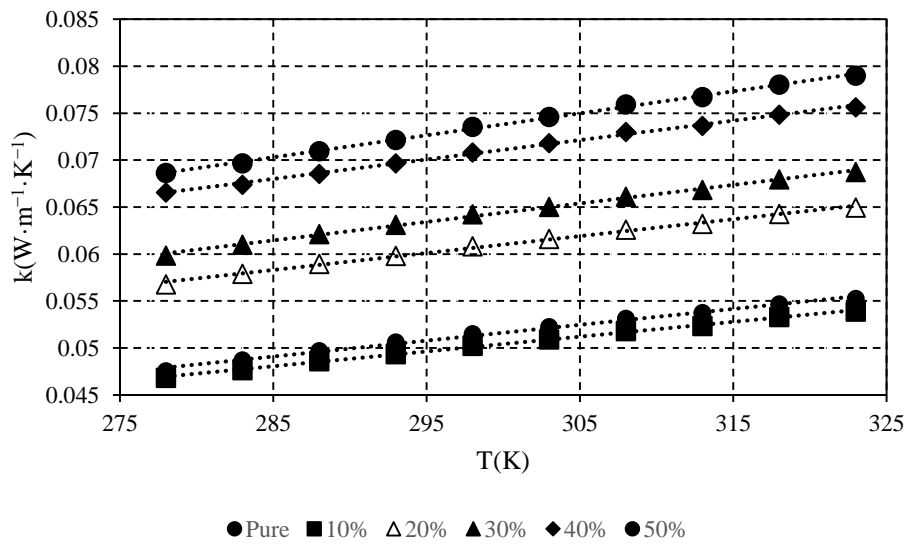


Fig. 65: Thermal conductivity of DVR-PS composites

Table 11: DVR-PS fitting parameters

Content	$C(W \cdot m^{-1} \cdot K^{-1})$	$m \times 10^{-3}(W \cdot m^{-1} \cdot K^{-2})$	R^2
Pure	0.00078	0.17	0.9974
10%	0.00313	0.16	0.9980
20%	0.00683	0.18	0.9970
30%	0.00547	0.20	0.9976
40%	0.00913	0.21	0.9973
50%	0.003590	0.23	0.9981

3.4.3 Buffing dust

Fig. 66 shows the effect of adding BD to PS on the thermal conductivity of BD-PS composite at 25 °C, while Fig. 67 demonstrates the variation in thermal conductivity of BD-PS composites in the temperature range of 5 to 50 °C. As may be seen from Fig. 66, the thermal conductivity was reduced to its lowest value at 10 wt. % before increasing again for the 15-BD, 20-BD and 25-BD composites. The thermal

conductivity of the 10-BD composite was 0.0447 W/m-K, which was 13.29 % lower than that for pure PS. Furthermore, the thermal conductivity of the 15-BD composite was almost as same as that of pure PS. BD wastes have a low thermal conductivity [76]. In addition, BD reduced the number of air voids in the sample, as shown in Fig. 59. These two factors control the trend in thermal conductivity (Fig. 67). The first factor reduced the thermal conductivity to some extent since the PS, which has higher thermal conductivity than BD, was replaced by BD. The second effect increased the thermal conductivity since the thermal conductivity of air is lower than that of BD. In other words, while the positive effect of replacing a portion of PS with BD was dominant for filler contents less than 10 wt. %, the negative effect of removing air voids from the composite was dominant for filler content higher than 10 wt. %. The BD-PS composites had superior thermal conductivity. The composite has a very low thermal conductivity compared with other BD developed composites [75] or other developed thermal insulation composites [39, 121]. In addition, it offers the prospect of an ingenious recycling solution for leather waste [64] and a method for reducing the use of non-biodegradable PS [124]. Moreover, when a linear equation was fitted to the change of thermal conductivity with temperature relationship, as with the DPP-PS and DVR-PS composites, the slope values were very small, as shown in Table 12. This is a highly desirable property for thermal insulation materials, especially in hot climate countries.

The previously-used Equation 3, which relates density and thermal conductivity linearly, was not used in this section. This equation is not applicable to this particular filler, as the relationship between filler content and thermal conductivity is nonlinear.

If the thermal conductivity of a wall is assumed equal to 1.01 W/m-K, according to [113], replacing one-third of the wall with 10-BD results in an 87.80% reduction in the overall thermal conductivity, as calculated below.

$$\frac{1}{K_{overall}} = \sum_{i=1}^n \frac{w_i}{k_i} = \frac{0.667}{1.01} + \frac{0.333}{0.044655} = 8.12 \text{ m} - \text{K/W}$$

$$K_{overall} = 0.123 \text{ m} - \text{K/W}$$

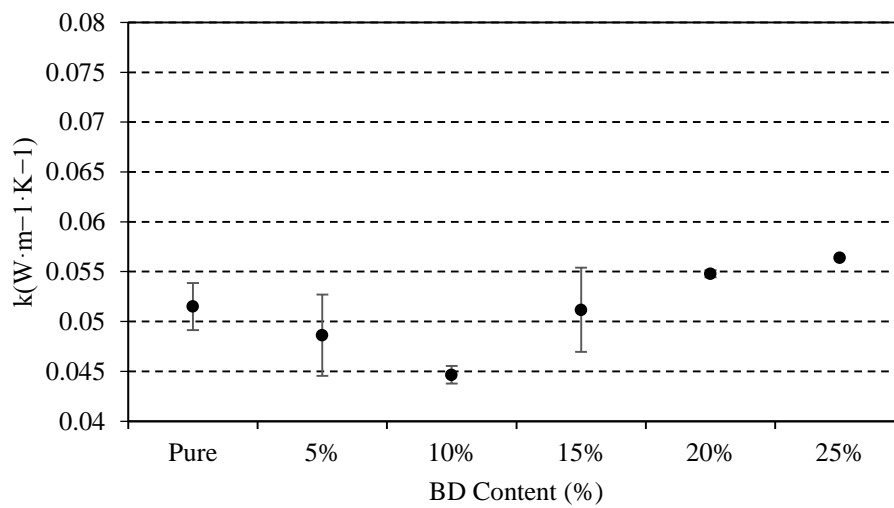


Fig. 66: Variation in thermal conductivity of BD-PS composites at 25 °C

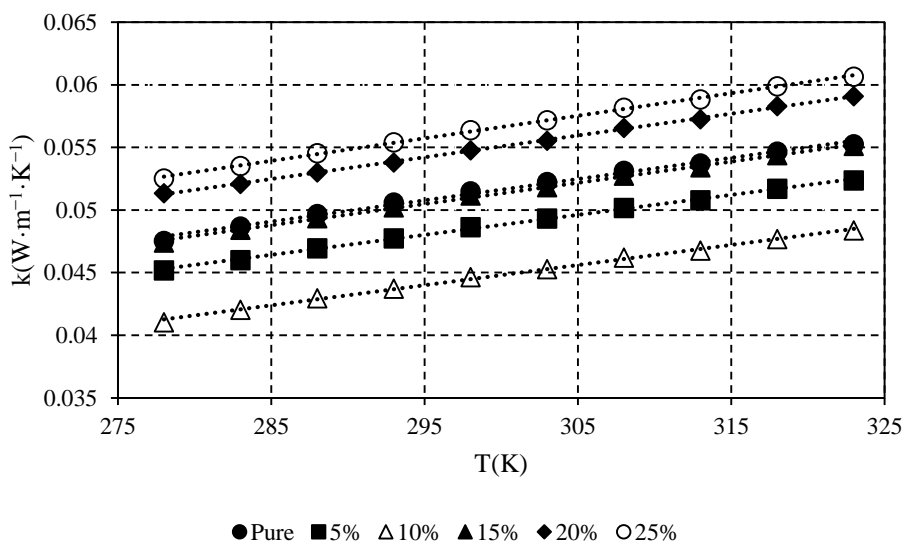


Fig. 67: Thermal conductivity in BD-PS composites

Table 12: BD-PS fitting parameters

Content	$C(W \cdot m^{-1} \cdot K^{-1})$	$m \times 10^{-3}(W \cdot m^{-1} \cdot K^{-2})$	R^2
Pure	0.00078	0.17	0.9974
10%	0.00089	0.16	0.9985
20%	0.00348	0.16	0.9975
30%	0.00506	0.17	0.9983
40%	0.002912	0.17	0.9992
50%	0.002619	0.18	0.9987

3.4.4 Treated fillers

The effect of NaOH treatment on the thermal conductivity of the developed composites is discussed in this section. As shown in Fig. 68, the thermal conductivity of all composites decreased with NaOH treatment. Thermal conductivity of the treated 25-BD composite decreased slightly, while the thermal conductivities of the 30-DPP and 30-DVR composites reduced by 14 % compared with their original values.

Agrawal, Saxena, Sreekala, and Thomas [126] reported that treatment of oil-palm fibers with alkali leads to irreversible mercerization and an increase in fiber diameter, which resulted in a slight increase in the thermal conductivity of the composite. It was reported by Ibraheem, Ali, and Khalina [127] that treatment of kenaf fiber with alkali increases thermal conductivity of the composite by 38.15 % by improving the contact area between the fiber and the matrix. Thus, treatment of the developed composites in the current research was expected to increase thermal conductivity, as it enhances the interlocking between the fillers and the matrix and consequently improves the mechanical properties. However, the results showed a reduction in the thermal conductivity of the composite. This may be explained by improved filler distribution. In other words, increasing the homogeneity of the composites enabled the instrument to measure the thermal conductivity more accurately, so the observed reduction may be due to measurement accuracy, rather than the chemical treatment.

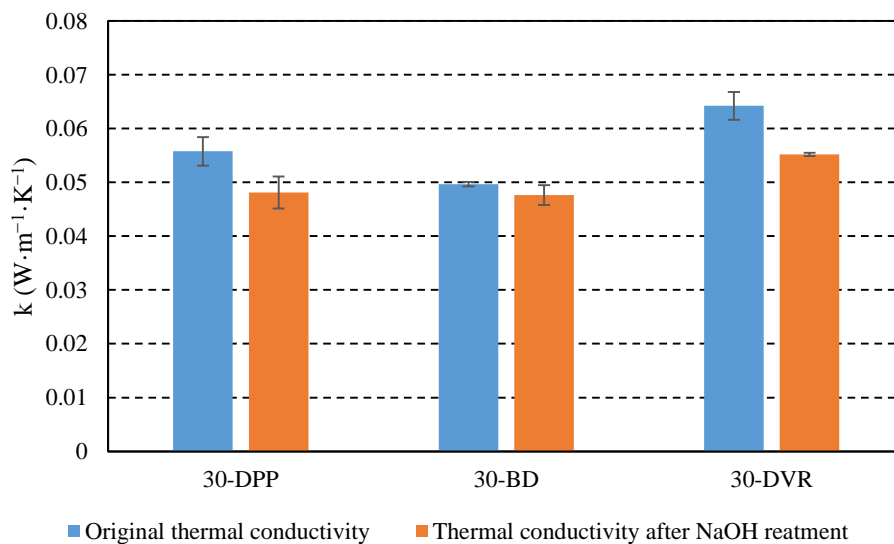


Fig. 68: Thermal conductivity of treated fibers composites

3.5 Thermogravimetric analyses

3.5.1 Date pits

Fig. 69 shows the weight loss versus the temperature for pure PS, DPP and their composites with filler contents varying from 0 to 50 wt. %. The main TGA results are reported in Table 13. Pure PS showed one principal stage of degradation, while DPP showed three stages of degradation. The first stage in all composites was a loss of moisture content, although this did not represent a large weight loss. Date pits consist mainly of three components with decomposition temperatures between 200 and 700 °C: hemicellulose, cellulose and lignin. These observations were in agreement with the results of Wu, Schott, and Lodewijks [128]. Hemicellulose decomposes between 160 and 360 °C, and cellulose decomposes between 240 and 390 °C. The decomposition temperature range of lignin is wider and higher, i.e., between 250 and 700 °C [129]. Thus, the first peak in Fig. 70, which shows the variations of the weight change of pure date pits (i.e., the differential TGA (DTGA) curve), may be due to the decomposition of hemicellulose. The second peak may be due to decomposition of cellulose while the third peak may be due to decomposition of lignin. The date pits show an initial loss of 5 % at 87 °C, a 50 % weight loss at 289 °C, and a total weight loss of 96.11%. Pure PS exhibited an initial degradation of 5% at 286 °C, a 50% weight loss at 355 °C, and a total weight loss of 99.87%.

The thermal behavior of the composite with higher filler contents was closer to that of pure date pits. The composites with higher than 20 % date pits (10-DPP and 20-DPP) degraded in four stages; however, the 10-DPP composite and pure polymer degraded in three stages. Briones, Serrano, Younes, Mondragon, and Labidi [130] reported a similar result using Deglet-Nour date seed fruit. Fig. 69 shows that both the

initial degradation temperature and the total weight loss decreased with increasing filler content. In general, the thermal stability of the matrix reduced slightly. Thermal stability generally affects shrinkage of the insulation materials in case of fire.

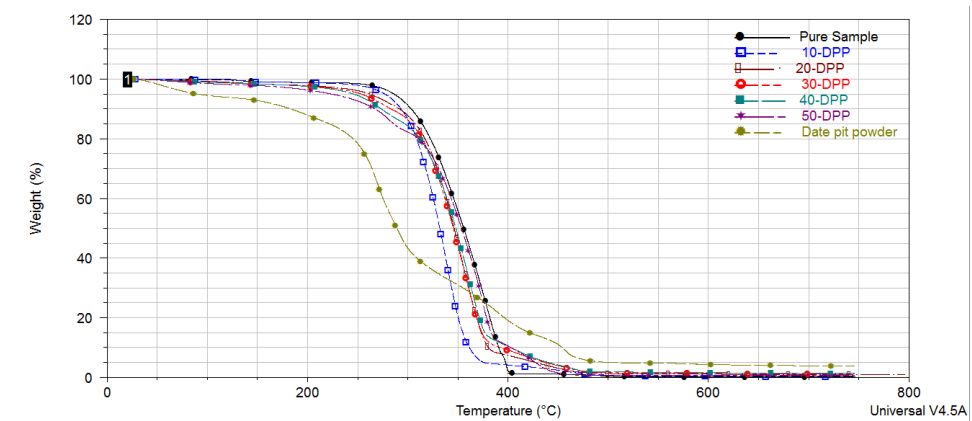


Fig. 69: Thermograms of DPP–PS composites with different filler content

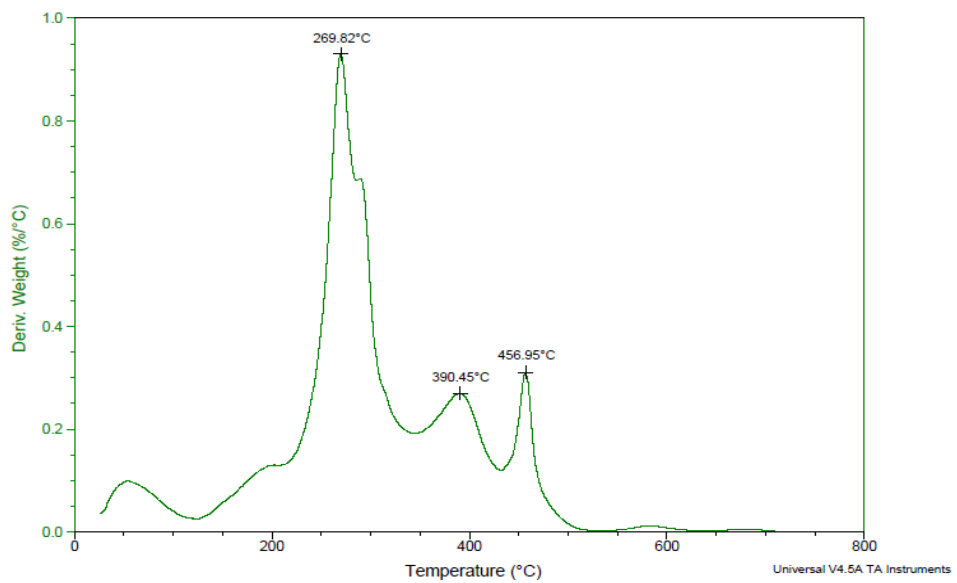


Fig. 70: DTGA curve of DPP

Table 13: Decomposition temperature of the DPP-PS composites

Samples	T5* (°C)	T50** (°C)	T _{max} (°C)	Overall change (%)
Pure PS	286	355	402	99.87%
10-DPP	274.7	333	501	99.62%
20-DPP	265	345.7	500	99.03%
30-DPP	251	345	497.1	98.74%
40-DPP	246.8	347.4	497	98.66%
50-DPP	236.7	352	494.5	99.10%
DPP	87	289	504	96.11%

*Temperature at which 5 % weight loss occurs

** Temperature at which 50 % weight loss occurs

3.5.2 Devulcanized rubber

Weight change with temperature of DVR, DVR-PS composites and pure PS is shown in Fig. 71. As discussed above, the pure PS decomposed in one stage, while the DVR degraded mainly over three stages. The weight of DVR was almost constant until it reached a temperature of 150 °C. After that, the weight of the DVR sample reduced moderately in the temperature range of 150 to 310 °C before dropping sharply between 310 and 400 °C. In the next stage, the weight reduced steadily until 700 °C. The first stage of degradation may be due to the decomposition of extender oil and other organic non-polymeric additives [131]. The second degradation stage may be due to decomposition of natural rubber, while the degradation of styrene–butadiene rubber and/or polybutadiene rubber may explain the third degradation stage [132]. Similar

degradation behavior was observed by Hassan, Badway, Elnaggar, and Hegazy [133] for DVR-polypropylene blends. The maximum weight loss occurred at 346 °C (Fig. 72).

Table 14 shows the main degradation temperatures of the pure DVR, pure PS and their composites. The addition of rubber to the PS composites had two effects: a reduction in the initial degradation temperature of the composites, as shown in Fig. 71; and a positive effect on weight loss of the composite. Increasing the filler content reduced the weight loss significantly, especially for high filler content composites, e.g. 30 to 50 wt. % composites for temperatures less than 600 °C. In fact, these composites follow the degradation trend of pure rubber.

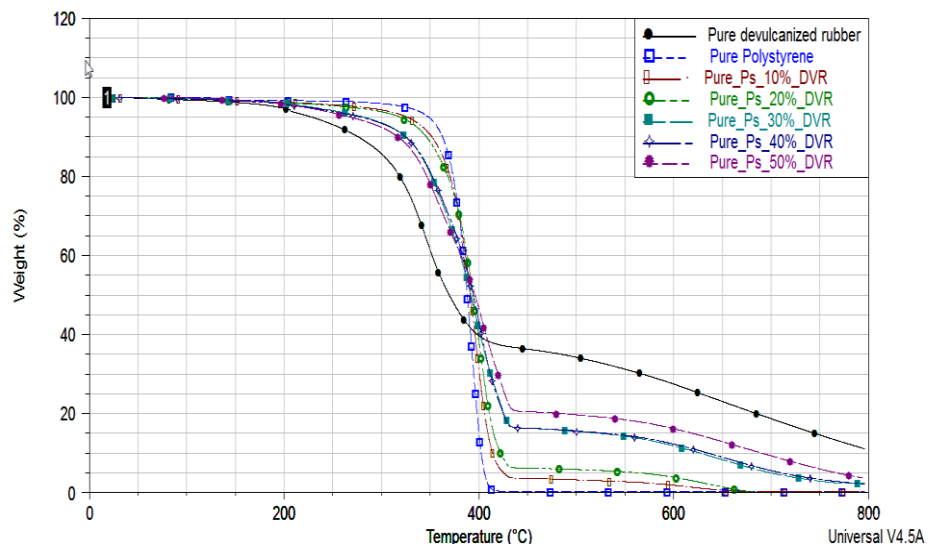


Fig. 71: Thermograms of DVR-PS composites for different filler content

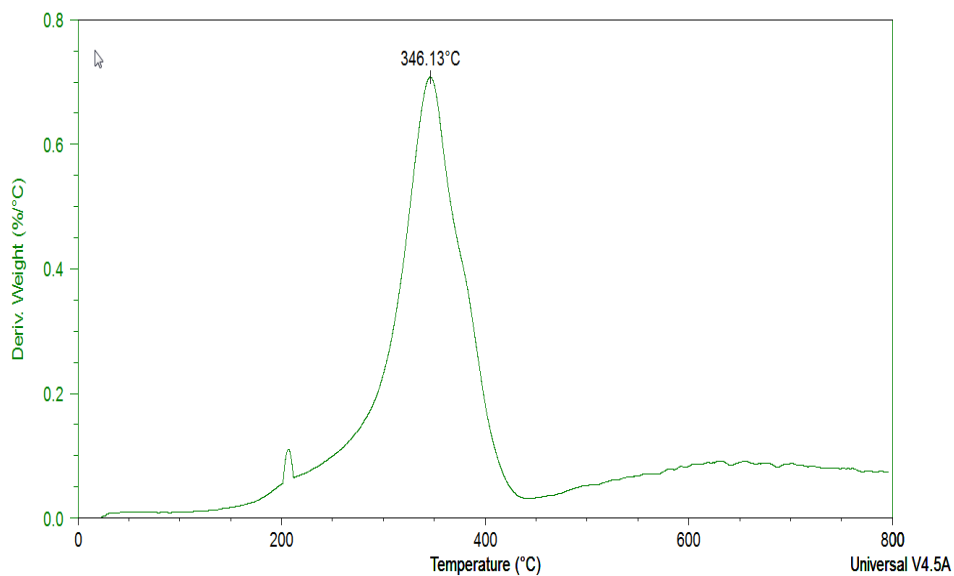


Fig. 72: DTGA curve of DVR

Table 14: Decomposition temperature of DVR-PS composites

Samples	T5* °C	T50** °C	T _{max} °C	Overall change (%)
Pure PS	286	355	402	99.87%
10-DVR	316	394	662	99.17%
20-DVR	324	391	648	99.24%
30-DVR	283	391	721	96.10%
40-DVR	284	394	743	96.44%
50-DVR	270	395	752	94.17%
Pure DVR	230	368	764	86.59%

*Temperature at which 5 % weight loss occurs

** Temperature at which 50 % weight loss occurs

3.5.3 Buffing dust

Weight loss of the BD-PS composites and the pure materials over the temperature range 30 to 800 °C is shown in Fig. 73. In addition, the main decomposition temperatures are listed in Table 15. BD decomposed mainly in two stages, as shown in Fig. 73 and Fig. 74. It may be noted from Fig. 73 that 10 % of the

BD weight was lost below 150 °C. The relative high weight loss may be explained by the high moisture content of BD waste. Madera-santan, Torres, and Lucero [134] reported that a BD moisture content of 7 %. Similar weight reductions at low temperatures for BD were observed in other studies, e.g. [64, 134, 135]. The pure BD experienced a moderate weight reduction over the temperature range 140 to 260 °C. This moderate weight reduction may be due to the crystallized water, oils and greases [134]. Furthermore, the higher temperature range weight loss may be due to decomposition of the collagen or protein. The weight loss peaks for BD were found to occur at 49 °C and 296 °C. A similar degradation trend of BD was noted in [134] and Joseph et al. [135], where they studied BD obtained from chrome tanned leather.

The composites with a BD content of 10 % or less display the same degradation characteristics as pure PS. On the other hand, composites with higher BD content (e.g. 25-BD) display the degradation characteristics of pure BD. As Fig. 73 indicates, total weight loss decreased with increasing BD filler content. However, the initial degradation temperature decreased with increasing BD content, which caused a slight decline in the thermal stability of the BD-PS composites.

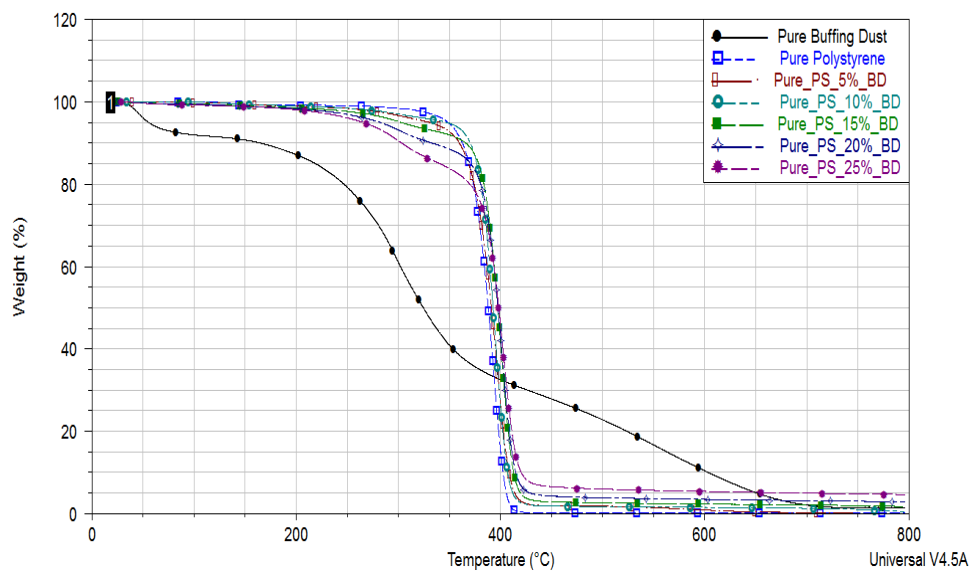


Fig. 73: Thermograms of BD-PS composites for different filler content

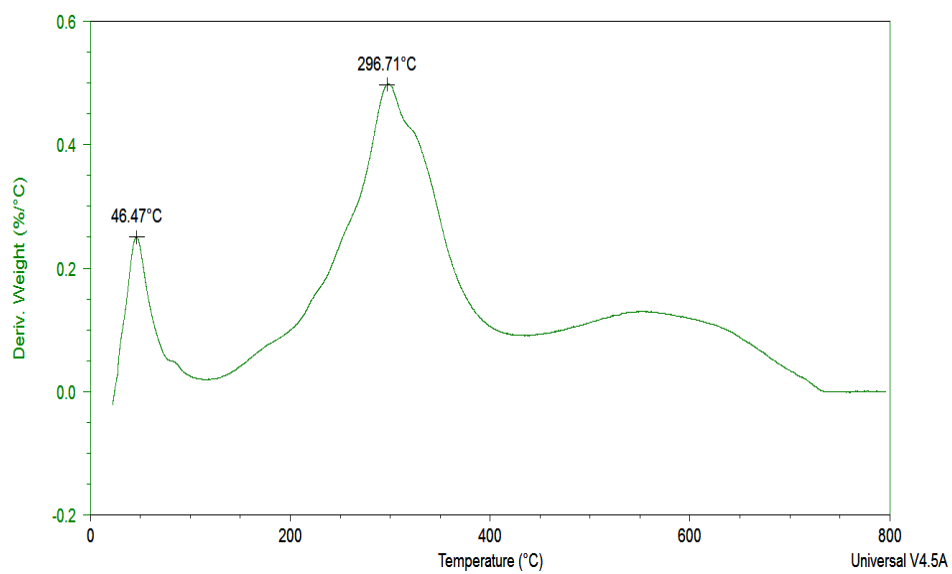


Fig. 74: DTGA curve of BD

Table 15: Decomposition temperature of BD-PS composites

Samples	T5* (°C)	T50** (°C)	T _{max} (°C)	Overall change (%)
Pure PS	286	355	402	99.87%
5-BD	329	391	551	98.54%
10-BD	349	392	641	98.4%
15-BD	302	397.39	616	97.67%
20-BD	282	397.57	606	96.55%
25-BD	265	398.41	611	94.63%
Pure BD	55	323	715	98.33 %

*Temperature at which 5 % weight loss occurs

** Temperature at which 50 % weight loss occurs

3.5.4 Treated fillers

In this section, the thermogravimetric properties of the treated fillers DPP, DVR and BD, are investigated. Fig. 75 shows the thermal events of treated and untreated DPP, while Fig. 76 and Fig. 77 show the thermal events of treated and untreated DVR and BD. It is noted that the treated DPP had less moisture content because the treated DPP was dried for 8 hours after the NaOH treatment. The second thermal event, which occurred between 240 °C and 300 °C is due to the degradation of hemicellulose, as discussed in section 3.5.1. The resultant weight loss in this event was found to be 35.7 % for treated DPP, which is 15 % lower than that for untreated DPP in this stage. Furthermore, treatment of DPP with NaOH caused a 5 % weight loss reduction for the cellulose thermal event, compared with the same event for untreated DPP cellulose, which occurred between 300 °C and 450 °C. The TGA results show a significant reduction in the hydrophilic components of DPP, which enhanced the adhesion between the DPP and the PS matrix and, consequently, its mechanical properties. In addition, the total weight loss of treated DPP at 600 °C was 30 % higher

than that of untreated DPP. That resulted in a significant improvement in the thermal stability of the treated DPP, and consequently in the developed DPP-PS insulator composites. In respect of DVR, it may be noted from Fig. 76 that the filler treatment had a positive effect on the thermal stability of the DVR filler for temperatures below 500 °C. The first degradation event (150 to 310 °C) was attributed to the decomposition of extender oil and non-polymeric additives (section 3.5.2). To investigate the effect of the treatment on the first thermal event, weight loss in both treated and untreated samples was measured at 300 °C by the TA Instruments Universal Analysis program. Weight loss of the non-treated DVR was found to be 4 % higher than that for the treated DVR, which indicates that part of the extender oil layer was removed by NaOH treatment. This explains the increased roughness in treated DVR samples observed under SEM (Fig. 46). At high temperatures (i.e., above 500 °C), thermal stability of the treated filler was found to be less than the untreated DVR. This indicates that the NaOH had attacked the styrene-butadiene rubber or polybutadiene rubber chains, causing a drop in the thermal stability of DVR filler at high temperatures. However, thermal stability in a high temperature range is insignificant since, in typical applications, building thermal insulators are intended perform at much lower temperatures. Fig. 77 shows that the treatment of BD filler increased thermal stability significantly, and the weight loss at 600 °C was reduced by 34 % for the treated filler. The first two thermal events, which were due to the removal of moisture content and crystallized water, oils and greases, was slightly affected. Furthermore, the weight loss of untreated and treated BD was found to be 89.64 % and 55.62 % at 600 °C, respectively. This indicates that a large fraction of the collagen was either removed from the BD or its structure was modified by NaOH treatment. The above events caused a crucial increase in the thermal stability of the BD filler. In fact,

BD SEM images (Fig. 47) support the view that the NaOH could alter the collagen structure, which was clearly evident in the change to the filler shape. The mechanical properties of the treated composites were boosted because of the improved distribution of the shape-modified BD particles in the PS matrix. In addition, the NaOH treatment interacted with hydrogen molecules in collagen chains, causing a change in the surface charge of the collagen molecule. The compatibility improvement between the BD filler and PS may be due to the induced surface charges.

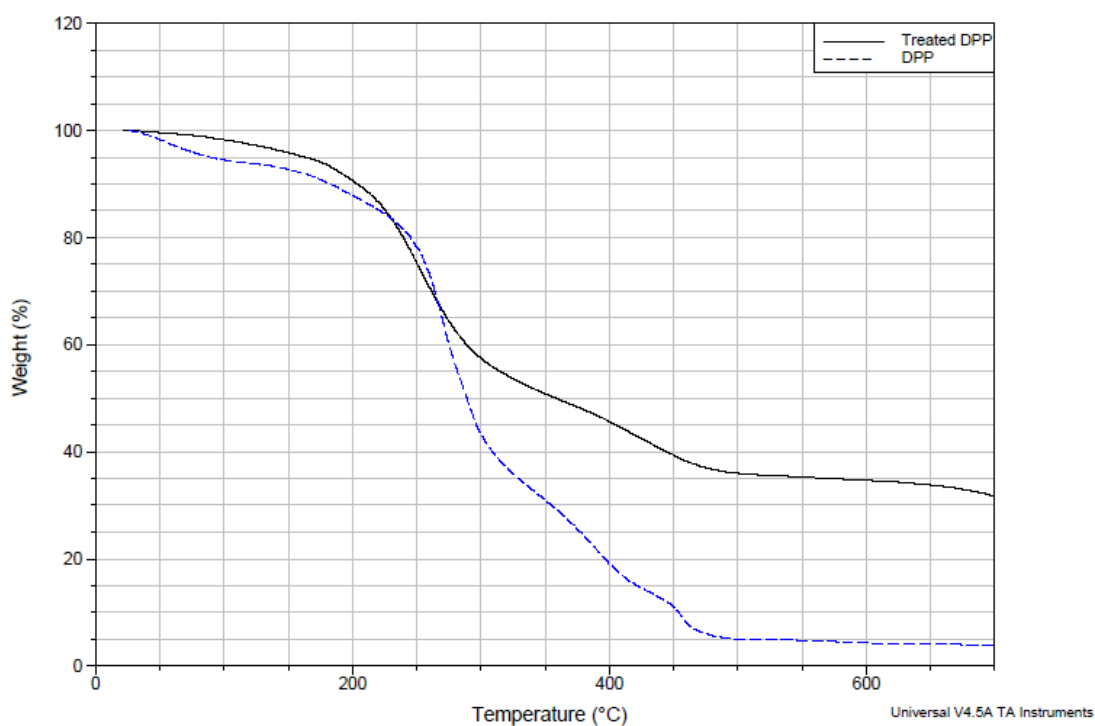


Fig. 75: Thermograms of untreated DPP and treated DPP

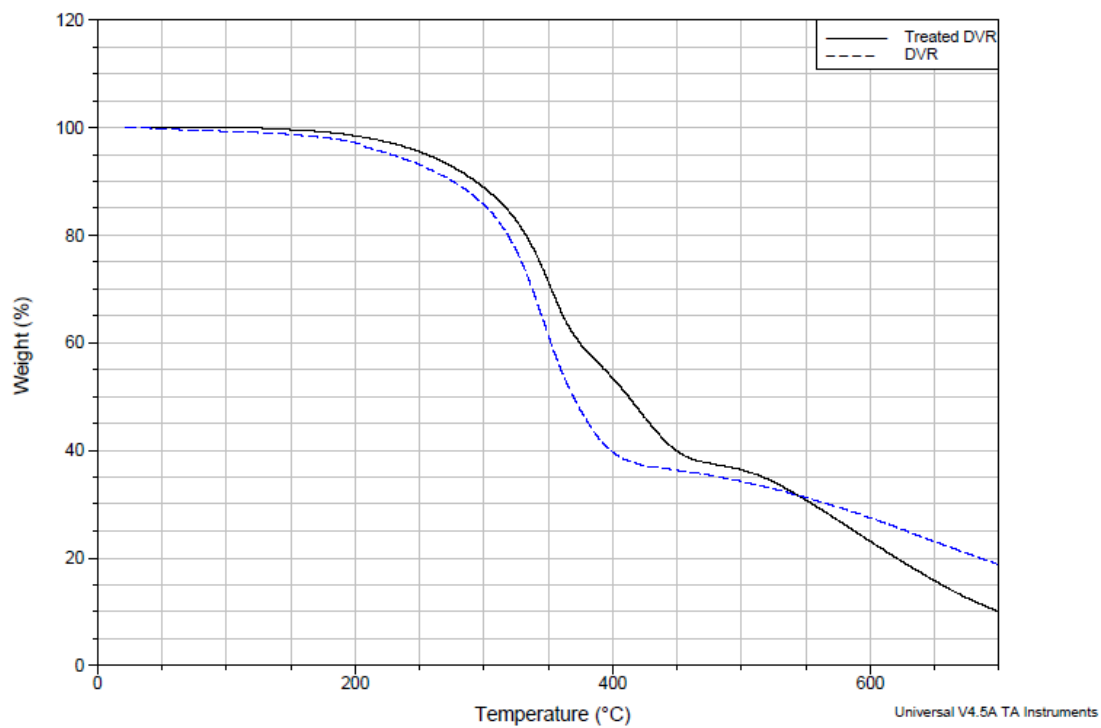


Fig. 76: Thermograms of untreated DVR and treated DVR

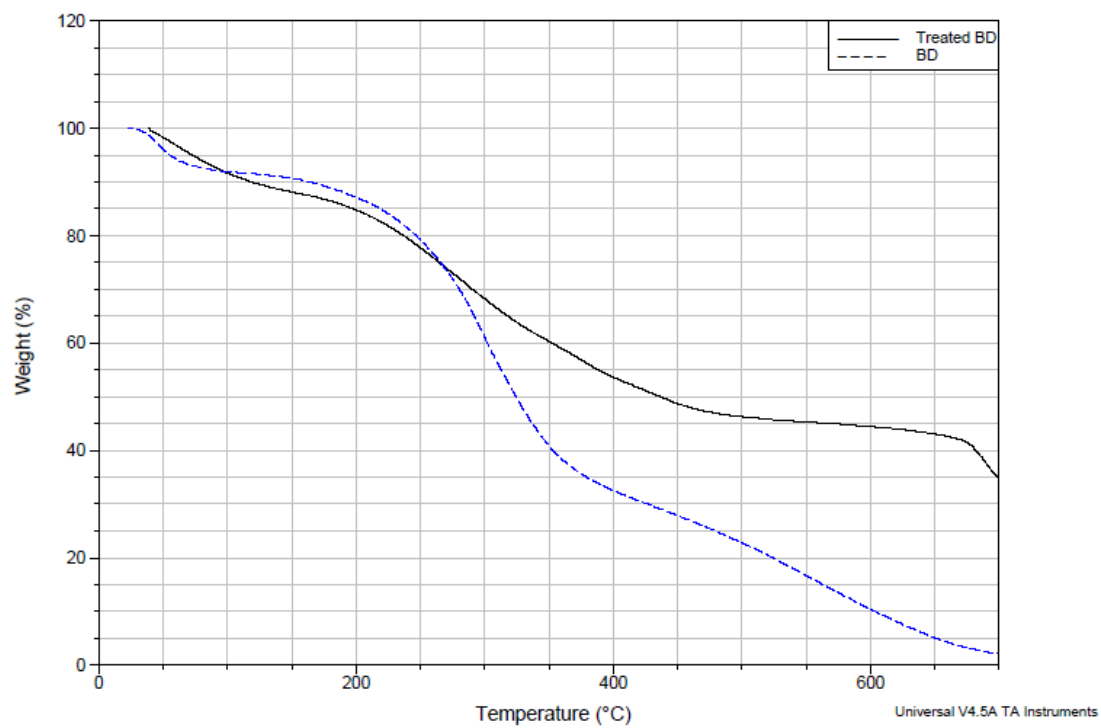


Fig. 77: Thermograms of untreated BD and treated BD

3.6 IR spectroscopy

In this section, IR analysis was performed to investigate the main functional groups of the pure fillers, DPP, DVR and BD. Furthermore, these fillers were tested again after the NaOH treatment in order to study the changes in the main functional groups. The IR spectra of untreated and treated DPP are shown in Fig. 78. The DPP result was found to be similar to the result obtained by [136]. While the broad band at 3412 cm^{-1} was due to O–H vibration and N–H stretching, the band at 2926 cm^{-1} and 2848 cm^{-1} were because of C–H stretching in the alkane group. The observed changes in the bands at 1247 cm^{-1} and 814 cm^{-1} are related to the lignocellulosic content [137]; a comparison of the spectra for untreated with treated DPP offers clear evidence that the lignocellulosic content was affected by the NaOH. Furthermore, the C=O bands at 1744 cm^{-1} and 1378 cm^{-1} were observed in the IR spectra of untreated DPP only. According to [138], this bond is found in one of the main functional groups of hemicellulose. The band almost disappeared with NaOH treatment, which supports the TGA results showing that a significant fraction of the hemicellulose was removed from the DPP, effecting an improvement in adhesion between the DPP and the PS matrix.

The DVR filler IR spectra is shown in Fig. 79. The IR spectra of the DVR used in this work were found to be in good agreement with that the rubber prepared in [58] using microwaves with power varying between 350 and 700 watts. The DVR spectra were in four main bands. The band at 3458 cm^{-1} was due to O–H vibration and the band at 2920 cm^{-1} was due to C–H in the main backbone chain of the rubber. Furthermore, the two bands at 1638 cm^{-1} and 1055 cm^{-1} are explained by the presences of C=C and S=O functional groups. An additional functional group was present in the treated DVR at 1448 cm^{-1} , which is related to C–O–H bending. Unfortunately, the S=S

and other sulfur bonds could not be studied because of the noise present at low wavelengths.

The BD IR spectra shown in Fig. 80 were similar to the BD spectra obtained by Swarnalatha, Srinivasulu, Srimurali, and Sekaran [139]. The O–H band centered at 3446 cm^{-1} decreased with NaOH treatment, which indicates a modification in the carboxylic acid. The bands at 3077 cm^{-1} , 2848 cm^{-1} and 1656 cm^{-1} were due to C–H and C=O stretching, and these were not affected by the chemical treatment. However, the bands at 1551 cm^{-1} and 1243 cm^{-1} , which resulted from N–H bending and N–O stretching, disappeared with NaOH treatment. This suggests that the collagen structure was affected by the treatment and explains the observed changes noted by SEM. The structural change in collagen caused a significant increase in the thermal stability of the BD. In addition, it allowed a better distribution of the filler in the PS matrix.

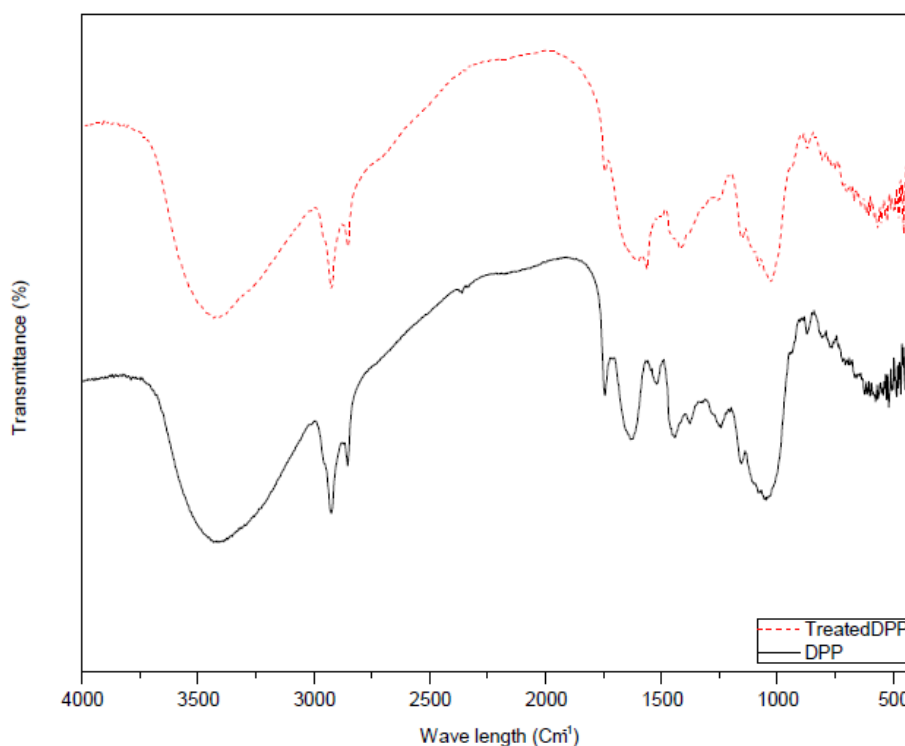


Fig. 78: FTIR spectra of DPP and treated DPP

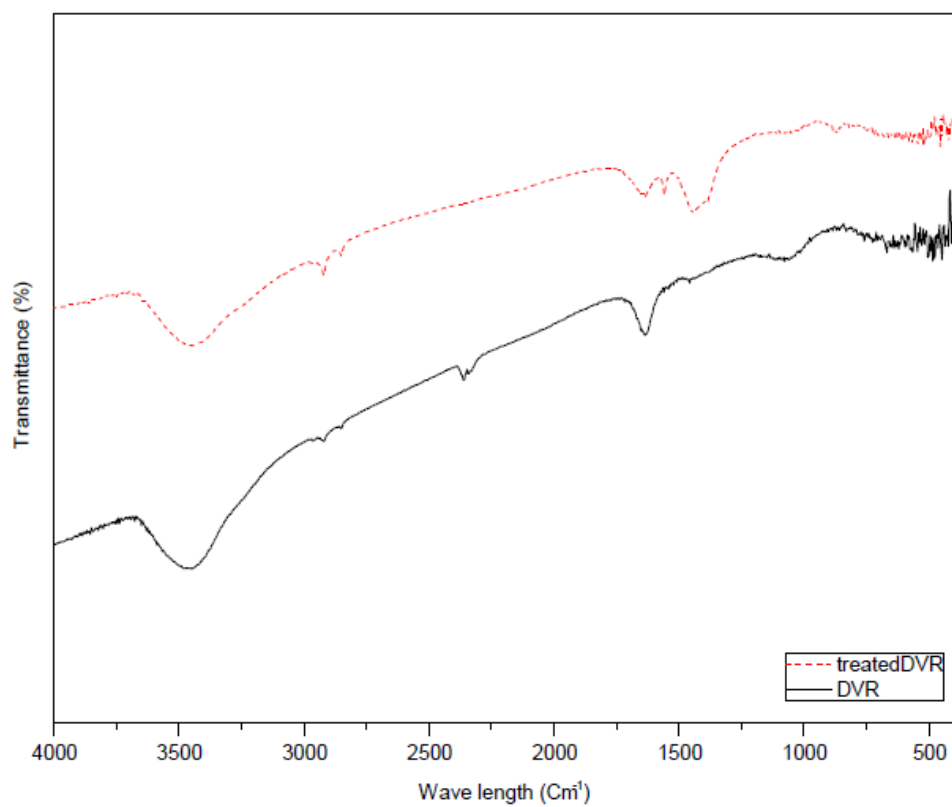


Fig. 79: FTIR spectra of DVR and treated DVR

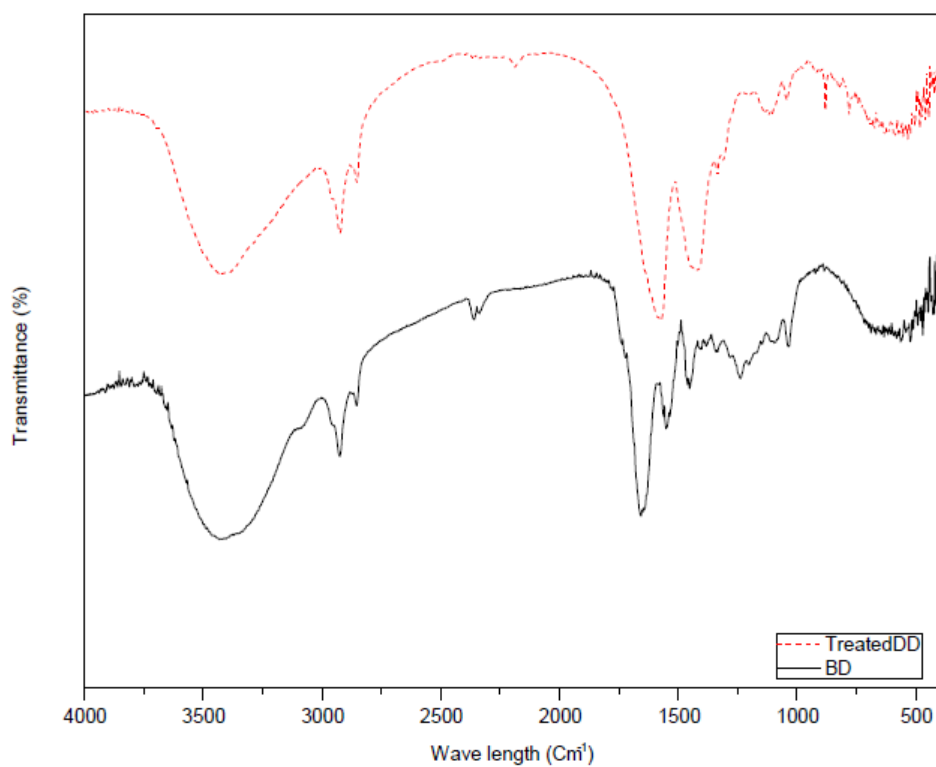


Fig. 80: FTIR spectra of BD and treated BD

3.7 Water retention

3.7.1 Date pits

Fig. 81 represents the water retention for the different samples in room temperature (25 °C) and hot (50 °C) water. The water retention for the 10-DPP and 20-DPP composites in cold water was quite low, i.e., around 5 % of sample weight. However, for the 30-DPP, 40-DPP and 50-DPP composites, the water retention values were 14 %, 26 %, and 57 % of the sample weight, respectively. In addition, water retention increased with increasing DPP filler content. This may be attributed to the hydrophilicity of DPP due to their hydroxyl groups and the voids induced by the poor compatibility between the DPP filler and the polymer matrix [108]. Ameh, Isa, and Sanusi [140] observed a similar behavior in water retention, which increased with increasing date seed concentration in date seed-polyester composites. Moreover, water absorption increased with increasing particle size in the date pits in the studied composites. A similar water retention trend was observed in [39] when polyester was combined with a non-natural fiber (crumbed rubber). As expected, the water retention in hot water was higher than that in cold water. Specifically, the water retention values in hot water were 0.31 %, 6 %, 21 %, 32 %, 53 % of the 10-DPP, 20-DPP, 30-DPP, 40-DPP and 50-DPP samples, respectively.

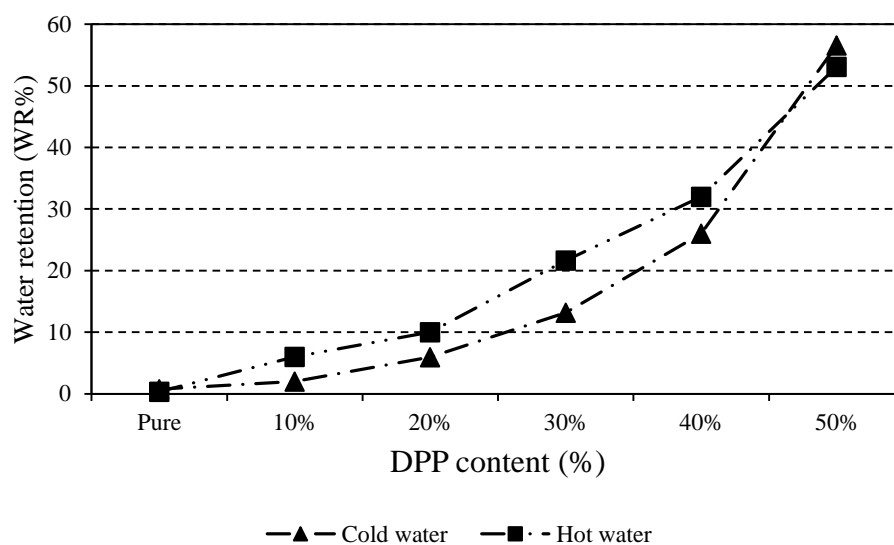


Fig. 81: Water retention of DPP-PS composites

3.7.2 Devulcanized rubber

The water retention of the DVR-PS composites is shown in Fig. 82. The test was conducted in two different environments: in the first test, samples were immersed in water at room temperature; in the second test, the water temperature was 50 °C. During the two tests, it was observed that water retention increased with increasing filler content. The water retention values for hot water test were higher than the cold water values. Water retention in the DVR-PS composites was much lower than in the DPP-PS composites. The DVR-PS composites had superior water retention values, with all samples recording water retention values of less than 0.5 %. The cold water retention test results were 0.145 %, 0.253 %, 0.478 %, 0.488 % and 0.449 % for the 10-DVR, 20-DVR, 30-DVR, 40-DVR and 50-DVR composites, respectively. In the hot water tests, water retention values were less than 1 % for all prepared composites, except the 40-DVR and 50-DVR composites. The water retention in the DVR-PS composites was lower than for other polymeric insulation materials, e.g. polyester-

scrap tire [39]. Although the DVR filler is hydrophobic, this filler increased the water retention. That may be due to the irregularity of the particle distribution and the poor interface evident in SEM images of the composites.

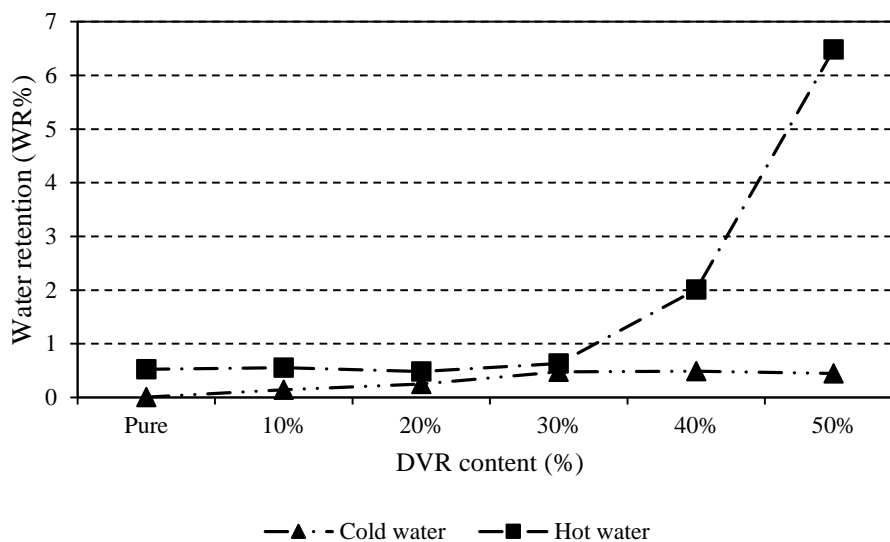


Fig. 82: Water retention of DVR-PS composites

3.7.3 Buffing dust

Fig. 83 shows the water retention behavior of the BD-PS composites after 24 hours. In the cold water tests, the water retention values for the 5-BD, 10-BD, 15-BD, 20-BD and 25-BD composites were 1.29 %, 1.61 %, 2.55 %, 2.80 % and 4.29 %. As observed above, water retention among samples immersed in hot water was higher than for those immersed in cold water. Fig. 83 also shows that water retention rose with increasing BD content. For both tests, the water retention of all composites with less than 20 wt. % filler content BD was below 3 %. Furthermore, the maximum water retention value was found to be about 5 % for the two tests. To the best of author's knowledge, no water retention test has been performed previously on BD composites. The water retention value is within the same range as that of other thermal insulators

composites such as rubber-polyester composite and Bentonite-polyester composite [39, 141]. Again, increasing of water retention with BD content may be due to the poor interface between the BD particles and the PS matrix (Fig. 53).

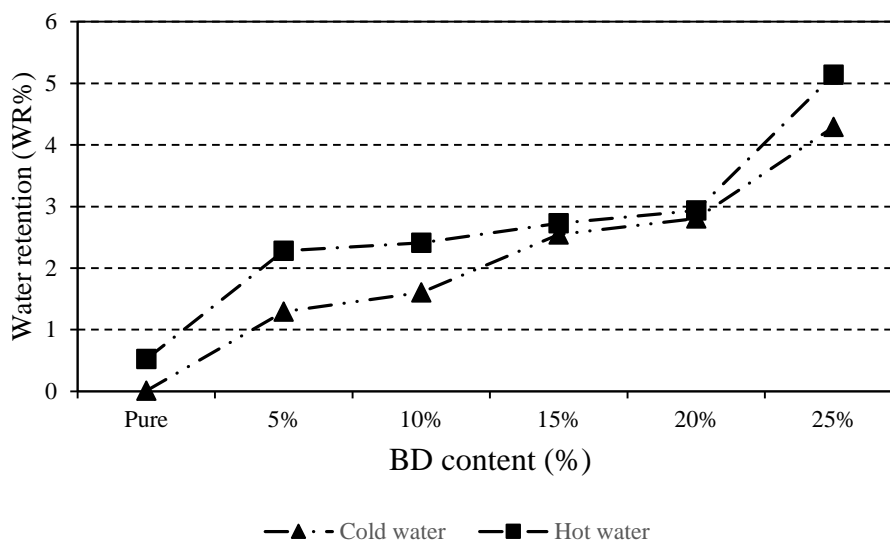


Fig. 83: Water retention of BD-PS composites

Chapter 4: Conclusion

In this study, waste-based thermal insulators were developed with different filler contents (0 to 50 wt. %). The addition of DPP, DVR and BD waste on PS properties was studied. Composites were characterized in terms of their mechanical, thermal and physical properties. Furthermore, chemical treatment was implemented and the mechanical and thermal properties of the treated composites were studied. The microstructure of both treated and untreated fillers and the composites prepared from them were investigated by SEM. In addition, the main functional groups of treated and untreated DPP, DVR and BD were investigated by IR spectroscopy.

Fig. 84 shows that the addition of the three fillers with a content of 20 wt. % had an acceptable negative effect on the compression strength of the composite. Furthermore, higher filler content (up to 40 wt. %) had a minimal effect on the compression strength of DPP-PS composites.

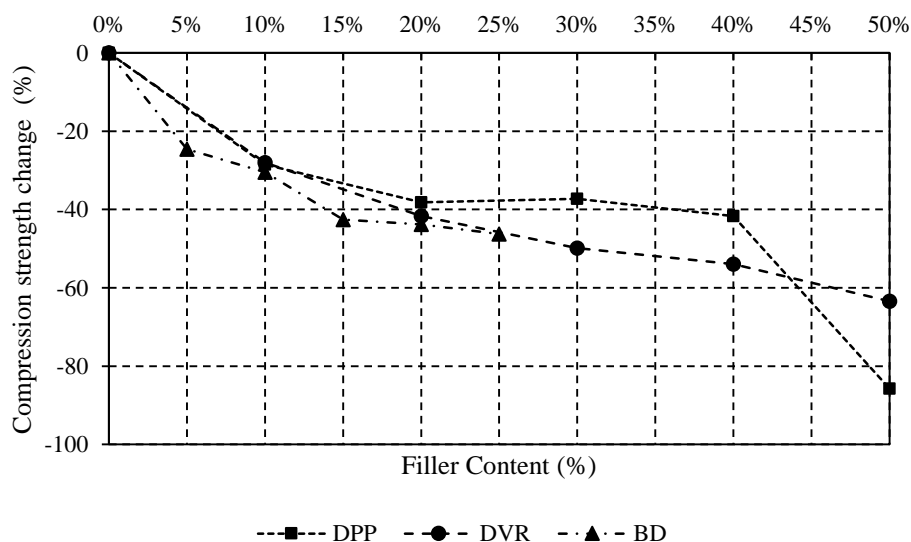


Fig. 84: Effect of different fillers on the compression strength

The change of tensile strength of the developed composites is shown in Fig. 85. The addition of a small proportion (10 wt. %) of BD and DVR improved the tensile strength of the composite. This may be due to a good distribution of the filler in the matrix and the strong adhesion between these two fillers and the matrix at low filler proportions. However, increasing the filler content above 15 % degraded the mechanical properties of the developed composites. Poor interface between the added fillers and the PS matrix caused a degradation in mechanical strength. Although the tensile strength of DVR-PS composites degraded as do the other two composites, the strength values for all DVR-PS composites was still higher than that of the pure matrix.

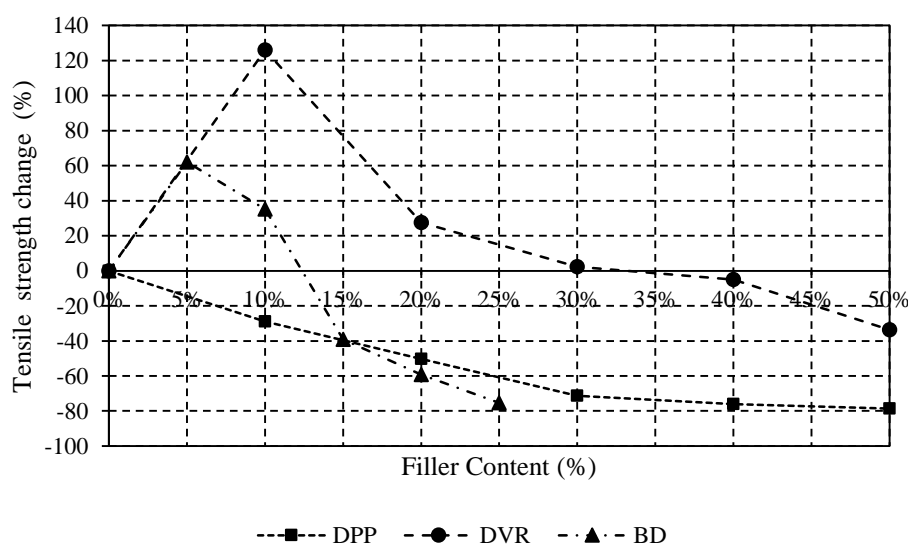


Fig. 85: Effect of different fillers on tensile strength

The flexural strength of the three developed composites is shown in Fig. 86. The flexural strength of DPP-PS and BD-PS, compared with that of the pure PS matrix, was found to reduce by 50 % with the addition of a small proportion of filler content. Above that, the flexural strength of these composites did not change significantly with

higher proportions of filler content. On the other hand, the flexural strength of the DVR-PS composite monotonically reduced with DVR addition.

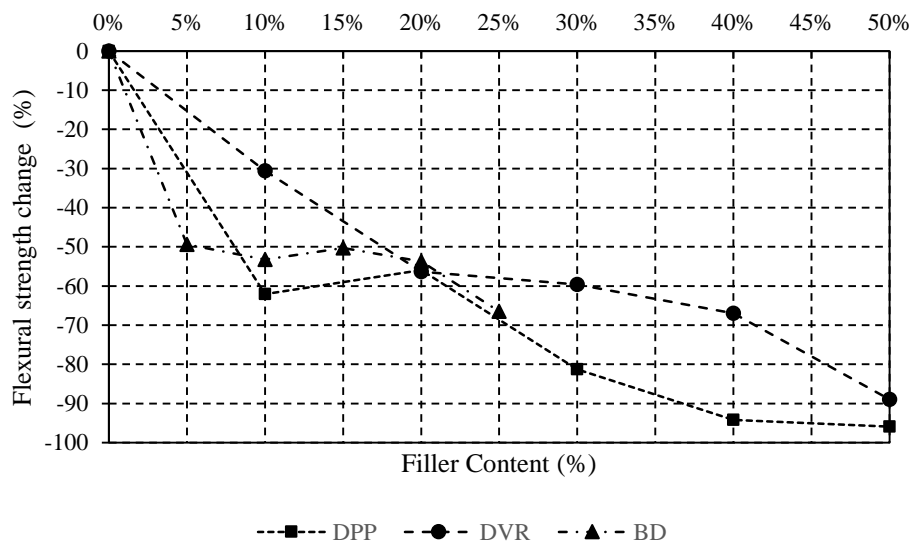


Fig. 86: Effect of different fillers on flexural strength

Fig. 87 shows that the addition of high proportions of DPP and BD had a minimal effect on thermal conductivity. For example, the addition of 20 wt. % DPP, DVR and BD increased the thermal conductivity by 2.9 %, 18% and 6.4 %, respectively. The addition of DVR in proportions less than 20 wt. % had an acceptable effect on thermal conductivity; however, the addition of more filler increased thermal conductivity significantly. It is worth noting in particular that replacing 10 wt. % of PS with DVR and BD reduced the thermal conductivity of pure PS matrix by 4 % and 13.5 %, respectively. Thermal conductivity changes may be explained by the presence of air voids and the thermal conductivity of the added fillers. The thermal stability of all composites decreased slightly before chemical treatment.

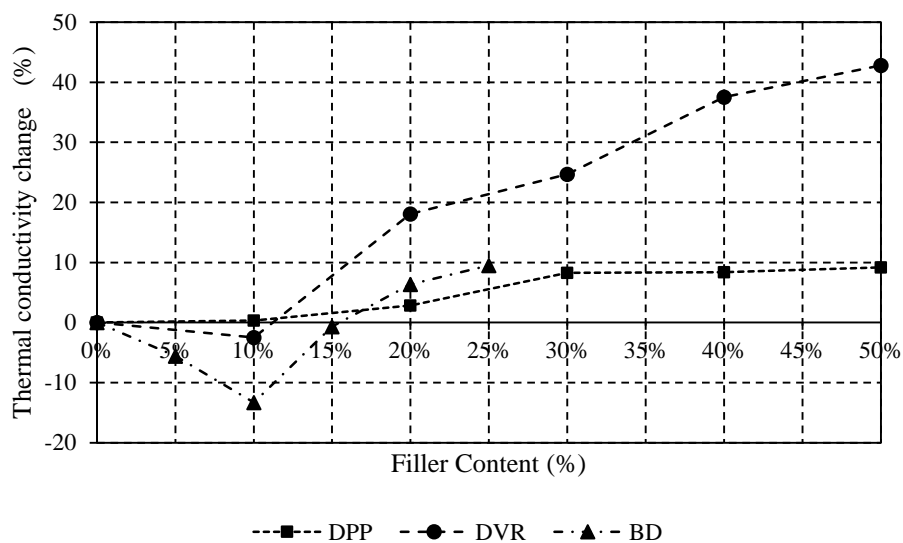


Fig. 87: Effect of different fillers on thermal conductivity

Water retention measurements of the composites are shown in Fig. 88. Overall, water retention by DVR-PS and BD-PS composites was excellent. However, DPP-PS's water retention was good only for low content composites. The maximum water retention values for the 50-DVR and 25-BD composite were measured at 2 % and 5 %, respectively.

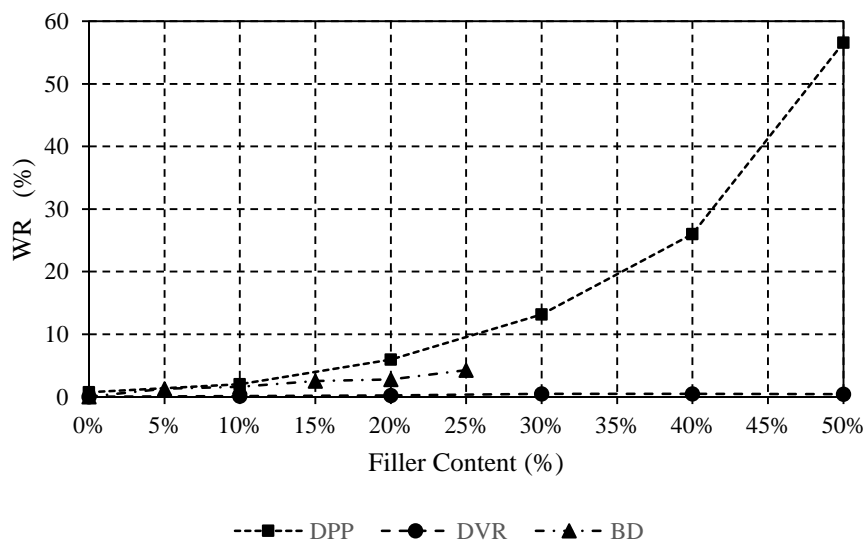


Fig. 88: Effect of different fillers on water retention

Finally, NaOH treatment effectively increased the tensile and flexural strength of all prepared composites. The treatment improved the compatibility between the matrix and the natural fillers. The SEM images demonstrate that the treatment effectively changed the surface roughness of the DPP and DVR and the shape of the BD filler. In addition, SEM show that the treatment enhanced the interference between the fillers and the PS matrix. TGA analysis indicates that the observed improvement in adhesion was due to removal of hydrophilic components from DPP, removal of oil from DVR and modifications to the structure of collagen in the BD. The IR spectra of the fillers were consistent with the TGA findings. Moreover, it showed that the chemical treatment created new functional groups in DVR.

The proposed composites were found suitable to be used as an insulation material, especially composites with 30 wt. % or less, when compared with other commercially available thermal insulation materials that are discussed in the literature [142] (Fig. 89 and Fig. 90). Replacing one-third of the thickness of a building wall with DPP-PS, DVR-PS and BD-PS composites reduced the heat transfer coefficient by 85 %, 87.8 % and 83 %, respectively.

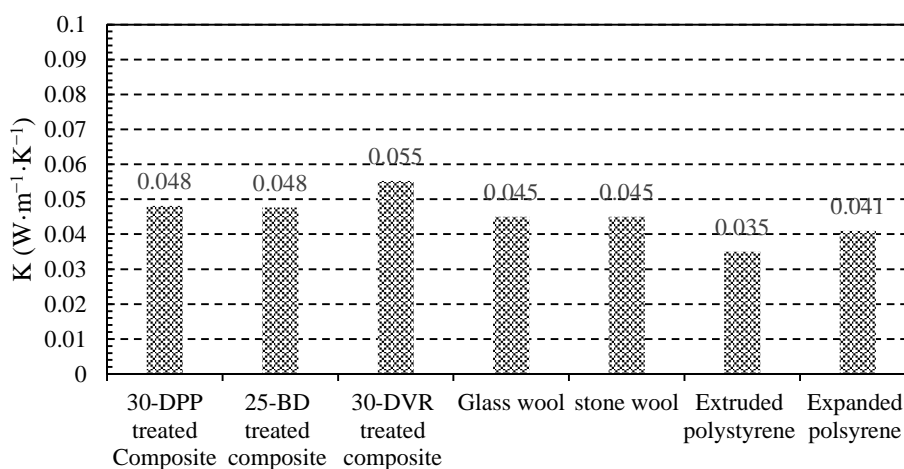


Fig. 89: Thermal conductivity comparison

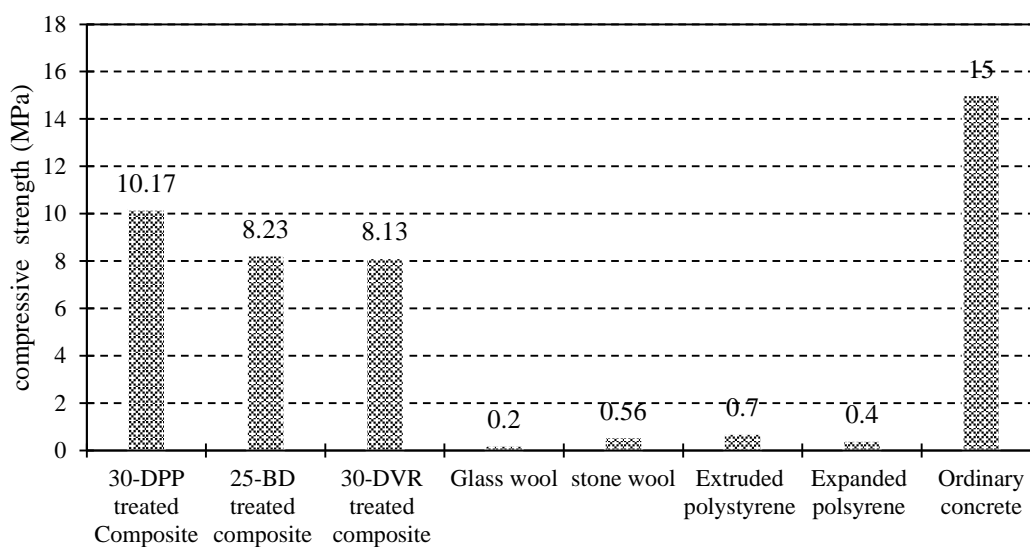


Fig. 90: Mechanical strength comparison

Finally, it is noted that air voids had a significant effect on the mechanical and thermal properties of the composites. Further investigation is required to study the effect of process parameters (e.g. temperature and pressure) on the number and size of voids. Moreover, the effect of different moulding techniques on the mechanical and thermal properties should be examined. Although BD has low thermal conductivity, the addition of a high proportion of BD increases the thermal conductivity of the composite because BD fills the voids. Finding a method to add BD to PS matrix without affecting the existing voids would enable the recycling large amounts of BD, as well as decrease the thermal conductivity of the PS. Furthermore, finding methods to control void size, number and location would be a worthwhile objective for future research. In addition, the effects of advanced mixing techniques such as a screw extruder is recommended for further study. Advanced mixing and other moulding techniques may effectively increase the mechanical strength of the composites.

References

- [1] D. Ürge-Vorsatz, L. F. Cabeza, S. Serrano, C. Barreneche, and K. Petrichenko, "Heating and cooling energy trends and drivers in buildings," *Renewable and Sustainable Energy Reviews*, vol. 41, pp. 85–98, 2015.
- [2] International Energy Agency (IEA), "Key World Energy Statistics," 2014.
- [3] U. S. E. I. Administration, "Annual Energy Outlook 2017 with projections to 2050," 2017.
- [4] A. M. Kazim, "Assessments of primary energy consumption and its environmental consequences in the United Arab Emirates," *Renewable and Sustainable Energy Reviews*, vol. 11, pp. 426–446, 2007.
- [5] A. Mokri, M. A. Ali, and M. Emziane, "Solar energy in the United Arab Emirates: A review," *Renewable and Sustainable Energy Reviews*, vol. 28, pp. 340–375, 2013.
- [6] A. A. Kader and A. M. Hussein, "Harvesting and postharvest handling of dates," *ICARDA*, vol. 1, pp. 1–15, 2009.
- [7] H. Almana and R. Mahmoud, "Palm date seeds as an alternative source of dietary fiber in Saudi bread," *Ecology of Food and Nutrition*, vol. 32, pp. 261–270, 1994.
- [8] R. Siddique and T. R. Naik, "Properties of concrete containing scrap-tire rubber—an overview," *Waste Management*, vol. 24, pp. 563–569, 2004.
- [9] E. M. Brown, M. M. Taylor, and W. N. Marmer, "Production and potential uses of co-products from solid tannery waste," *The Journal of the American Leather Chemists Association (USA)*, pp. 270–276, 1996.
- [10] J. Shi, L. Lu, W. Guo, J. Zhang, and Y. Cao, "Heat insulation performance, mechanics and hydrophobic modification of cellulose–SiO₂ composite aerogels," *Carbohydrate Polymers*, vol. 98, pp. 282–289, 2013.
- [11] F. Asdrubali, A. L. Pisello, F. D. Alessandro, F. Bianchi, M. Cornicchia, and C. Fabiani, "Innovative Cardboard Based Panels with Recycled Materials from the Packaging Industry: Thermal and Acoustic Performance Analysis," *Energy Procedia*, vol. 78, pp. 321–326, 2015.
- [12] G. Balčiūnas, J. Žvironaitė, S. Vėjelis, A. Jagniatinskis, and S. Gaidučis, "Ecological, thermal and acoustical insulating composite from hempshives and spropel binder," *Industrial Crops and Products*, vol. 91, pp. 286–294, 2016.
- [13] Y. Dieye, V. Sambou, M. Faye, A. Thiama, M. Adj, and D. Azilinson, "Thermo-mechanical characterization of a building material based on Typha Australis," *Journal of Building Engineering*, vol. 9, pp. 142–146, 2017.

- [14] D. Belkharouché and A. Chaker, "Effects of moisture on thermal conductivity of the lightened construction material," *International Journal of Hydrogen Energy*, vol. 41, pp. 7119–7125, 2016.
- [15] F. Balo, "Feasibility study of 'green' insulation materials including tall oil: Environmental, economical and thermal properties," *Energy and Buildings*, vol. 486, pp. 182–191 2015.
- [16] H. Binici, R. Gemci, O. Aksogan, and H. Kaplan, "Insulation properties of bricks made with cotton and textile ash wastes," *International Journal of Materials Research*, vol. 101, pp. 894–899, 2010.
- [17] H. Binici, R. Gemci, A. Kucukonder, and H. H. Solak, "Investigating sound insulation, thermal conductivity and radioactivity of chipboards produced with cotton waste, fly ash and barite," *Construction and Building Materials*, vol. 30, pp. 826–832, 2012.
- [18] H. Binici, M. Eken, M. Dolaz, O. Aksogan, and M. Kara, "An environmentally friendly thermal insulation material from sunflower stalk, textile waste and stubble fibres," *Construction and Building Materials*, vol. 51, pp. 24–33, 2014.
- [19] H. Binici, O. Aksogan, and C. Demirhan, "Mechanical, thermal and acoustical characterizations of an insulation composite made of bio-based materials," *Sustainable Cities and Society*, vol. 20, pp. 17–26, 2016.
- [20] Y.-F. Shih, J.-X. Cai, C.-S. Kuan, and C.-F. Hsieh, "Plant fibers and wasted fiber/epoxy green composites," *Composites Part B: Engineering*, vol. 43, pp. 2817–2821, 2012.
- [21] P. Anand, "Chemical and Mechanical Treatment of Banana Waste to Develop an Efficient Insulating Material," *Biochemistry & Analytical Biochemistry*, vol. 4, pp. 1–4, 2015.
- [22] L. C. da Rosa, C. G. Santor, A. Lovato, C. S. da Rosa, and S. Güths, "Use of rice husk and sunflower stalk as a substitute for glass wool in thermal insulation of solar collector," *Journal of Cleaner Production*, vol. 104, pp. 90–97, 2015.
- [23] J. C. Damfeu, P. Meukam, and Y. Jannot, "Modeling and measuring of the thermal properties of insulating vegetable fibers by the asymmetrical hot plate method and the radial flux method: Kapok, coconut, groundnut shell fiber and rattan," *Thermochimica Acta*, vol. 630, pp. 67–77, 2016.
- [24] H. Binici and O. Aksogan, "Insulation material production from onion skin and peanut shell fibres, fly ash, pumice, perlite, barite, cement and gypsum," *Materials Today Communications*, vol. 10, pp. 14–24, 2017.
- [25] A. Limam, A. Zerizer, D. Quenard, H. Sallee, and A. Chenak, "Experimental thermal characterization of bio-based materials (Aleppo Pine wood, cork and

- their composites) for building insulation," *Energy and Buildings*, vol. 116, pp. 89–95, 2016.
- [26] N. Makul and G. Sua-iam, "Characteristics and utilization of sugarcane filter cake waste in the production of lightweight foamed concrete," *Journal of Cleaner Production*, vol. 126, pp. 118–133, 2016.
- [27] J. S. Hamada, I. B. Hashim, and F. A. Sharif, "Preliminary analysis and potential uses of date pits in foods," *Food Chemistry*, vol. 76, pp. 135–137, 2002.
- [28] A. Oushabi, S. Sair, Y. Abboud, O. Tanane, and A. EL-Bouari, "Natural thermal-insulation materials composed of renewable resources: characterization of local date palm fibers (LDPF)," *Journal of Materials and Environmental Science*, vol. 6, pp. 3395–3402, 2015.
- [29] A. H. Alami, "Mechanical and thermal properties of solid waste-based clay composites utilized as insulating materials," *International Journal of Thermal and Environmental Engineering*, vol. 6, pp. 89–94, 2013.
- [30] F. Alsewailem and Y. A. Binkhder, "Preparation and characterization of polymer/date pits composites," *Journal of Reinforced Plastics and Composites*, pp. 1743–1749, 2009.
- [31] B. Abu-Jdayil and A.-H. Mourad, "Thermal Insulation Material. US Patent " United Arab Emirates Patent US 9347216 B2, 2016.
- [32] K. S. Rebeiz and A. P. Craft, "Plastic waste management in construction: technological and institutional issues," *Resources, Conservation and Recycling*, vol. 15, pp. 245–257, 1995.
- [33] J. L. Ruiz-Herrero, D. Velasco Nieto, A. López-Gil, A. Arranz, A. Fernández, A. Lorenzana, *et al.*, "Mechanical and thermal performance of concrete and mortar cellular materials containing plastic waste," *Construction and Building Materials*, vol. 104, pp. 298–310, 2016.
- [34] A. Patnaik, M. Mvubu, S. Muniyasamy, A. Botha, and R. D. Anandjiwala, "Thermal and sound insulation materials from waste wool and recycled polyester fibers and their biodegradation studies," *Energy and Buildings*, vol. 92, pp. 161–169, 2015.
- [35] A. Abdou and I. Budaiwi, "The variation of thermal conductivity of fibrous insulation materials under different levels of moisture content," *Construction and Building Materials*, vol. 43, pp. 533–544, 2013.
- [36] J. W. Van De Lindt, J. A. H. Carraro, P. R. Heyliger, and C. Choi, "Application and feasibility of coal fly ash and scrap tire fiber as wood wall insulation supplements in residential buildings," *Resources, Conservation and Recycling*, vol. 52, pp. 1235–1240, 2008.

- [37] R. Sulcis, L. Lotti, S. Coiai, F. Ciardelli, and E. Passaglia, "Novel HDPE/ground tyre rubber composite materials obtained through in-situ polymerization and polymerization filling technique," *Journal of Applied Polymer Science*, vol. 131, pp. 40313 1–13, 2014.
- [38] Ł. Piszczyk, A. Hejna, K. Formela, M. Danowska, and M. Strankowski, "Effect of ground tire rubber on structural, mechanical and thermal properties of flexible polyurethane foams," *Iranian Polymer Journal*, vol. 24, pp. 75–84, 2015.
- [39] B. Abu-Jdayil, A.-H. Mourad, and A. Hussain, "Thermal and physical characteristics of polyester–scrap tire composites," *Construction and Building Materials*, vol. 105, pp. 472–479, 2016.
- [40] B. Abu-Jdayil, A.-H. Mourad, and A. Hussain., "Investigation on the mechanical behavior of polyester-scrap tire composites," *Construction and Building Materials*, vol. 127, pp. 896–903, 2016.
- [41] B. Yesilata, H. Bulut, and P. Turgut, "Experimental study on thermal behavior of a building structure using rubberized exterior-walls," *Energy and Buildings*, vol. 43, pp. 393–399, 2011.
- [42] S. Herrero, P. Mayor, and F. Hernández-Olivares, "Influence of proportion and particle size gradation of rubber from end-of-life tires on mechanical, thermal and acoustic properties of plaster-rubber mortars," *Materials & Design*, vol. 47, pp. 633–642, 2013.
- [43] J. Eiras, F. Segovia, M. Borrachero, J. Monzó, M. Bonilla, and J. Payá, "Physical and mechanical properties of foamed Portland cement composite containing crumb rubber from worn tires," *Materials & Design*, vol. 59, pp. 550–557, 2014.
- [44] L. Rincon, J. Coma, G. Pérez, A. Castell, D. Boer, and L. F. Cabeza, "Environmental performance of recycled rubber as drainage layer in extensive green roofs. A comparative Life Cycle Assessment," *Building and Environment*, vol. 74, pp. 22–30, 2014.
- [45] A. Benazzouk, O. Douzane, K. Mezreb, B. Laidoudi, and M. Quéneudec, "Thermal conductivity of cement composites containing rubber waste particles: Experimental study and modelling," *Construction and Building Materials*, vol. 22, pp. 573–579, 2008.
- [46] H. Oktay, R. Yumrutaş, and A. Akpolat, "Mechanical and thermophysical properties of lightweight aggregate concretes," *Construction and Building Materials*, vol. 96, pp. 217–225, 2015.
- [47] J. Norambuena-Contreras, E. Silva-Robles, I. Gonzalez-Torre, and Y. Saravia-Montero, "Experimental evaluation of mechanical and thermal properties of recycled rubber membranes reinforced with crushed polyethylene particles," *Journal of Cleaner Production*, vol. 145, pp. 85–97, 2017.

- [48] S. Schiavoni, F. D'Alessandro, F. Bianchi, and F. Asdrubali, "Insulation materials for the building sector: A review and comparative analysis," *Renewable and Sustainable Energy Reviews*, vol. 62, pp. 988–1011, 2016.
- [49] R. Mujal-Rosas, M. Marin-Genesca, J. Orrit-Prat, A. Rahhali, and X. Colom-Fajula, "Dielectric, mechanical, and thermal characterization of high-density polyethylene composites with ground tire rubber," *Journal of Thermoplastic Composite Materials*, vol. 25, pp. 537–559, 2012.
- [50] I. Mangili, M. Lasagni, M. Anzano, E. Collina, V. Tatangelo, A. Franzetti, *et al.*, "Mechanical and rheological properties of natural rubber compounds containing devulcanized ground tire rubber from several methods," *Polymer Degradation and Stability*, vol. 121, pp. 369–377, 2015.
- [51] M. Kojima, K. Ogawa, H. Mizushima, M. Tosaka, S. Kohjiya, and Y. Ikeda, "Devulcanization of sulfur-cured isoprene rubber in supercritical carbon dioxide," *Rubber chemistry and technology*, vol. 76, pp. 957–968, 2003.
- [52] A. Isayev, J. Chen, and A. Tukachinsky, "Novel ultrasonic technology for devulcanization of waste rubbers," *Rubber Chemistry and Technology*, vol. 68, pp. 267–280, 1995.
- [53] R. A. Romine and M. F. Romine, "Rubbercycle: a bioprocess for surface modification of waste tyre rubber," *Polymer Degradation and Stability*, vol. 59, pp. 353–358, 1998.
- [54] I. Mangili, E. Collina, M. Anzano, D. Pitea, and M. Lasagni, "Characterization and supercritical CO₂ devulcanization of cryo-ground tire rubber: Influence of devulcanization process on reclaimed material," *Polymer Degradation and Stability*, vol. 102, pp. 15–24, 2014.
- [55] Z. Liu, X. Li, X. Xu, X. Wang, C. Dong, F. Liu, *et al.*, "Devulcanization of waste tread rubber in supercritical carbon dioxide: Operating parameters and product characterization," *Polymer Degradation and Stability*, vol. 119, pp. 198–207, 2015.
- [56] J. Shi, K. Jiang, D. Ren, H. Zou, Y. Wang, X. Lv, *et al.*, "Structure and performance of reclaimed rubber obtained by different methods," *Journal of Applied Polymer Science*, vol. 129, pp. 999–1007, 2013.
- [57] F. D. de Sousa, C. H. Scuracchio, G.-H. Hu, and S. Hoppe, "Devulcanization of waste tire rubber by microwaves," *Polymer Degradation and Stability*, vol. 138, pp. 169–181, 2017.
- [58] K. Aoudia, S. Azem, N. A. Hocine, M. Gratton, V. Pettarin, and S. Seghar, "Recycling of waste tire rubber: Microwave devulcanization and incorporation in a thermoset resin," *Waste Management*, vol. 60, pp. 471–481, 2017.
- [59] Ł. Piszczyk, A. Hejna, K. Formela, M. Danowska, and M. Strankowski, "Effect of ground tire rubber on structural, mechanical and thermal properties

- of flexible polyurethane foams," *Iranian Polymer Journal*, vol. 24, pp. 75-84, 2015.
- [60] P. Punnarak, S. Tantayanon, and V. Tangpasuthadol, "Dynamic vulcanization of reclaimed tire rubber and high density polyethylene blends," *Polymer Degradation and Stability*, vol. 91, pp. 3456–3462, 2006.
- [61] S. Tantayanon and S. Juikham, "Enhanced toughening of poly (propylene) with reclaimed-tire rubber," *Journal of Applied Polymer Science*, vol. 91, pp. 510–515, 2004.
- [62] M. M. Hassan, R. O. Aly, S. A. Aal, A. M. El-Masry, and E. Fathy, "Mechanochemical devulcanization and gamma irradiation of devulcanized waste rubber/high density polyethylene thermoplastic elastomer," *Journal of Industrial and Engineering Chemistry*, vol. 19, pp. 1722–1729, 2013.
- [63] X. Zhang, Z. Lu, D. Tian, H. Li, and C. Lu, "Mechanochemical devulcanization of ground tire rubber and its application in acoustic absorbent polyurethane foamed composites," *Journal of Applied Polymer Science*, vol. 127, pp. 4006–4014, 2013.
- [64] G. Sekaran, K. Shanmugasundaram, and M. Mariappan, "Characterization and utilisation of buffing dust generated by the leather industry," *Journal of Hazardous Materials*, vol. 63, pp. 53–68, 1998.
- [65] T. Karak, R. Bhagat, and P. Bhattacharyya, "Municipal solid waste generation, composition, and management: The world scenario," *Critical Reviews In Environmental Science and Technology*, vol. 42, pp. 1509–1630, 2012.
- [66] O. Yılmaz, I. C. Kantarli, M. Yuksel, M. Saglam, and J. Yanik, "Conversion of leather wastes to useful products," *Resources, Conservation and Recycling*, vol. 49, pp. 436–448, 2007.
- [67] K. Chrońska-Olszewska and A. Przepiórkowska, "A mixture of buffing dust and chrome shavings as a filler for nitrile rubbers," *Journal of Applied Polymer Science*, vol. 122, pp. 2899–2906, 2011.
- [68] N. G. Garcia, E. A. P. Reis, E. R. Budemberg, D. L. d. S. Agostini, L. O. Salmazo, F. C. Cabrera, *et al.*, "Natural rubber/leather waste composite foam: A new eco-friendly material and recycling approach," *Journal of Applied Polymer Science*, vol. 132, pp. 416361 (1–10), 2015.
- [69] S. H. El-Sabbagh and O. A. Mohamed, "Recycling of chrome-tanned leather waste in acrylonitrile butadiene rubber," *Journal of Applied Polymer Science*, vol. 121, pp. 979–988, 2011.
- [70] K. Chronska and A. Przepiorkowska, "Buffing dust as a filler of carboxylated butadiene-acrylonitrile rubber and butadiene-acrylonitrile rubber," *Journal of Hazardous Materials*, vol. 151, pp. 348–355, 2008.

- [71] M. J. Ferreira, F. Freitas, and M. F. Almeida, "The effect of leather fibers on the properties of rubber-leather composites," *Journal of Composite Materials*, vol. 44, pp. 2801–2817, 2010.
- [72] A. Andreopoulos and P. Tarantili, "Waste leather particles as a filler for poly (vinyl chloride) plastisols," *Journal of Macromolecular Science-Pure and Applied Chemistry*, vol. 37, pp. 1353–1362, 2000.
- [73] K. P. Murugan, S. Swarnalatha, and G. Sekaran, "Utilization of Micro Fibrous Carbon Matrix from Tannery Solid Waste for Making Pavement Materials," *Procedia Environmental Sciences*, vol. 35, pp. 298–307, 2016.
- [74] B. Bitlisli and E. Karacaki, "Utilization of leather industry solid wastes in the production of porous clay brick," *Journal of the Society of Leather Technologists and Chemists*, vol. 90, pp. 19–22, 2006.
- [75] H. Lakraflı, S. Tahiri, A. Albizane, and M. El Otmani, "Effect of wet blue chrome shaving and buffing dust of leather industry on the thermal conductivity of cement and plaster based materials," *Construction and Building Materials*, vol. 30, pp. 590–596, 2012.
- [76] H. Lakraflı, S. Tahiri, A. Albizane, M. Bouhria, and M. El Otmani, "Experimental study of thermal conductivity of leather and carpentry wastes," *Construction and Building Materials*, vol. 48, pp. 566–574, 2013.
- [77] V. A. Alvarez, R. A. Ruseckaite, and A. Vazquez, "Mechanical Properties and Water Absorption Behavior of Composites Made from a Biodegradable Matrix and Alkaline-Treated Sisal Fibers," *Journal of Composite Materials*, vol. 37, pp. 1575–1588, 2003.
- [78] R. Raj, B. Kokta, F. Dembele, and B. Sanschagrain, "Compounding of cellulose fibers with polypropylene: Effect of fiber treatment on dispersion in the polymer matrix," *Journal of Applied Polymer Science*, vol. 38, pp. 1987–1996, 1989.
- [79] M. Kazayawoko, J. Balatinez, and L. Matuana, "Surface modification and adhesion mechanisms in woodfiber-polypropylene composites," *Journal of Materials Science*, vol. 34, pp. 6189–6199, 1999.
- [80] I. Van de Weyenberg, J. Ivens, A. De Coster, B. Kino, E. Baetens, and I. Verpoest, "Influence of processing and chemical treatment of flax fibres on their composites," *Composites Science and Technology*, vol. 63, pp. 1241–1246, 2003.
- [81] C. Vallo, J. M. Kenny, A. Vazquez, and V. P. Cyras, "Effect of chemical treatment on the mechanical properties of starch-based blends reinforced with sisal fibre," *Journal of Composite Materials*, vol. 38, pp. 1387–1399, 2004.
- [82] K. Joseph, S. Thomas, and C. Pavithran, "Effect of chemical treatment on the tensile properties of short sisal fibre-reinforced polyethylene composites," *Polymer*, vol. 37, pp. 5139–5149, 1996.

- [83] K. M. Nair, S. Thomas, and G. Groeninckx, "Thermal and dynamic mechanical analysis of polystyrene composites reinforced with short sisal fibres," *Composites Science and Technology*, vol. 61, pp. 2519–2529, 2001.
- [84] S. Mohanty, S. Nayak, S. Verma, and S. Tripathy, "Effect of MAPP as a coupling agent on the performance of jute–PP composites," *Journal of Reinforced Plastics and Composites*, vol. 23, pp. 625–637, 2004.
- [85] Y. Xie, C. A. Hill, Z. Xiao, H. Militz, and C. Mai, "Silane coupling agents used for natural fiber/polymer composites: A review," *Composites Part A: Applied Science and Manufacturing*, vol. 41, pp. 806–819, 2010.
- [86] A. Valadez-Gonzalez, J. Cervantes-Uc, R. Olayo, and P. Herrera-Franco, "Effect of fiber surface treatment on the fiber–matrix bond strength of natural fiber reinforced composites," *Composites Part B: Engineering*, vol. 30, pp. 309–320, 1999.
- [87] L. M. Matuana, R. T. Woodhams, J. J. Balatinecz, and C. B. Park, "Influence of interfacial interactions on the properties of PVC/cellulosic fiber composites," *Polymer Composites*, vol. 19, pp. 446–455, 1998.
- [88] S. M. Nachtigall, G. S. Cerveira, and S. M. Rosa, "New polymeric-coupling agent for polypropylene/wood-flour composites," *Polymer Testing*, vol. 26, pp. 619–628, 2007.
- [89] M. Bengtsson, K. Oksman, and N. M. Stark, "Profile extrusion and mechanical properties of crosslinked wood–thermoplastic composites," *Polymer composites*, vol. 27, pp. 184–194, 2006.
- [90] M. Bengtsson and K. Oksman, "The use of silane technology in crosslinking polyethylene/wood flour composites," *Composites Part A: Applied Science and Manufacturing*, vol. 37, pp. 752–765, 2006.
- [91] R. Raj, B. V. Kokta, D. Maldas, and C. Daneault, "Use of wood fibers in thermoplastics. VII. The effect of coupling agents in polyethylene–wood fiber composites," *Journal of Applied Polymer Science*, vol. 37, pp. 1089–1103, 1989.
- [92] J. Arenas, J. Marcos, J. Otero, I. Tocon, and J. Soto, "Nitrenes as intermediates in the thermal decomposition of aliphatic azides," *International Journal of Quantum Chemistry*, vol. 84, pp. 241–248, 2001.
- [93] G. A. McFarren, T. F. Sanderson, and F. G. Schappell, "Azidosilane polymer–filler coupling agent," *Polymer Engineering & Science*, vol. 17, pp. 46–49, 1977.
- [94] D. Maldas, B. Kokta, and C. Daneault, "Influence of coupling agents and treatments on the mechanical properties of cellulose fiber–polystyrene composites," *Journal of Applied Polymer Science*, vol. 37, pp. 751–775, 1989.

- [95] M. A. Alam, S. Arif, and M. Shariq, "Enhancement in Mechanical Properties of Polystyrene-ZnO Nanocomposites," *International Journal of Innovative Research in Advanced Engineering*, vol. 2, pp. 122–129, 2015 2014.
- [96] V. Vergnat, T. Roland, G. Pourroy, and P. Masson, "Effect of covalent grafting on mechanical properties of TiO₂/polystyrene composites," *Materials Chemistry and Physics*, vol. 147, pp. 261–267, 2014.
- [97] A. Berge and P. Johansson, "Literature review of high performance thermal insulation," Chalmers University of Technology 2012 2012.
- [98] V. J. Sundar, J. Raghavarao, C. Muralidharan, and A. Mandal, "Recovery and utilization of chromium-tanned proteinous wastes of leather making: A review," *Critical Reviews In Environmental Science and Technology*, vol. 41, pp. 2048–2075, 2011.
- [99] ASTM International, "Standard Test Method for Compressive Properties of Rigid Plastics," in *ASTM D695-15*, ed, 2015.
- [100] A. International, "Standard Test Method for Tensile Properties of Plastics," in *ASTM D638-14*, ed, 2014.
- [101] A. International, "Standard Test Methods for Flexural Properties of Unreinforced and Reinforced Plastics and Electrical Insulating Materials," in *ASTM D638-14*, ed, 2002.
- [102] A. International, "Standard Practice for Calculating Thermal Transmission Properties Under Steady-State Conditions," in *ASTM D638-14*, ed, 2013.
- [103] A. International, "Standard Test Method for Water Absorption of Plastics," in *ASTM D638-14*, ed, 2010.
- [104] S. H. Aziz and M. P. Ansell, "The effect of alkalization and fibre alignment on the mechanical and thermal properties of kenaf and hemp bast fibre composites: Part 1—polyester resin matrix," *Composites Science and Technology*, vol. 64, pp. 1219–1230, 2004.
- [105] S. K. De, A. Isayev, and K. Khait, *Rubber Recycling*: Boca Raton, Florida: Taylor & Francis/CRC Press, 2005.
- [106] J. Khedari, B. Suttisonk, N. Pratinthong, and J. Hirunlabh, "New lightweight composite construction materials with low thermal conductivity," *Cement and Concrete Composites*, vol. 23, pp. 65–70, 2001.
- [107] L. L. C. Owen Corning Foam Insulation. *FOAMULAR® Extruded Polystyrene Insulation Commercial Product Directory of Availability and Physical Properties*, 2007. Available: www.owenscorning.com
- [108] X. Li, L. G. Tabil, and S. Panigrahi, "Chemical treatments of natural fiber for use in natural fiber-reinforced composites: a review," *Journal of Polymers and the Environment*, vol. 15, pp. 25–33, 2007.

- [109] I. B. Topcu, "The properties of rubberized concretes," *Cement and Concrete Research*, vol. 25, pp. 304–310, 1995.
- [110] N. Marcovich, M. Aranguren, and M. Reboledo, "Modified woodflour as thermoset fillers Part I. Effect of the chemical modification and percentage of filler on the mechanical properties," *Polymer*, vol. 42, pp. 815–825, 2001.
- [111] E. T. N. Bisanda and M. P. Ansell, "The effect of silane treatment on the mechanical and physical properties of sisal-epoxy composites," *Composites Science and Technology*, vol. 41, pp. 165–178, 1991 1991.
- [112] E. Mıhlayanlar, Ş. Dilmaç, and A. Güner, "Analysis of the effect of production process parameters and density of expanded polystyrene insulation boards on mechanical properties and thermal conductivity," *Materials & Design*, vol. 29, pp. 344–352, 2008.
- [113] F. Karabork, E. Pehlivan, and A. Akdemir, "Characterization of styrene butadiene rubber and microwave devulcanized ground tire rubber composites," *Journal of Polymer Engineering*, vol. 34, pp. 543–554, 2014.
- [114] J. I. P. Singh, V. Dhawan, S. Singh, and K. Jangid, "Study of Effect of Surface Treatment on Mechanical Properties of Natural Fiber Reinforced Composites," *Materials Today: Proceedings*, vol. 4, pp. 2793–2799, 2017.
- [115] M. Poletto, J. Dettenborn, M. Zeni, and A. J. Zattera, "Characterization of composites based on expanded polystyrene wastes and wood flour," *Waste Management*, vol. 31, pp. 779–784, 2011.
- [116] X.-y. Zhou, F. Zheng, H.-g. Li, and C.-l. Lu, "An environment-friendly thermal insulation material from cotton stalk fibers," *Energy and Buildings*, vol. 42, pp. 1070–1074, 2010.
- [117] N. F. Medina, D. F. Medina, F. Hernández-Olivares, and M. Navacerrada, "Mechanical and thermal properties of concrete incorporating rubber and fibres from tyre recycling," *Construction and Building Materials*, vol. 144, pp. 563–573, 2017.
- [118] N. Segre and I. Joekes, "Use of tire rubber particles as addition to cement paste," *Cement and Concrete Research*, vol. 30, pp. 1421–1425, 2000.
- [119] A. Adefemi, M. H. Nensok, E. T. Kaase, and I. A. Wuna, "Exploratory study of date seed as coarse aggregate in concrete production," *Civil and Environmental Research*, vol. 3, pp. 85–92, 2013.
- [120] R. Demirboğa and R. Gül, "The effects of expanded perlite aggregate, silica fume and fly ash on the thermal conductivity of lightweight concrete," *Cement and Concrete Research*, vol. 33, pp. 723–727, 2003.
- [121] B. Abu-Jdayil, A. H. Mourad, and M. Hassan, "Development of polymeric heat insulators based on emirati red shale filler: Thermal and physical properties," *Polymer Composites*, 10.1002/pc.24356, 2017.

- [122] K. Al Rim, A. Ledhem, O. Douzane, R. M. Dheilly, and M. Queneudec, "Influence of the proportion of wood on the thermal and mechanical performances of clay-cement-wood composites," *Cement and Concrete Composites*, vol. 21, pp. 269–276, 1999.
- [123] B. Abu-Jdayil, A.-H. Mourad, and A. Hussain, "Date Pits and Date Palm Wood-Based Heat Insulator Composites," presented at the 10th International Conference on Composite Science and Technology (ICCST), Lisbon, Portugal, 2015.
- [124] D. Allsopp, K. J. Seal, and C. C. Gaylarde, *Introduction to biodeterioration*: New York: Cambridge University Press, 2nd edition, 2004.
- [125] Z. Cheheb, P. Mousseau, A. Sarda, and R. Deterre, "Thermal conductivity of rubber compounds versus the state of cure," *Macromolecular Materials and Engineering*, vol. 297, pp. 228–236, 2012.
- [126] R. Agrawal, N. Saxena, M. Sreekala, and S. Thomas, "Effect of treatment on the thermal conductivity and thermal diffusivity of oil-palm-fiber-reinforced phenolformaldehyde composites," *Journal of Polymer Science Part B: Polymer Physics*, vol. 38, pp. 916–921, 2000.
- [127] S. Ibraheem, A. Ali, and A. Khalina, "Development of green insulation boards from kenaf fibres and polyurethane," *Polymer-Plastics Technology and Engineering*, vol. 50, pp. 613–621, 2011.
- [128] M. R. Wu, D. L. Schott, and G. Lodewijks, "Physical properties of solid biomass," *Biomass and Bioenergy*, vol. 35, pp. 2093–2105, 2011.
- [129] M. E. Babiker, A. R. A. Aziz, M. Heikal, and S. Yusup, "Pyrolysis characteristics of Phoenix dactylifera date palm seeds using thermogravimetric analysis (TGA)," *International Journal of Environmental Science and Development*, vol. 4, pp. 521–524, 2013.
- [130] R. Briones, L. Serrano, R. B. Younes, I. Mondragon, and J. Labidi, "Polyol production by chemical modification of date seeds," *Industrial Crops and Products*, vol. 34, pp. 1035–1040, 2011.
- [131] C. H. Scuracchio, D. A. Waki, and M. L. C. P. da Silva, "Thermal analysis of ground tire rubber devulcanized by microwaves," *Journal of Thermal Analysis and Calorimetry*, vol. 87, pp. 893–897, 2007.
- [132] W. W. Sułkowski, A. Danch, M. Moczyński, A. Radoń, A. Sułkowska, and J. Borek, "Thermogravimetric study of rubber waste-polyurethane composites," *Journal of Thermal Analysis and Calorimetry*, vol. 78, pp. 905–921, 2004.
- [133] M. M. Hassan, N. A. Badway, M. Y. Elnaggar, and E.-S. A. Hegazy, "Thermo-mechanical properties of devulcanized rubber/high crystalline polypropylene blends modified by ionizing radiation," *Journal of Industrial and Engineering Chemistry*, vol. 19, pp. 1241–1250, 2013.

- [134] T. J. Madera-Santana, A. C. Torres, and A. M. Lucero, "Extrusion and mechanical characterization of PVC-leather fiber composites," *Polymer Composites*, vol. 19, pp. 431–439, 1998.
- [135] S. Joseph, T. S. Ambone, A. V. Salvekar, S. Jaisankar, P. Saravanan, and E. Deenadayalan, "Processing and characterization of waste leather based polycaprolactone biocomposites," *Polymer Composites*, pp. 2889–2897, 2015.
- [136] A.-N. A. El-Hendawy, "Variation in the FTIR spectra of a biomass under impregnation, carbonization and oxidation conditions," *Journal of Analytical and Applied Pyrolysis*, vol. 75, pp. 159–166, 2006.
- [137] V. Gomez-Serrano, J. Pastor-Villegas, A. Perez-Florindo, C. Duran-Valle, and C. Valenzuela-Calahorro, "FT-IR study of rockrose and of char and activated carbon," *Journal of Analytical and Applied Pyrolysis*, vol. 36, pp. 71–80, 1996.
- [138] H. Yang, R. Yan, H. Chen, D. H. Lee, and C. Zheng, "Characteristics of hemicellulose, cellulose and lignin pyrolysis," *Fuel*, vol. 86, pp. 1781–1788, 2007.
- [139] S. Swarnalatha, T. Srinivasulu, M. Srimurali, and G. Sekaran, "Safe disposal of toxic chrome buffing dust generated from leather industries," *Journal of Hazardous Materials*, vol. 150, pp. 290–299, 2008.
- [140] A. O. Ameh, M. T. Isa, and I. Sanusi, "Effect of particle size and concentration on the mechanical properties of polyester/date palm seed particulate composites," *Leonardo Electronic Journal of Practices and Technologies*, vol. 26, pp. 65–78, 2015.
- [141] K. Al-Malah and B. Abu-Jdayil, "Clay-based heat insulator composites: Thermal and water retention properties," *Applied Clay Science*, vol. 37, pp. 90–96, 2007.
- [142] A. M. Papadopoulos, "State of the art in thermal insulation materials and aims for future developments," *Energy and Buildings*, vol. 37, pp. 77–86, 2005.